Influence of CFRP Confinement on Bond Behavior of Steel Bars Embedded in Concrete Exposed to Elevated Temperatures

Mehdi Hosseinpour

Submitted to the
Institute of Graduate Studies and Research
In partial fulfillment of the requirements for the degree of

Doctor of Philosophy
in
Civil Engineering

Eastern Mediterranean University
January 2018
Gazimağusa, North Cyprus

ABSTRACT

This study is presented in two parts. The first part reports the results of an experimental study where the axial capacity of fire-damaged specimens repaired by expansive cement concrete and CFRP wrap were investigated. Specimens were subjected to axial compressive loading and their resulting stress-strain curves were recorded. The cross section for some of the specimens were changed from square to circle shape. To modify the shape, expansive cement concrete has been utilized to fill the gap between the circular and the square cross sections. The test results indicated that heating the specimens up to 500°C caused a severe decline in compressive strength and the elastic modulus of concrete. Two layers of CFRP wrap around the concrete not only compensated the drop in compressive strength but furthermore it increased the strength beyond that of unheated specimen. After heating the square specimens, that were first subjected to shape modification and then wrapped by CFRP sheet, experienced increase in the strength and the elastic modulus. Therefore, the stiffness and the compression strength of fire-damaged square concrete specimens could be compensated fully by the use of shape modification and the CFRP wrapping of the cross section. The second part of the thesis has comprehensively studied the effectiveness of strengthening with CFRP wrapping for maintenance of bond behavior between bar and heat-damaged concrete. The effects of temperature (room temperature as reference, 200°C, 400°C, 600°C and 800°C), concrete cover (25 mm and 35 mm), concrete compressive strength (30 MPa and 40 MPa) and CFRP sheets have been investigated by performing bond test. The results show that strengthening with CFRP can effectively increase the bond strength of samples subjected to high temperature and also can change the failure mode from brittle to a more ductile one. Moreover, the

mechanical properties decreased as the temperature increased, especially after 400°C, so that at 800°C, the compressive strength reduces to around 80%. It was observed that exposure to heat reduced the concrete-bar bond strength particularly for samples with thicker cover and higher compressive strength. But confinement with CFRP improved the bond strength significantly and this was particularly true for samples exposed to high temperature. The effectiveness of wrapped were more significant for samples with low compressive strength and thin concrete cover.

Keywords: Fire Damaged Concrete, Bond Behavior, Strengthening, Shape Modification, CFRP Wrapping.

ÖZ

Bu doktora tezi yangında hasar görmüş bir yapı elemanının tamiri konusu ve de tamiri neticesinde betonun kapasindesindeki değişimlerin incelenmesini içermektedir. Tez çalışması, iki ana bölüm olarak özetlenebilir. Tezin birinci bölümü, yapılmış olan deneysel çalışma sonuçlarını içermektedir. Deney çalışmasında; yangında hasar görmüş deney numunelerinin, genleşen çimento kullanılarak ve de CFRP bandı ile sarılarak iyileştirilmesi neticesinde eksenel basınç dayanım kapasitelerindeki değişim araştırılmıştır. Bu amaç için; basınç dayanımına tabii tutulmuş numunelerin gerilme-şekil değiştirme eğrileri elde edilmiştir. Yükleme neticesinde, kesit alanda oluşmuş olan hasar veya değişim genleşebilen çimentodan üretilmiş beton ile kapatılmıştır. Deney neticeleri göstermiştir ki; beton numunelerinin 500°C'ye maruz kalmaları, hem basınç dayanımını hem de elastic modulusu ciddi miktarlarda azaltmıştır. Fakat, beton numunesi etrafına iki katman olarak uygulanmış olan CFRP, yalnızca basınç dayanımındaki kayıbı gidermekle kalmayıp, hiç ısıya maruz kalmamış olan numunelerin basınç dayanımlarının da üzerine çıkmıştır. Bu uygulama ile aynı zamanda elastik modulus da artış göstermiştir. Böylece, yangında hasar gönmüş kare beton numunelerinde hem elastic modulus hem de basınç dayanımı kayıpları, CFRP uygulaması ile bütünüyle giderilebilir neticesine varılmiştır.

Tezin ikinci bölümünde; numunelerin etrafına sarılmış olan CFRP bandı uygulamasının, donate çeliği ile ısıdan hasar görmüş beton arasındaki bağın iyileştirilmesi konusuna etkileri, farklı ısı uygulamaları için araştırılmıştır. Çalışmanın bu bölümünde oda sıcaklığı referans alınarak 200°C, 400°C, 600°C ve 800°C sıcaklığa maruz kalmış beton numuneleri, iki farlı pas payı, 25 mm and 35 mm; iki farklı beton

tipi, 30 MPa and 40 MPa ve de CFRP band uygulaması dikkate alınarak çekme dayanımına etkileri araştırılmıştır. Neticeler göstermiştir ki, beton numunelerinin CFRP bandı ile güçlendirilmeleri neticesinde, numunelerin bağ dayanımlarının önemli ölçude arttığı ve de gevrek davranış yerine daha çok sünek davranış sergiledikleri gözlemlenmiştir. Bunun yanısıra CFRP band uygulamasının düşuk dayanımlı ve de düşük pas payı olan beton numunelerde daha etkili olduğu anlaşılmıştır.

Anahtar Kelimeler: Yangın hasarlı beton, Bağ dayanımı, Güçlendirme, Şekil değişimi, CFRP band uygulaması.

This dissertation is dedicated to my lovely wife and admiration and to my family especially my father and mother with thanks and appreciation.

ACKNOWLEDGMENT

I would like to thank my supervisor Assoc. Prof. Dr. Murude Çelikağ for her support in the preparation and help in various issues of this thesis, appreciate Assoc. Prof. Dr. Murude Çelikağ. Also I gratefully and sincerely acknowledge the invaluable advice, supervision expertise and encouragement of my co-supervisor, Asst. Prof. Dr. Habib Akbarzadeh Bengar. I would like to express my deepest gratitude to Prof. Dr. Metin Hüsem, Prof. Dr. Turan Özturan, Assoc. Prof. Dr. Giray Özay, Asst. Prof. Dr. Tülin Akçaoğlu and Assoc. Prof. Dr. Mehmet Cemal Geneş for accepting to be the jury members on my thesis defense.

I am very grateful to all academic staff of EMU Civil Engineering Department, who always supported me. Furthermore, I would like to thanks M. Nima Tazehzadeh who helped me for my thesis format.

A special thanks to my family. Words cannot express how grateful I am to my mother and father for all of the sacrifices that you've made on my behalf. Your prayer for me was what sustained me thus far. At the end I would like express appreciation to my beloved wife who spent sleepless nights with and was always my support in the moments when there was no one to answer my queries.

TABLE OF CONTENTS

LIST OF TABLES

LIST OF FIGURES

LIST OF ABBREVIATIONS

ACI	American Concrete Institute
ASTM	American Society for Testing and Materials
ANSI	American National Standard Institute
ASCE	American Society of Civil Engineers
AFRP	Aramid Fiber Reinforced Concrete
BFRP	Basalt Fiber Reinforced Concrete
BSI	British Standard Institute
CFRP	Carbon Fiber Reinforced Concrete
C	Circular
CSH	Calcium Silicate Hydrate
FRP	Fiber Reinforced Concrete
FDC	Fire Damaged Concrete
FM	Fineness Modulus
GFRP	Glass Fiber Reinforced Concrete
G-2	Grout II expander additive
ISO	International Organization for Standardization

LVDT	Linear Variable Displacement Transducer
M	Modified
P	Post heated
PVC	Poly Vinyl Chloride
RPC	Reactive Powder Concrete
RC	Reinforced Concrete
SMA	Shape Modification Alloy
S	Square
US	United State
UTM	Universal Testing Machine
U-S-O	Unheated Square without wrapping
U-C-O	Unheated Circular without wrapping
U-M-O	Unheated Modified without wrapping
WR	Wrapped

Chapter 1

INTRODUCTION

1.1 Background

The sustainability and durability of concrete buildings and infrastructures are very challenging issues in construction industries around the world. The preservation of the environment and conservation of natural resources have been some of the main concerns for the past decades. One of the most widely used building materials in the world is concrete. This popularity is because of its mechanical properties, durability, cost effectiveness and availability. The statistics showed that the annual average concrete production rate is around one ton per person based on the world population [1].

Concrete is known as a product of several components designed to reach the final specification. Its various components, including cement, coarse aggregate, fine aggregate, additives and water. The disadvantages of low tensile strength of concrete is why it has low ductility and high brittleness. To fix this steel bars are used in concrete [2]. Complete correlation and cohesion between concrete and steel is a major factor in the performance of a sample of reinforced concrete as a monolithic object. Bond failure mechanism is different for plain and ribbed bars. The ribbed bars are used to improve friction between steel and concrete.

On the other hand, the resistance of a concrete structure depends on the strength of materials from which it is made. Knowledge of material properties and behavior under load and environmental impact, is essential for understanding the performance of reinforced concrete structures. Mechanical properties of reinforced concrete elements under loading and environmental effects, such as, high temperature, is very important. One of the most devastating environmental impact for reinforced concrete structures, is exposure to high temperatures during a fire. Concrete and steel rebar have different reaction to heat and the behavior of the composite system for modeling the heat is difficult. The effects of high temperatures on the mechanical response of concrete have been investigated since the mid-twentieth century [3-6] to date.

The use of polymer composites in retrofitting reinforced concrete structures are widely grown in recent years. Maintaining composite action requires transfer of load between the concrete and steel. According to the growing concern on durability of concrete structures, fiber reinforced polymers (FRPs) have been used as an alternative to reinforcement [7].

These materials consist of fibers embedded in polymeric resin. There are different kinds of fibers and resins that are commonly used in FRPs. Glass FRP (GFRP), carbon FRP (CFRP) and aramid FRP (AFRP) are the examples of the most common FRP bars in the current global market of construction. Their lightweight, high tensile strength, non-corrosive nature, and non-conductivity are main advantages of this type of reinforcements. They can be produced with smooth surface, or with deformation like ribbed bars and surface treatments, such as, sand coated bars, in order to improve the FRP-concrete bond characteristics [8 and 9].

In recent years, many experimental studies and analytical methods were carried out for the performance of FRP for circular and square concrete columns at ambient temperature. But few studies on the impact of FRP-concrete columns exposed to high temperature were carried out and there is little research on the repair of RC columns subjected to high temperatures.

Many studies [10-15] have been carried out to investigate the bond behavior of FRP reinforced concretes. However, because of different types of commercially available CFRP and variation in their effective parameters, such as, type of fiber, fiber volume, type of resin, fiber orientation, rate of curing, and service temperature, a plenary model for predicting the bond strength has not been determined yet.

Previous studies on concrete exposed to high temperature the information bond behavior between steel reinforcement and concrete is less than the studies on mechanical properties. Bond behavior between steel and concrete is studied by using Pull-out test. Some studies linked with this type of work were carried out by Morley and Roles [16] Haddad and Shannis [17] Hadad et al. [18] Bingol and Gull [19]. The results reported indicates that the bond strength reduces significantly when the temperature rises.

1.2 Objectives of the Study

This thesis has two important objectives relating to the fire behavior of concrete structural elements strengthened with CFRP systems.

Objective 1: The primary objective is to investigate the effect of CFRP wrapping and the shape modification of the repair of fire-damaged concrete columns.

Objective 2: The secondary objective is to investigate the influence of CFRP confinement on the bond behaviour of steel bars embedded in concrete exposed to elevated temperatures.

Originality of the study is about investigation of reinforcing bars bond behaviour with concrete specimens exposed to temperature. In this thesis numerous variables were used in the experimental work as follows:

- Four different mix design
- Four different concrete compressive strength
- Six different temperatures
- Shape modification of square specimens
- Two different concrete cover of the reinforcement rebar
- Strengthening with and without CFRP wrapping
- Bond behaviour of heated and unheated specimens

Hence, as oppose to the past research, the above given variables were used to investigate concrete specimens with reinforcing bars, when exposed to fire.

1.3 Thesis Organization and Outline

This thesis is organized in 6 chapters.

Chapter 1 – Introduction: There is a brief introduction and overview on the effects of fire on concrete and retrofitting with modification and expansive cement. Furthermore, investigation of the bond behavior between steel rebar and concrete and the effects of carbon fiber reinforced polymer (CFRP).

Chapter 2 – Literature Review: This chapter presents a literature review of the fire behavior of concrete structural elements strengthened with CFRP systems and influence of CFRP confinement on bond behavior of steel bars embedded in concrete exposed to elevated temperatures. This chapter discusses the effect of different parameters on the bond behavior of steel bar and CFRP wrap on concrete after being exposed to fire. It highlights the gaps in the available literature on the compressive bond behavior of rebar in concrete and thereby, sets the research objectives.

Chapter 3 – Methodology: This chapter of thesis is about characteristics of materials and the laboratory test setup. The chapter describes the experimental procedure along with the results for fire behavior of concrete structural elements strengthened with CFRP systems and influence of CFRP confinement on bond behavior of steel bars embedded in concrete exposed to elevated temperatures.

Chapter 4 – Test results and discussion first part: In this chapter, the results of the first part of the study are presented. The results related to the effect of heat, retrofitting with expansive cement shape modification and CFRP sheets on the compressive strength of concrete were presented. The results obtained from sensitivity analysis has also been discussed.

Chapter 5 – Test results and discussion second part: This chapter present the results of the accomplished tests for specimens embedded with steel rebar and CFRP wrap and discuss the influence of different factors including compressive strength of concrete, concrete cover of rebar, amount of temperatures and CFRP wrapping on the bond strength between concrete and rebar. The results obtained from sensitivity analysis has been discussed in this chapter as well.

Chapter 6 – Conclusions: This chapter presents the conclusions derived from this study and provides recommendations for future research work.

Chapter 2

BACKGROUND INFORMATION AND LITERATURE REVIEW

2.1 Introduction

The following chapter presents an overview of CFRP sheet properties and fire behavior of concrete structural elements strengthened with CFRP systems and influence of CFRP confinement on bond behavior of steel bars embedded in concrete exposed to elevated temperatures.

Concrete is one of the most widely used structural material in the world. Concrete structures show good performance during a fire owing to the low thermal conductivity of concrete. Past experience of real fires indicates that it is rare for a reinforced concrete building to collapse as a result of a fire and the concrete structures that are severely damaged by fires can successfully be repaired [20]. The effect of temperature on the behavior of structures is inevitable to achieve the principle design criteria or retrofitting the fire. In fire damaged concrete structures, the knowledge of the residual properties of materials is required as a basis for the decision of reconstructing or repairing and for the economical design of the repair structure.

Many methods for repairing and strengthening of concrete structures after being exposed to fire, have been used in the past [21, 22]. Unfortunately, all previous traditional available techniques for repairing and strengthening of concrete structures

are associated with a time consuming and deafening process of removing and replacing the damaged materials with new and stronger materials. In recent years, fiber-reinforced polymer (FRP) has been recognized as a strengthening and repairing advanced technology especially in the speedy repair and strengthening measures for civil engineering subtractions all around the world. In this advanced technology, reinforced concrete columns can be easily and effectively being strengthened by wrapping layers of FRP around columns in existing conditions.

This chapter have a focus on some of the available background information and literature relevant to the current study are summarized as below.

2.2 Effects of Fire on Concrete Structures

Temperatures greater than 500°C are common in fires within concrete buildings [23-26]. In terms of structural performance under fire exposure, concrete structures generally accomplish very well primarily due to the concrete's low thermal conductance which results in the structure being increased in temperature at a slow rate during a fire. Experience from real fires shows that it is infrequent for a concrete building to collapse as a result of fire and most fire-damaged concrete structures can be reinstalled successfully. In fire damaged concrete structures, the knowledge of the residual properties of materials are required as a basis for the decision of its reinstatement.

The reduction in load-bearing capacity of the concrete structural members in fire depends on many factors [27-31]:

1) Variety and quality of reinforcement.
2) Type of aggregates.

3) Duration time and the severity of fire exposure.
4) Conditions of testing: the concrete is tested in hot conditions or after cooling down; it is extinguished with water or allowed to cool down slowly in the furnace or in open air before testing.
5) Conditions of the loading during heating regime of the specimens and whether the concrete specimens are restrained or unrestrained during heating.
6) The amount of dampness content present in the concrete specimens at the time of heating.
7) Shape and dimensions of the structural concrete member.
8) Concrete cover and other protection of the reinforcement.

The mechanical properties of concrete such as compressive strength, tensile strength, Poisson's ratio and modulus of elasticity are changeable after heating with different temperatures. These changes depend upon the peak temperature, the rate of heating and cooling, the fire duration, the type of concrete and kind of testing. Three kinds of test conditions, stressed, un-stressed, and un-stressed residual strength tests, have been used to investigate the performance of concrete structure after being exposed to fire [32]. In a stressed test condition, a load beforehand, normally in the range of 20 to 40 percent of the ultimate compressive strength at room temperature is applied to the concrete specimen prior to heating, and the load is maintained during the heating period. The specimen is heated continuously at a prescribed rate until a specified temperature is reached, and the temperature is maintained constant until a thermal stable state is achieved [32]. After reaching for uniform temperature, the load is then increased at a prescribed rate until the specimen fails. In the un-stressed test method, the specimen is heated without any loading at an assigned rate to the determinate

temperature and is maintained constant until a thermal steady state is achieved within the specimen. After reaching for the purpose temperature, the specimen is loaded at a prescribed rate until failure occurs. The stressed and un-stressed test methods were carried out to assess the properties of concrete at elevated temperature [32].

2.3 Residual Compressive Strength of Concrete

Concrete strength decreases with increase in temperature and there is further decrease on cooling probably because of additional micro cracking. When concrete cools down, the quicklime (calcium oxide) absorbs moisture and converts to slaked lime (calcium hydroxide). When this happens, disintegration of the affected concrete will occur [33]. Generally, the residual strength of concrete remains approximately in the range of 75% to 25% of the original strength when heated in the range of 300°C to 600°C respectively in most concrete structures [24-26, 33].

Many researchers investigated the effects of high temperatures on the compressive strength of concrete made with Ordinary Portland Cement tested at elevated temperatures and after cooling. Hertz [28] investigated the behaviour of siliceous, limestone, granite, sea gravel, pumice and expanded clay aggregate concrete at elevated temperatures and after cooling down. It was found that the relative residual compressive strength of heated siliceous concrete was about 20% smaller than the hot strength for temperatures above 400°C. Hertz [28] also investigated the behaviour of the granite, basalt, limestone, and sea gravel, which belongs to a group of aggregates that has lower thermal expansion and suffers less damage than siliceous aggregate concrete during fire. It was found that the reduction in compressive strength and the standard deviation for this reduction was nearly the same for granite, basalt, limestone, and sea gravel. The concretes made of aggregates (granite, basalt, limestone, and sea

gravel) were tested considering one group called the main group by Hertz [28]. It was observed that the main group aggregate concrete showed higher compressive strength values than siliceous aggregate concrete after cooling. It was also confirmed by Abrams [34] that, at temperatures above about 430°C, siliceous aggregate concrete lost a greater proportion of its strength than concretes made with limestone or lightweight aggregates but when the temperature reached approximately 800°C the difference disappeared [35].

Lankard et al. [36] reported the results of compressive strength tests carried out on two concretes made with gravel aggregates and with limestone aggregate, at temperatures up to 260°C. The results demonstrated that limestone and gravel aggregate concretes behaved similarly when heated up to 260°C. The unsealed unstressed gravel aggregate concrete showed higher compressive strength than sealed unstressed gravel aggregate concrete when tested in both the hot and cold conditions. For both unsealed gravel and limestone aggregate concretes, there was an increase in the hot and cold strengths after heating at about 80°C and 120°C respectively. Specimens heated to above 190°C and cooled to room temperature before testing generally showed losses of strength in the range of 10% to 20%.

Kaplan et al. [37] conducted tests on unsealed concrete specimens made with siliceous aggregates and reported that for temperatures below 150°C the strength after cooling was greater than that tested while hot, whereas for temperatures above 150°C the hot specimens were stronger than cooled ones. The compressive strength of specimens tested at 400°C while hot was up to 20% less than the values of original unheated specimens, whereas after cooling to room temperature the specimens showed up to 40% reduction in compressive strength.

Khoury et al. [38] reported the results of compressive strengths of concrete made with limestone, basalt, siliceous and light weight aggregates. It was observed that after heating to 600°C, the residual strengths of the unstressed specimens were about 20, 30, and 40% for limestone, lightweight, and basalt aggregate respectively. It was found that the siliceous gravel aggregate concrete at 600°C was so badly damaged and it could not be tested.

Harada et al. [39] investigated the compressive strength, elasticity and thermal properties of concrete during and after heating at various temperatures. The results showed that the residual compressive strengths of concrete were 80%, 75% and 60% of the original value at 100°C, 300°C, and 450°C respectively. The findings of Harada [39] were very close to Abrams [34].

Purkiss [40] reported the results of the variation of residual compressive strength of concrete with temperature. It was found that the percentage loss in compressive strength of concrete quoted by Purkiss [40] was lower when compared to Malhotra [29] and Abrams [34].

The Concrete Society TR15 [23] suggested a strength reduction curve based on the research of unstressed residual strength of concrete, as shown in Figure 2.1.

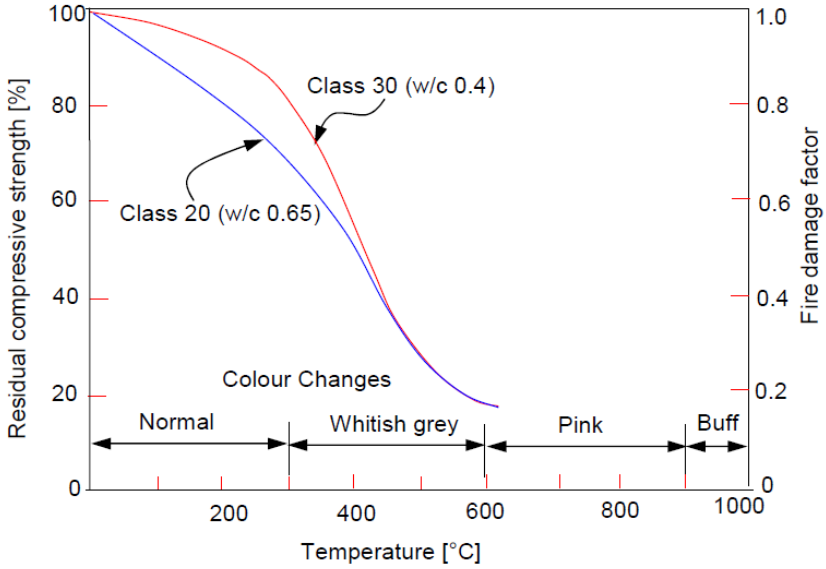

Figure 2.1: Residual strength of heated un-stressed dense aggregate concrete after cooling [23]

It has been found that the strength of the loaded specimens is generally higher than those of unloaded specimens during heating [28, 34]. Therefore, the unstressed residual strength test is considered more conservative for assessing the post-fire or residual properties of concrete [28, 32, 34 and 40]. In reality, all concrete structures would be stressed, at least under dead load, at the time of heating. Therefore, the Concrete Society had made some modifications in the TR33 report [24] and proposed the strength reduction curve shown in Figure 2.2 based on the residual strength of heated stressed concrete after cooling.

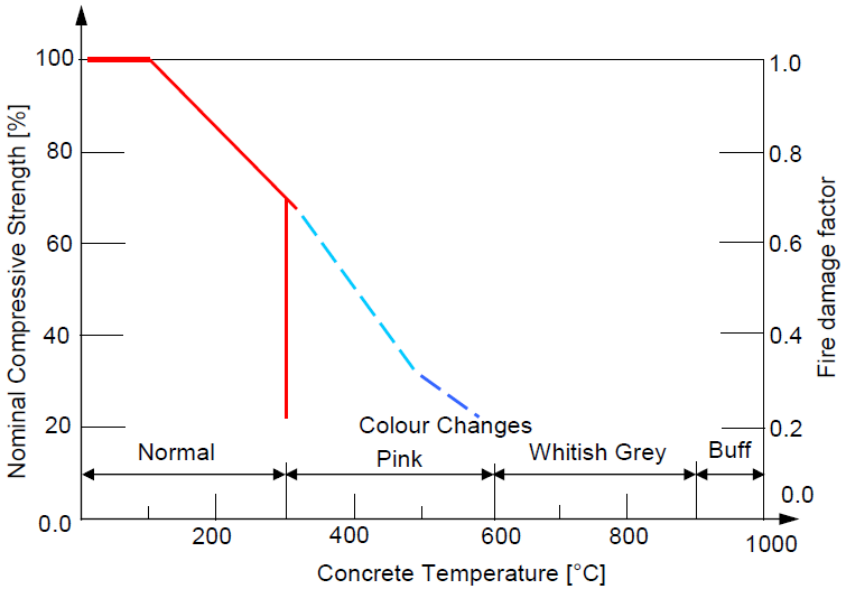

Figure 2.2: Residual strength of heated stressed dense aggregate concrete after cooling [24]

Recently, the Concrete Society published a report TR68 [21] in which it is assumed that the concrete heated to above 300°C has lost all of its strength. It has been found that the normal grey colour of Ordinary Portland Cement Concrete turns to light pink at around 300°C [41]. Therefore, the 300°C temperature is considered as the boundary for the pink colour and it identifies the limit of damaged concrete. Since the change of colour is not evident for all types of aggregates. Therefore, the concrete exposed to more than 300°C should be removed prior to repairing. For the sake of assessment of fire damaged concrete structure on the safer side, the Concrete Society TR68 [21] assumed the zero strength of concrete above 300°C (Figure 2.3). It is worth mentioning here that the colour changes shown in Figures 2.1 to 2.2 are applicable for siliceous aggregate and may not be applicable for calcareous or crushed flint aggregate. Marchant [22] reported that concrete retains 50% of its compressive strength after being exposed to 500°C temperature (Figure 2.4).

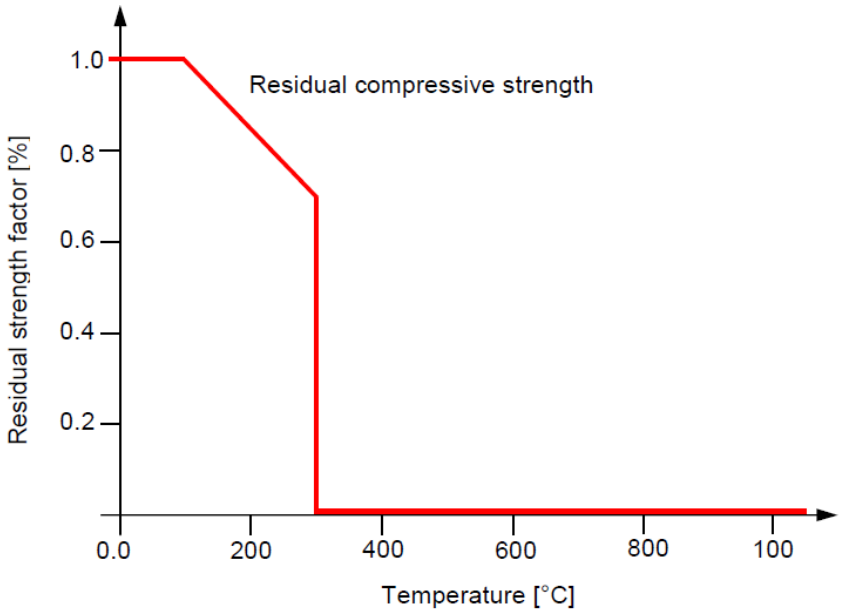

Figure 2.3: Residual compressive strength of concrete after cooling [21]

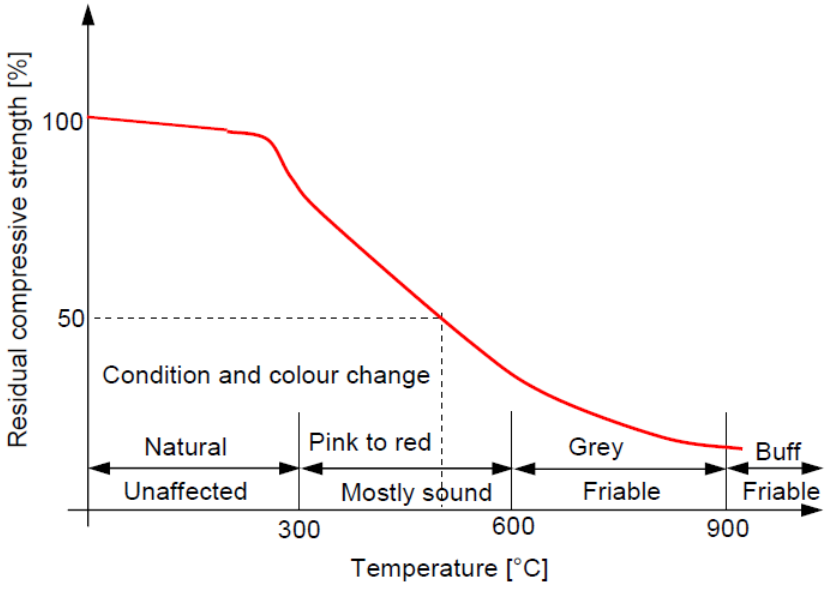

Figure 2.4: Residual compressive strength of concrete after cooling [22]

2.4 Effect of Shape and Size of Specimens on the Compressive Strength of Concrete

The shape and size of the specimens may affect the compressive strength of Portland Cement Concrete at high temperatures [42]. The temperature at the center of the larger size specimen will be lower than those of smaller size specimens due to the delay of

the heat transfer. Consequently, the loss of strength would be higher in the smaller size concrete specimen than in the larger size specimens when exposed to same fire duration [42-44]. However, the effect of specimen size on the retained compressive strength of concrete is not manifested when heated uniformly [45].

2.5 Effect of Long Term Exposure to High Temperature on the Compressive Strength of Concrete

The longer the period of exposure to high temperatures, the greater would be the deterioration in compressive strength due to crack generation and material decay. Most of the reduction occurs within the first 30 days of long term exposure [35, 36, 39, 46-50]. The residual strengths after one hour of exposure at 200, 400, 600 and 800°C were about 80, 70, 60, and 30%, respectively, while the residual strengths after 2 hours or more exposure were found to be about 70, 60, 45, and 25% [50]. At 300°C, residual compressive strength of about 65% was found after two days and 50% at the end of four months [49].

2.6 Effect of Temperature on the Modulus of Elasticity of Concrete

In the evaluation of deformation of fire-damaged concrete structures, it is important to consider the effect of temperature on the elastic modulus of the concrete since concrete is softening with increasing temperature [51]. Concrete is normally made of carbonate, siliceous and lightweight aggregates. In all the three concretes, the modulus of elasticity is affected by the temperature increase [27]. The type of aggregates had a significant effect on the elastic modulus with increasing temperature [27]. The modulus of elasticity of the high strength concrete is decreased by 5 to10 % when exposed to temperatures in the range of 100 to 300°C. At 800°C, the modulus of elasticity was only 20 to 25% of the value at room temperature [52]. The rate of heating affects the elastic modulus and compressive strength in a similar manner. The faster

the heating, the lower would be the elastic modulus due to higher thermal stresses, higher pore pressure, higher stresses from thermal shrinkage, and greater damage to the microstructure [53-56].

For the siliceous aggregate concrete heated to 400°C, the value of elastic modulus after cooling was the same as that prevailing at the highest temperature [54]. The same finding was quoted by Harada [53] that the value of residual elastic modulus (after cooling) showed a similar drop with maximum temperature. This indicated that the elastic modulus experiences a permanent reduction in its value [49] due to the change of microstructure and bonding with increase in temperature. The reduction in elastic modulus is more than that in the compressive strength when exposed to fire [51]. The original strength has no significant effect on the elastic modulus after heating to various temperatures [51]. It was found that the values of elastic modulus at 200°C 400°C, and 600°C were about 80%, 40% and 6% of the original unheated value, respectively [51].

2.7 Fiber Reinforce Polymer Composites

2.7.1 Introduction to FRP Composites

Fiber Reinforce Polymer (FRP) composites have been used externally for reinforcing concrete structures since the mid-1980s. The number of projects that have been used with FRPs composites around the world has grown dramatically for the last ten years. Structural members reinforced with these composites include beams, slabs, columns, walls, joints and structures such as furnaces and chimneys, arches, domes, tunnels, silos, pipes and trusses. The various shapes and types of fiber reinforced polymers are shown in Figure 2.5.

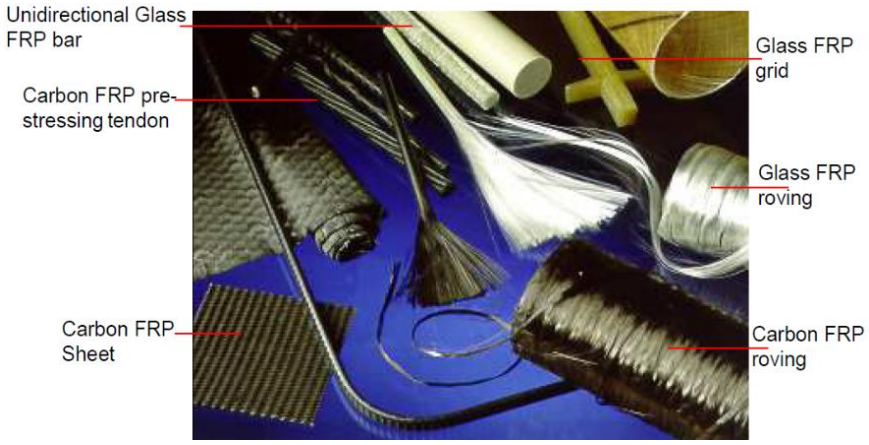

Figure 2.5: Various shapes and types of FRP [57]

2.7.2 Advantages of Using FRP Composites for Strengthening

The main advantage of FRP materials is its high strength to lightweight and high corrosion resistance. Their high strength, while having a low weight, makes it easier to transport and the cost of using them is reduced. Also, the high strength of fiber reinforce polymer composite to corrosion increases their durability. FRP plates have at least twice the resistance of steel plates [57-61].

2.7.3 Classification of FRP Composite Materials

The composites consist of two components: fibers and matrix. There are more types of fibers dominating civil engineering structures:

1- Carbon Fiber Reinforce Polymer (CFRP)

2- Glass Fiber Reinforce Polymer (GFRP)

3- Aramid Fiber Reinforce Polymer (AFRP)

4- Basalt Fiber Reinforce Polymer (BFRP)

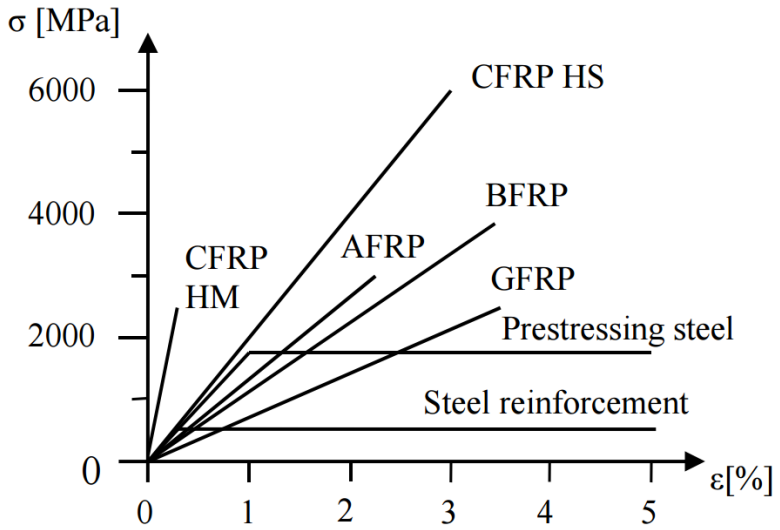

Figure 2.6: Stress-strain diagram for the steel and FRP materials [62]

2.7.3.1 Carbon Fiber Reinforce Polymer (CFRP)

Carbon fibers are anisotropic in nature (Figure 2.7) and it is produced at 1300ºC. High strength, excellent creep level, resistance to chemical effects, low conductivity, low density and high elastic modulus are the advantages of carbon fibers. The weak sides of carbon fibers are being expensive and anisotropic materials with low compressive strength [58].

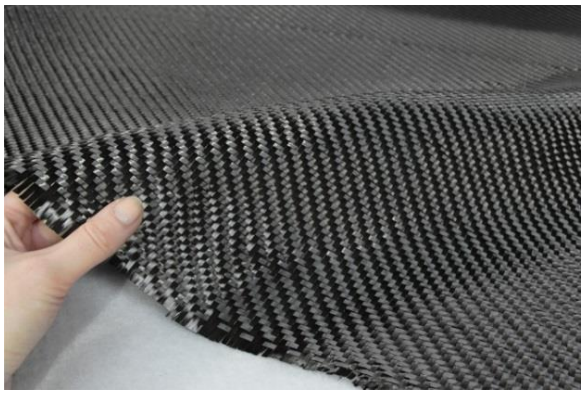
Figure 2.7: Carbon Fiber Reinforce Polymer (CFRP) sheet

2.7.3.2 Glass Fiber Reinforce Polymer (GFRP)

Glass fibers, typical form shown in Figure 2.8, are isotropic in nature and most widely used filament. Common types of glass fibers are E-Glass, S-Glass and C-Glass. The

characteristic properties of glass fibers are high strength, low cost with good water resistance and resistance to chemicals [58].

Figure 2.8: Glass Fiber Reinforce Polymer (GFRP) sheet [62]

2.7.3.3 Aramid Fiber Reinforce Polymer (AFRP)

Aramid fibers widespread known as a Kevlar fiber in the markets as shown in Figure 2.9. The structure of Aramid fiber is anisotropic in nature and usually yellow in colors. Aramid fibers are more expensive than glass moderate stiffness, good in tension applications (Cables and tendons) but lower strength in compression. Aramids have high tensile strength, high stiffness, high modulus and low weigh and density [58].

Figure 2.9: Aramid Fiber Reinforce Polymer (AFRP) sheet [62]

2.7.3.4 Basalt Fiber Reinforce Polymer (BFRP)

Basalt is a type of igneous rock formed by the rapid cooling of lava at the surface of the planet. The production of the basalt and the glass fibers is similar. Compared to FRPs made from carbon, glass and aramid fiber, its use in the civil infrastructure market is very low [58].

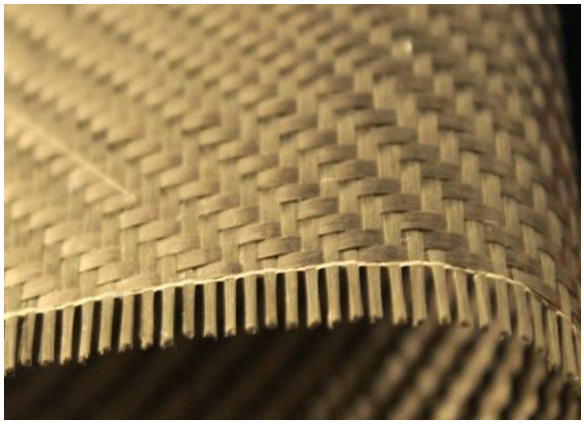

Figure 2.10: Basalt Fiber Reinforce Polymer (BFRP) sheet [62]

In this thesis, Carbon Fiber Reinforce Polymer (CFRP) is used for strengthening specimens.

2.8 Research Carried Out on Strengthening of Fire Damaged Concrete with Expansive Cement and CFRP Wrap

Concrete structures show good performance during a fire owing to the low thermal conductivity of concrete. Past experience of real fires indicates that it is rare for a reinforced concrete building to collapse as a result of a fire and the concrete structures that are severely damaged by fires can successfully be repaired [20].

Once a reinforced concrete (RC) structure gets heated up, changes in some mechanical properties and the deformation caused by heating would lead to a reduction in compressive strength of the concrete and a change in stress-strain response both during

heating and cooling time. The residual strength of RC structure after being exposed to fire is somewhat less than its capacity before heating even if the damage is not observable [63, 64]. These changes will bring a breakdown in the structure of concrete, affecting its mechanical properties. Therefore, concrete members without visible damage may have reduced strength due to elevated temperatures. The decision for repairing or demolishing of a structure should be based on economic considerations, such as direct costs and time.

Compressive strength of concrete at an elevated temperature is of primary interest in fire resistance design. Compressive strength of concrete at ambient temperature depends upon water-cement ratio, aggregate-paste interface transition zone, curing conditions, type and size of aggregate, type of admixture and type of stress [65]. At high temperature, compressive strength is highly influenced by room temperature strength, rate of heating, and binders in batch mix (such as silica fume, fly ash, and slag). Over the years, numerous studies have examined the effect of high temperature on mechanical properties and compressive strength of concrete [66-72].

In previous studies, various kinds of materials for external covering of concrete, such as, Shape Memory Alloy (SMA) wires [73, 78], steel wrapping plates [79], and Carbon Fiber Reinforced Polymer (CFRP) sheets [80], were used to increase the strength. The use of CFRP wrap for strengthening RC is widely used and there has been growing number of studies to evaluate the fire performance of such applications [81, 82].

Repairing and strengthening of the RC structures have become more common in the past decade due to increased knowledge and confidence in the use of CFRP. There is

many research for retrofitting design with CFRP to increase the load capacity of concrete members at ambient temperature [79-88].

One of the simple and fast methods for repairing reinforced concrete columns is the use of CFRP wrapping. In recent years CFRP wrap is used by prominent researchers for repairing, reinforcing and strengthening of concrete column [89-92]. However, until now only few studies have been carried out to investigate the reinforced concrete structures damaged by fire and using CFRP for their repair [93-97].

According to Karbhari and Gao externally bonded CFRP composite jackets could have a significant effect on the confinement of the concrete columns with circular section [98]. The study carried out by Rochette and Labossière indicated that CFRP confinement is relatively less effective in increasing the compressive strength of columns with square and rectangular sections as opposed to columns with circular sections [99]. The square and rectangular columns were largely remained unconfined and the CFRP jackets were only effective along the two diagonals of the cross-section. The presence of internal bars could limit the ability of rounding the corners of square and rectangular columns. The lack of confinement in these columns affects the softening behavior and causes premature rupture in CFRP, so the inherent capacity of CFRP is not used [100]. One possible method of improving the effect of CFPR jackets on square and rectangular columns is to make shape modification of the cross-section into an elliptical, oval, or circular section [100, 101]; and Experiments indicate that the elliptical sections provide supreme performance compared to confined rectangular columns. It should be mentioned that one way to do this improvement is the use of non-shrinkable cement concrete in the annular gap space. Then the formworks of non-shrinkable concrete are removed and the section is wrapped with CFRP jackets. There

are few studies in the literature regarding the use of an expansive factor in the gap between column and CFRP jacket to reach active confinement [101-103].

Nevertheless, there is no specimens in the literature in which the shape of a fire-damaged concrete sample has been modified using an expansive agent and actively confined with CFRP shells.

2.9 Research Carried Out on Influence of CFRP Confinement on Bond Behaviour of Steel Deformed Dar Embedded in Concrete Exposed to High Temperature

Knowledge of the properties of materials and behaviour under the influence of load and environmental effects is fundamental to understanding the performance of the RC structures. Determining the mechanical properties of reinforced concrete elements is very important under environmental impacts such as high temperatures when exposed to load [104]. Fire occurs in the building for various reasons often due to human and natural factors [105]. Exposure to high temperatures during a fire is one of the most devastating environmental impacts for RC structures. Concrete and steel, each have a particular reaction to heat and it is difficult to model the behavior of the reinforced concrete composite system after being subjected to heat [104]. When a reinforced concrete (RC) element is exposed to high temperatures, some physical and chemical changes will occur mainly in concrete. The effects of high temperatures on the mechanical response of concrete have been investigated since the mid-twentieth century [106-109] and continued to this day. Previous research can be separated into two: material testing and element testing. The results of the material tests provide information on the effects of temperature on the mechanical properties of the concrete (such as, compressive and tensile strength, modulus of elasticity). While the test results

of elements were used to evaluate the heat resistance of RC elements (such as, beams columns and slabs). It has been reported that changes in mechanical properties due to heat may vary depending on the parameters like the chemical and physical properties of concrete compounds, the thermal temperature of concrete structures exposed to it, the size of concrete structures, and also the exerted external loads and cooling conditions of structural members [110-119]. Previous studies on the strength of bonding between reinforcement and concrete are less frequent than studies on the mechanical properties of concrete subjected to high temperatures. Concrete bonding behaviour is investigated using pull-out tests examples. The variations in the bond strength between the reinforcing arm and the concrete with change in temperature vary with different parameters. For this reason, it's very difficult to find a direct relationship between the increase in temperature and the residual bond strength. In fact, it is very useful for engineers to find a relationship that involves the effects of different parameters together to assess the strength of existing buildings exposed to fire. The bond failure between steel and concrete bars occurs in two ways: splitting or sliding. If the concrete coating is high or the concrete is well enclosed the existing deflection failure takes place by pulling out the concrete or by breaking the concrete keys between the reinforcement tents. On the other hand, if the concrete coating is relatively small or the medium is enclosed in concrete or the steel bars are in close proximity the tensile splitting cracks around the concrete will expand leading to a continuity failure before splitting the concrete keys between the treads [120-123].

For most reinforced concrete structures, the failure of the conjunction occurs in a splitting mode. Examples of critical areas of reinforced concrete structures that are prone to joint failure especially under seismic loading are: Bridge foundation, column

connection to the roof slab in reinforced concrete buildings [124] (the base of bridge piers or the junction of columns and floor slabs in a concrete building where the reinforcement is spliced with starter bars for reinforcement continuity and case of construction). Some related studies have been reported by Pothisiri and Panedpojman [106], Kodur and Agrawal [126], Abdallah et al [127] Gul and Bingol [128]. According to the results reported by them as the temperature rises the consistency resistance is significantly lost. The findings of these studies indicate that the residual continuity resistance varies between 30% and 70% depending on the factors studied, such as the temperature, the properties of the concrete and the reinforcement, the diameter and embedment length of the reinforcement, the amount of concrete cover and the heating and cooling regime [125-128]. The pull-out failure mode provides more versatile resistance and behaviour than fracture failure [129-130]. Therefore, in areas where fracture failure is expected to occur, it is necessary to change the fission to the outflow by using external jackets. In previous studies various types of materials for external coatings have been used to increase bond strength between rebar and concrete, such as, SMA wires (shape memory alloy) [131 and 132] FRP sheets. Also the use of external FRP jackets for seismic reinforcement in areas with joint formation potential in reinforced concrete columns which are located at low distance reinforcing steel bars is very effective and delayed the failure of split fusion and resulting in improved seismic performance in the area [132- 139].

Chapter 3

METHODOLOGY (CHARACTERISTICS OF MATERIALS AND LABORATORY TEST SETUP)

3.1 Introduction

In order to obtain concrete with the desired characteristics and performance the first step is to select the components of the material; the next step is the process known as mixing ratio by which the correct combination of concrete components is obtained although there are some methods for determining mixing ratio. Determining the ratio of concrete mixtures also known as mixing ratios or concrete mix designs is the process by which the correct combination of cement, aggregate and water can be obtained to produce concrete according to the specifications given. According to reasons prepared below although it need scientific basis, it can be seen as an art, too.

One of the objectives of determining the mixture ratio is to obtain a product that meets the requirements of the predetermined requirements. The most important of these needs are the performance of new concrete and the strength of hardened concrete at a certain age. Another goal is to determine the mixture ratio to obtain a concrete mix that will meet required performance at the lowest possible cost; this includes decision making on materials that are not only suitable but also affordable.

Engineers have limited tools to achieve these goals. This is due to the fact that the required properties of concrete can be affected by changing a given variable with

another variable. For example, adding water to a concrete mixture with a given amount of cement improves the flow ability of fresh concrete but at the same time reduces its strength. In fact, the performance of the concrete consists of two main components: the fluency (ease of flowing) and adhesion (resistance to separation) both of these two components tend to counteract to each other when water is added to the concrete mixture. Therefore, the process of mixing up improves to the art of balancing various opposing things as described above. For building materials of concrete with specified characteristics and for specified working conditions (i.e. specific design and concrete transfer equipment) the variables under the control of mixing are usually as follows: The ratio of cement paste to aggregates in the mixture, the ratio of water to cement in the cement paste, the proportion of sand to the large aggregate in aggregates, and the use of its excess and its amount.

The reaction of the structure in an event depends on several factors such as the characteristics of the underlying soil, structural properties and structural qualities. In many cases, concrete structures do not respond elastically to the events occur during their life time. Under loading, stress in a structural member may lead to a brittle response in the absence of adequate reinforcement. After this step, the remained strength needs to be sufficient in order to ensure that the structure remains stable against the subsequent severe loading conditions that may be due to an earthquake and large deformations [135].

Analysis is a tool used by engineers to achieve the ultimate design of the structure. The good analytical tool predicts the structural reliability and compares its performance with the criteria adopted in the design [136]. This study is limited to construction materials. This section describes the materials used in the construction of the concrete

as well as the details of the experiments carried out to evaluate the physical and mechanical properties of the concrete.

The main aim of this research is divided into two parts:

1) Investigating the compressive behavior of concrete damaged by heat and the impact of the CFRP wrappers on this behaviour.
2) The investigation of the bonding behavior between steel bar and concrete for fire exposed reinforced concrete members and also the effect of using CFRP wrappers on bond strength.

The experiments carried out are divided into two sections: fresh concrete and hardened concrete tests. The main test of concrete was the slump test. Concrete's hardness properties tests included: compressive strength determination of stress -strain behavior and bonding strength of steel bar in concrete.

3.2 Materials Used

3.2.1 Aggregates

The aggregates used in concrete generally consist of coarse aggregate (gravel) and fine aggregate (sand) aggregates. Gravel as coarse aggregate plays a very important role in bearing loads on concrete. Therefore, applying aggregate with higher resistance, such as, granite aggregate has a significant effect on the strength of concrete. Sand is also used as a fine-grained material to fill the gap between coarse aggregate. The aggregation test is used to determine the distribution of the size of the aggregate, which is carried out via separation by bolter based on ACI 211 standard ASTM C33 [140].

There are many reasons to determine the extent of aggregation and the maximum size of aggregates used in concrete. Aggregating and maximum aggregate size, in addition

to affecting the aggregate composition ratio, affect cement and water requirements, efficiency, pumping capacity, cost effectiveness, porosity, concentration and durability of concrete. Aggregate changes can seriously affect the uniformity of concrete. In general, aggregates with a continuous aggregation curve yield the most satisfactory results so that some of the aggregate sizes are not very small or very large. In this study an ACI 211 [140] has been used to obtain concrete mix design. This study uses three weight, volumetric and quick methods to achieve the desired concrete mixture. It should be noted that most concrete mix design methods are based on the properties of the materials that are available in each region or country and their application in another region will not be sufficiently precise.

The US regulation or ACI 211 has the advantages that in the final stages of design by constructing a laboratory specimen and performing a few simple tests on this specimen the results of the previous steps are corrected and involved the effect of the special properties of the materials of each area in the design results appropriately. Therefore, the rules of procedure in different regions will result more precisely. According to this regulation, sand and gravel used materials must be within the scope of ASTM C33 (C33Committee is one of the ASTM Institute committees that are investigating the properties of sand and gravel [138]).

3.2.1.1 Sand and Fineness Modulus (FM)

The fineness modulus is an indicator for the use of aggregates in concrete so that the fineness modulus for a given aggregate is much larger, the aggregate will be thicker. It should be noted that the fineness modulus does not provide any information on how the aggregate size is distributed so that different aggregate may have the same fineness

modulus. The fineness modulus of fine aggregate is useful in estimating the fine or coarse aggregate ratios in concrete mixtures.

In accordance with the ASTM C-125 standard (Standard Terminology Relating to Concrete and Concrete Aggregates), the fineness modulus of fine or coarse aggregates is obtained by collecting the weight of the cumulative percentages retained on each sieve in a specific group of sieve and dividing to 100. It was shown in equation (3.1). According to the standard, the fineness modulus for fine aggregates should not be less than 2.3 or more than 3.1.

$$\text{F.M}= \frac{\sum(\text{cumulative percentages retained on specified sieves})}{100} \qquad (3.1)$$

In order to make experimental specimens, washed sand was used with a fineness modulus of 3.19. The specific density of the used sand was equal to 2.64 and its unit weight was 1400 kg/m^3. In Figure 3.1 the gravel and sand curve and ASTM standard aggregation are plotted. Meanwhile in this research a vibrational device was used to sieve aggregates.

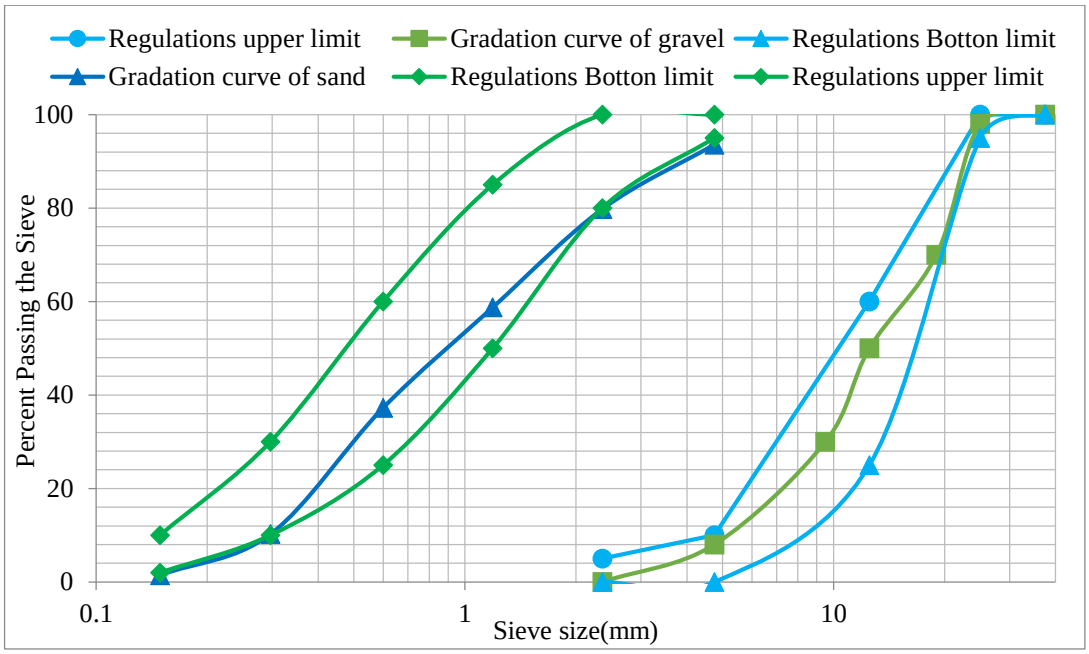

Figure 3.1: Gradation curve of fine and coarse aggregates

3.2.1.2 Gravel

The gravel used in the concrete construction was broken type with a maximum size of 19.5 mm. In addition, the specific gravity used was 2.68. The sand gradation curve is also presented in Figure 3.1 with standard limits.

3.2.2 Cement

The cement used is Portland cement type II. The density of the cement is equal to 3.15 and the physical and chemical properties of this cement were presented in Tables 3.1 and 3.2, respectively.

Table 3.1: Mechanical properties of type II cements [138]

Physical Properties of Used Cement	
Initial setting time	100 minutes
Final setting time	180 minutes
3-day strength	220N/mm2
7-daystrength	390N/mm2
28-daystrength	520N/mm2

Table 3.2: Chemical properties of type II cements [138]

Chemical mixture	Percentage	Chemical mixture	Percentage
SiO_2	21.25	CaO	64.07
Al_2O_3	4.95	MgO	1.20
Fe_2O_3	3.19	SO_3	2.04
K_2O	0.63	Na_2O	0.38

3.2.3 G-2 Expander Additive

Typically, shrinkage is occurred after flash set of concrete. In order to prevent this phenomenon, G-2 expander additive can be used in cases where concrete condensation causes problem. If added to the concrete during preparation reduces the proportion of water to cement, prevents loss of water from concrete, increases the mechanical strength, prevents concrete contraction and increases the strength. The use of this additive is recommended for the construction of resistant cement mortars, the foundation of heavy machinery, cranes, the foundation of heavy metal structures, and other similar structures.

The benefits of using this material include the following:

- Preventing the natural contraction of concrete
- Reducing the water to cement ratio
- Increasing mechanical resistance
- Preventing loss of water from concrete
- Consistency of concrete

Depending on the amount of expansion needed and the required strength and concrete gradation, the amount of additive added during the preparation of the mortar is 0.5% to 1.5% of the weight of cement used. Technical specifications are in accordance with Table 3.3.

Table 3.3: Technical Specifications of G-2

Physical state	Powder
Color	Light grey
Unit gravity	1.2gr/cm^3
Chlorine ion	No
Time and storage	Up to one year in indoor and dry environment
Standard	BS 8110 part 1

3.2.4 Steel Bars

For the production of pull out specimens with 20mm diameter reinforcement was used. Yield strength, ultimate strength and elastic modulus of steel bar were 374 MPa, 571 MPa and 210 GPa, respectively.

3.2.5 CFRP Sheets and Epoxy Resin

Composite shells used in this study were unidirectional carbon fiber reinforced polymer (quantum wrap 200c) (Figure 3.2). The material properties of CFRP sheets (from manufactures data) are presented in Table 3.4.

Table 3.4: Material properties for CFRP

Properties	**Value**
Thickness	0.11 mm
Density	1.76 gr/ cm^3
Tensile strength	3530 MPa
Tensile modulus	230 GPa
Strain	1.5%
Filament diameter	7 μm

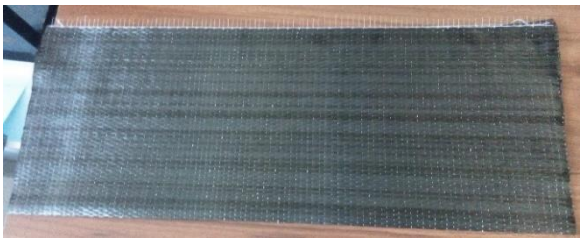

Figure 3.2: The CFRP sheets used in experiments

For the installation of CFRP sheets on concrete specimens an epoxy resin of Sikadur 330 type has been used which has a density of 1.3 gr/cm^3. Details of the adhesive are given in the Table 3.5.

Table 3.5: Material properties for epoxy resin (at 23°C)

Properties	**value**
Chemical base	Epoxy resin
Density	1300 Kg/m3
Viscosity	6000 mPas
Tensile strength	30 MPa
Elastic modulus (flexural)	3.8 GPa
Elastic modulus (tensile)	4.5 GPa
Elongation at break	0.9 %

3.3 Mix Design

Concrete mix design used in this study is in accordance with ACI 211-89. Due to the wide range of specimens required the content was divided into two parts. In the first part the effect of heat and strengthening with CFRP wrap on the compressive strength was studied. In the second part, the effect of heat on the bonding strength of concrete, concrete cover, concrete compressive strength and the impact of CFRP wrap on the bond strength parameter.

To achieve the goal in the first part, two types of concrete were used. The details of concrete designs are given in Table 3.6. The C1 design is for the production of specimens and the C2 design is an expanding concrete and it is used for the shape modification of the specimens. In the second part, two types of concrete (C30 and C40) were used and these concrete have two different compressive strengths as detailed of in Table 3.6.

Table 3.6: Details of the concrete mix design samples

Concrete Mixture	Kg/m^3				
	Gravel	**Sand**	**Cement**	**Water**	**G-2 (%)**
C1	1100	815	400	200	-
C2	1100	815	430	200	4.3
C30	1040	805	320	193	-
C40	1040	600	500	210	-

3.4 Construction of Concrete Specimens

To build the specimens, first of all, different proportions of the concrete mixing materials were determined for a certain amount of concrete. According to the experience in laboratory, before mixing the materials in the mixer, first water was added water in the mixer and the mixer was allowed to spin with water for several seconds so that the friction of the material, was reduced and the mixer body would prevent excess water being added to the cement material.

First of all, gravel and sand were mixed with a portion of water (of the water for mix design) which lasted for up to three minutes for pre-wetting of aggregates. Then the cement is added to the mixture and then the remaining water is added to the mixture. After this step, the fresh concrete tests were performed immediately after for each mix design.

Figure 3.3: Mixing of the materials for build the concrete by mixer

Then the concrete was poured into pre-prepared and lubricated molds and covered with wet sack for the better curing of specimens.

Figure 3.4: The concrete molding

Specimens were placed in laboratory for 24 hours to harden. After 24 hours, the specimens were removed from the molds and stored in a water pool.

3.5 Experiments to Determine the Characteristics of Fresh Concrete

Fresh concrete is having a liquidity or plasticity. But the most important issue is its workability. For the acceptability of concrete workability, it should:

- easily be mixed and transported.
- be uniform throughout a given batch and between batches.
- have the right consistency so that it can completely fill the concrete formworks for which it was designed.
- have the ability to be compacted without excessive loss of energy.
- not segregate during placing and consolidation.
- have good finishing characteristics.

The standard test used to determine the degree of workability is the slump test. In this test, an incomplete cone with a height of 30 cm is used (Figure 3.5).

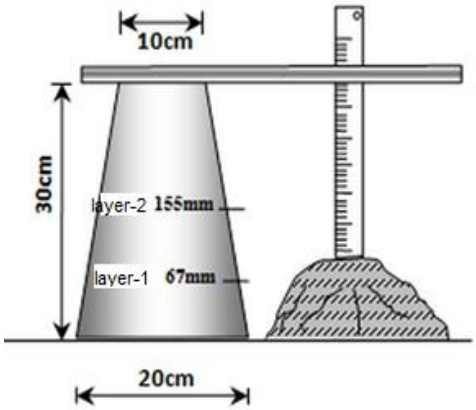

Figure 3.5: Abraham's incomplete cone for the Slump test

To test, fresh concrete is placed in three layers in the cone and vibrates. Then the top surface is flatted and the cone is moved upwards. The slump of the concrete is measured by measuring the distance from the top of the slumped concrete to the level of the top of the slump cone. The slumped concrete takes various shapes and according to the profile of slumped concrete, the slump is termed as true slump, shear slump or collapse slump. If a shear or collapse slump is achieved, a fresh sample should be taken and the test repeated. A collapsed slump is an indication that the mix is too wet. Only

a true slump is of any use in the test. A collapsed slump will generally mean that the mix is too wet or that it has a high workability mix, in which case the slump test is not appropriate. Very dry mixes having slump 0 – 25 mm are typically used in road making. Low workability mixes having slump 10 – 40 mm are typically used for foundations with light reinforcement. Medium workability mixes with slump 50 – 90 mm, are typically used for normal reinforced concrete placed with vibration. High workability concrete with slump > 100 mm is typically used where reinforcement has tight spacing, and/or the concrete has to flow a great distance. The slump used in this study was 8 centimeters.

3.6 Examination of Specimens

The main goal of the experiments in the first section of this study is to investigate the effect of CFRP wrapping and the shape modification on the repair of fire-damaged concrete columns. All specimens at the time of construction had the same cross sectional size; prismatic sections were 100 mm×100 mm and the ones with circular cross section had diameter of 150 mm. The height of all specimens were 300 mm.

The specimens were tested under the following conditions:

- Un-heated specimens
- Post- heated specimens without spalling
- Post- heated specimens without any spalling wrapped with carbon fiber reinforced polymer (CFRP) jacket
- Post- heated specimens repaired and shape modified with expansive cement concrete
- Post- heated specimens repaired with both expansive cement concrete and CFRP

The modeled specimens were given unique names. These names are formed of three parts. The first part indicates whether the specimen was un-heated (U) or post-heated (P). The second part is related to the cross section and shape modification. The square specimens without shape modification (S), the circular specimens without shape modification (C), and the shape-modified specimens (M). Furthermore, the third part represents the strengthening with CFRP. Hence, the specimens strengthened with CFRP wrapping (WR), and specimens without strengthening (O). The details of tested specimens are shown in Table 3.7.

Table 3.7: Details of tested specimens

Specimen ID	Original cross section (mm)		Modified cross section (circular) (d)	Area increase (%)	Heating	Wrapping
	Circular (d)	Square (a)				
U-S-O	-	100	-	-	-	-
P-S-O	-	100	-	-	✓	-
U-S-WR	-	100	-	-	-	✓
P-S-WR	-	100	-	-	✓	✓
U-C-O	150	-	-	-	-	-
P-C-O	150	-	-	-	✓	-
U-C-WR	150	-	-	-	-	✓
P-C-WR	150	-	-	-	✓	✓
P-M-O	-	100	150	76	✓	-
P-M-WR	-	100	150	76	✓	✓
(d): diameter of cylindrical cross section (a): Side of the square cross section						

For carrying out the second part of the study, eighty pull out specimens were prepared for this program (Figure 3.6). Variables include concrete compressive strength, clear cover thickness, different temperatures and wrapping with CFRP sheets as presented in Table 3.8.

Figure 3.6: All specimens used for pull-out test

Table 3.8: Characterization of test specimens

Sample ID	**Compressive strength (MPa)**	**Confinement with CFRP**	**Heating temperature (°C)**	**Cover thickness (mm)**	**Number of samples**
C30-U-20-25	30	-	20	25	2
C30-U-200-25	30	-	200	25	2
C30-U-400-25	30	-	400	25	2
C30-U-600-25	30	-	600	25	2
C30-U-800-25	30	-	800	25	2
C30-U-20-35	30	-	20	35	2
C30-U-200-35	30	-	200	35	2
C30-U-400-35	30	-	400	35	2
C30-U-600-35	30	-	600	35	2
C30-U-800-35	30	-	800	35	2
C30-W-20-25	30	✓	20	25	2
C30-W-200-25	30	✓	200	25	2

Sample ID	Compressive strength (MPa)	Confinement with CFRP	Heating temperature (°C)	Cover thickness (mm)	Number of samples
C30-W-400-25	30	✓	400	25	2
C30-W-600-25	30	✓	600	25	2
C30-W-800-25	30	✓	800	25	2
C30-W-20-35	30	✓	20	35	2
C30-W-200-35	30	✓	200	35	2
C30-W-400-35	30	✓	400	35	2
C30-W-600-35	30	✓	600	35	2
C30-W-800-35	30	✓	800	35	2
C40-U-20-25	40	-	20	25	2
C40-U-200-25	40	-	200	25	2
C40-U-400-25	40	-	400	25	2
C40-U-600-25	40	-	600	25	2
C40-U-800-25	40	-	800	25	2
C40-U-20-35	40	-	20	35	2
C40-U-200-35	40	-	200	35	2
C40-U-400-35	40	-	400	35	2
C40-U-600-35	40	-	600	35	2
C40-U-800-35	40	-	800	35	2
C40-W-20-25	40	✓	20	25	2
C40-W-200-25	40	✓	200	25	2
C40-W-400-25	40	✓	400	25	2
C40-W-600-25	40	✓	600	25	2
C40-W-800-25	40	✓	800	25	2
C40-W-20-35	40	✓	20	35	2
C40-W-200-35	40	✓	200	35	2
C40-W-400-35	40	✓	400	35	2
C40-W-600-35	40	✓	600	35	2
C40-W-800-35	40	✓	800	35	2

Figure 3.7 gives the schematic view of the pull out specimen. Pull out specimen had a cross-sectional area of 150 mm × 150 mm and a height of 250 mm. Deformed steel bar with 20 mm diameter is placed in one corner of the specimen so that the concrete cover for specimens is 25 mm and 35 mm. Also, 25 mm length of the top and bottom part of the bar is rolled with the PVC pipes and therefore the length embeded in the concrete was 200 mm.

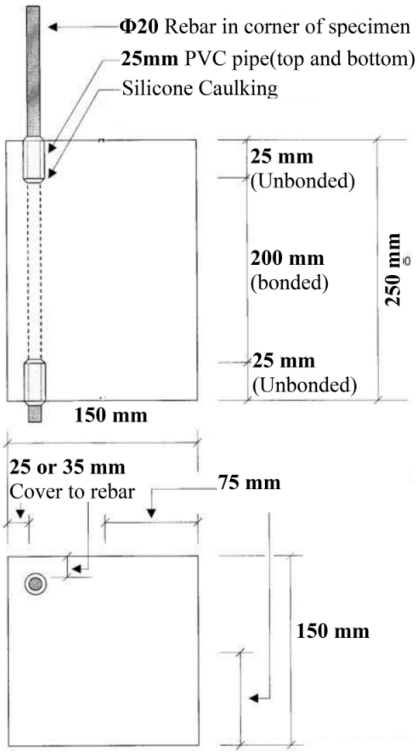

Figure 3.7: Pull-out specimen configuration

Figure 3.8: Mold for Pull-out specimen test

Figure 3.9: Molds manufacturing for Pull-out specimen test

The specimens consist of two series with different compression strengths: 30.1 MPa (C30) and 39.9 MPa (C40). Each series consisted of 40 pull out test and 30 cubic specimens for testing compressive strength (15cm × 15cm × 15cm). Each series includes 20 pull out specimen with 25 mm concrete cover and 20 specimens with a 35 mm concrete cover. These 20-member groups of pull out specimens are divided into five groups each of which is subjected to a specific temperature (ambient temperature, 200°C, 400°C, 600°C, 800°C).

The name of the pull out samples is composed of four parts. The first part expresses the compressive strength of the concrete specimen (C30 and C40) and the second part indicates the wrapped with CFRP (U represents the unwrapped specimens and W represents the wrapped specimens). The third part represents the temperature at which the specimen is located (20°C, 200°C, 400°C, 600°C and 800°C) and finally the fourth part indicates the amount of concrete covering on the bar in the sample (25mm and 35mm).

In this research, a standard cubic mold of 150mm × 150 mm × 150mm has been used to test the compressive strength.

3.7 Concrete Curing

Curing plays an important role on strength development and durability of concrete. Curing takes place immediately after concrete placing and finishing, and involves maintenance of desired moisture and temperature conditions, both at depth and near the surface, for extended periods of time. Properly cured concrete has an adequate amount of moisture for continued hydration and development of strength, volume stability, resistance to freezing and thawing, and abrasion and scaling resistance. In this study, concrete specimens made from different mix designs were kept in laboratory condition after 24 hours of concrete breaks and opening the frames to the desired age under wet conditions in the water pool.

3.8 Specimens Heating Regime

In first section of this study, specimens were heated about four months after the construction. An electric furnace with dimensions of 500mm×500mm×500mm was used to heat the specimens.

The method of placing specimens inside the furnace and the heating regimes are presented in Figures 3.10 and 3.11, respectively. To completely dry the specimens, they were placed in an electric furnace for a duration of 24 hours at temperature of 100°C.

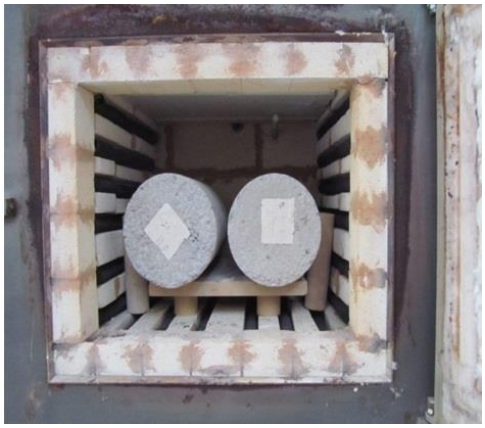

Figure 3.10: Furnace with concrete cylinders ready for heating (first part)

In previous researches, for high temperatures, heating rate of 1-10°C/min has been used [35-37]. Average rate of heating was 250 °C/h. However, it should be noted that the rate of heating used is considerably lower than ISO-834 regulation which is presented in Figure 3.11.

However, considering the capability of the furnace, the heating regime given in Figure 3.11 and also used by previous researchers, has been utilized. Once the average temperature of the furnace reached to 500 °C, the temperature is kept constant for two hours. After this time the furnace is turned off and the specimens were allowed to cool naturally in the furnace for 24 hours.

Afterwards, the specimens were removed from the furnace and kept under laboratory conditions until the time of testing.

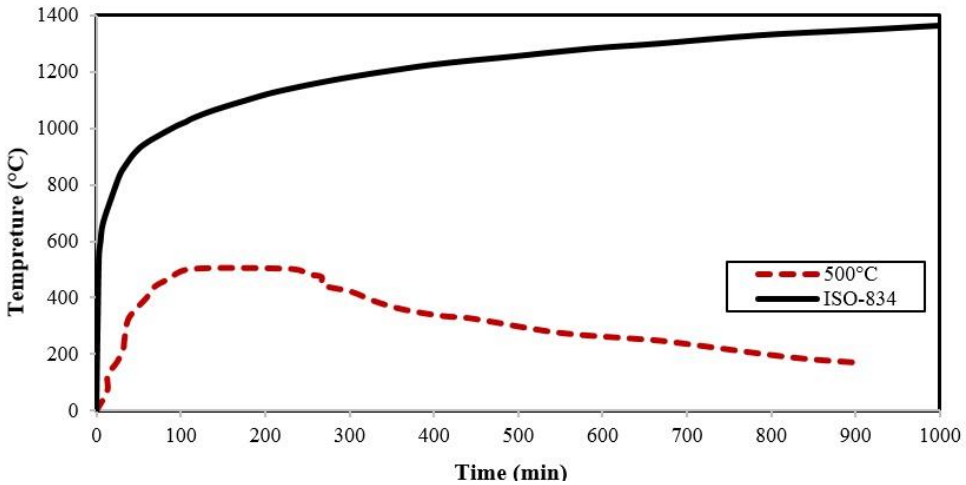

Figure 3.11: Time–temperature curves used in this study (first part)

In the second part of the study after constructing the specimens, they were cured for 28 days inside the water pool and laboratory conditions. After the completion of curing, the specimens were heated.

Before placing the specimens in an electric furnace, place it in a temperature of 100± 5° c for 24 hours to dry well. An electric furnace (Figure 3.12) with dimensions of 150cm × 150cm × 150cm is used to heat the specimens. The heating regime (Figure 3.13) was planned and the device was programmed to attain the desired temperature.


Figure 3.12: Heating cell (heating furnace for second part)

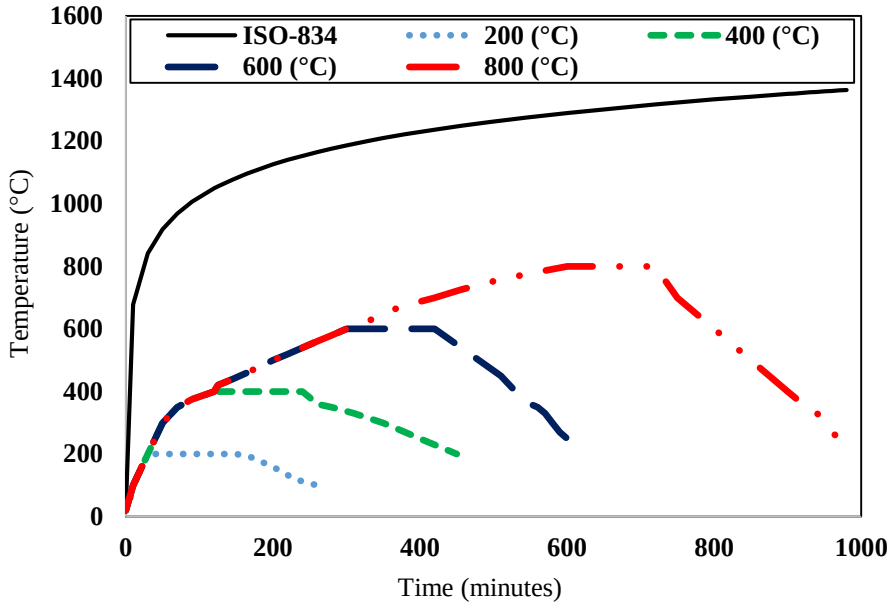

Figure 3.13: Heating rate curve used in this study (second part of thesis)

In this study, the average heating rate was about 250°c/h. When the furnace temperature reaches the target temperature, the temperature is kept constant for more than two hours (soaking period). Under this regime it can be assumed that the interior temperature the specimen is distributed monotonously [141, 142].


Figure 3.14: Placing the samples inside the electric furnace

After this time, the furnace is switched off and the specimens are allowed to cool naturally for 24 hours. After cooling and reaching the ambient temperature the specimens were taken out of the furnace and kept until they were tested under laboratory conditions.

Figure 3.15: Storing the specimens in the laboratory before CFRP wrapping

3.9 Repair Process of Heat Damaged Specimens

Due to the fact that the specimens, which are exposed to fire, have no severe damage and only small cracks were observed on their surface, there is no need for repair concrete surface before shape modification and performing CFRP wrap.

3.9.1 Shape Modification of Specimens with Expansive Cement

To modify the shape of specimens in the annular gap between cylindrical frameworks (150×300 mm) and prismatic specimens, expansive cement has been used. Before placing concrete in the corners of the cross-section, a 10 mm chamfer is created to make the aggregates move in the concrete easily (Figure 3.16). It is noteworthy that before implementing the expansive concrete, the surfaces of the specimen were prepared based on BS EN1504 standard [141]. The loose concrete is removed using a steel wire brush and the concrete substrate was prepared to make a better connection between regular concrete and expansive concrete. In addition, the specimens were

placed in water before using the expansive concrete since this would prevent regular concrete to absorb the water of the expansive concrete.

Figure 3.16: Shape-modification of square samples by using circular molds

The specimens were kept in steel formworks for four weeks after using the expansive concrete. Moreover, the top surface of concrete has been regularly moistened using wet clothes. This method of curing causes an increase in the volume of the expansive concrete. The formwork did not allow the volume of the concrete to increased, therefore, it could create compressive stress between regular and expansive concrete leading to a better connection between both types of concrete.

3.9.2 Wrapping of Specimens with CFRP Sheet

Wet lay-up technique has been used for wrapping up the specimens. Before the use of CFRP, the surface of specimens was prepared based on BSEN1504 standard. The epoxy resin called Sikador330 has been used before the CFRP wrapping around the concrete.

In the second part of the study, a layer of CFRP sheets is used to strengthen the specimens. An amount of 7 cm has been used as an overlap to increase the effectiveness of the fiber. The direction of the fiber is perpendicular to the direction of the main bar. The CFRP implementation process on concrete consists of four steps:

1) Surface preparation
2) Resin under coating
3) CFRP applying
4) Resin cover coating

Because after the heat, no concrete damage has been observed on concrete surfaces only small cracks have been seen; no special repair measurement has been made. The corner of the prismatic specimens was rounded to 20 mm radius in cross sections for more fiber effectiveness. It was shown in Figure 3.17. The side surfaces of the sample are grated through grinding stone and the wire brush is removed about one millimeter from the concrete layer.

Figure 3.17: Corner rounded specimens to 20 mm radius in cross sections

Finally, to clean the surfaces the specimen was washed with acetone-impregnated cloth. After the end of the first step, epoxy resin was used to prepare concrete surfaces and a thin layer of epoxy was applied on the specimen surfaces to connect the CFRP to the concrete surface. After this step, the CFRP sheet is implemented as wrapping. The trapped air bubbles press out by the rollers and the hand. Finally, a thin layer of resin is applied on the fibers to make the fibers completely saturated. One week is required for the resin on the wrapped specimens to become rigid. The sample prepared according to the standards before CFRP installation and after CFRP installation (Figure 3.18 and 3.19). Maintenance of samples under laboratory conditions for complete epoxy adhesive curing, is shown in Figure 3.20.

Figure 3.18: Sample prepared according to standard before installation

Figure 3.19: CFRP applied on specimens

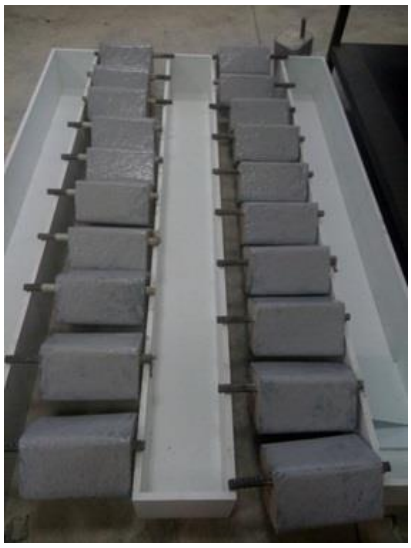
Figure 3.20: Storing samples under laboratory conditions for complete epoxy adhesive curing

3.10 Test Setup and Testing Procedure

3.10.1 Method of Stress Measurement

Before testing, all specimens were capped to achieve parallel surfaces and hence uniform load distribution. In order to measure strain, linear variable displacement transducers (LVDT) were used. As can be seen from Figure 3.21, two LVDTs were installed during loading time was used to test the specimens under axial pressure, up to failure by a machine with a capacity of 2000 KN. The test data was monitored and

logged by data logger. The strain measurement methods for square and circular specimens are presented in Figure 3.21.

(a) (b)

Figure 3.21: Strain measurement for (a) square and (b) circular specimens

3.10.2 Pull-out Test Setup

The test setup is presented in Figure 3.22.

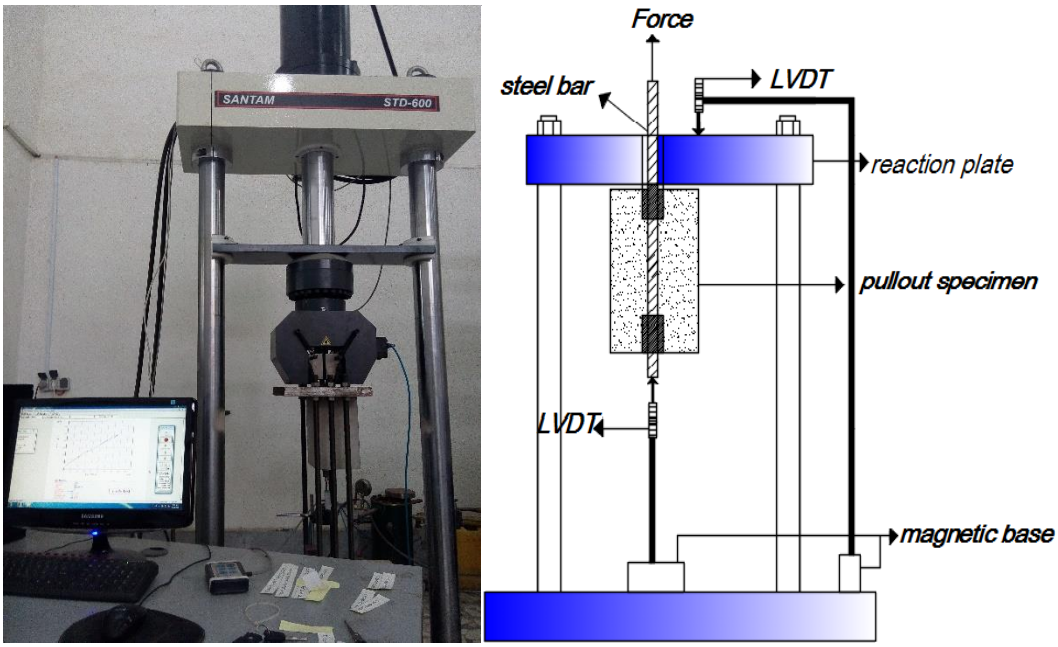

Figure 3.22: Loading device

A loading frame is designed, constructed and installed for testing (Figure 3.23). The loading frame consists of two 50 mm thick steel plates of joined by 6 steel bars with 25 mm diameter.

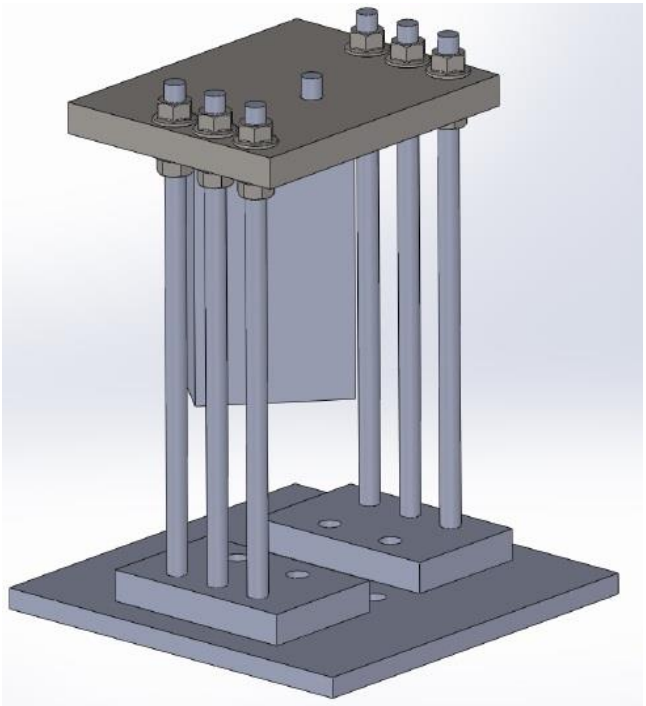

Figure 3.23: The loading frame constructed and installed for testing

The test is performed by pulling the bar in the specimen upward. A hydraulic universal test machine (UTM) performed the test with a capacity of 600 KN (Figure 3.24). 1(mm/min) rate was used for monotonic loading.

Figure 3.24: Hydraulic universal test machine (UTM SANTAM STD 600)

During loading, the load applied together with the output of the LVDTs is automatically collected and stored by the machine using the data acquisition system. Upon reaching the peak load, the loading is continuing in the downstream processing.

The pull out test was stopped when one of the following conditions occur.

1. Pull through or rupture the rebar that never happened
2. Splitting of surrounding concrete
3. The force applied to the extraction sample is less than 50% of the peak load

In this test the amount of bar displacement per load was measured and finally the maximum bond stress between concrete and bars was obtained from equation (3.2).

f_b = P/πDL (3.2)

f_b = Bond stress

P: Maximum applied tensile force

D: Bar diameter

L: The embedment length of the rebar

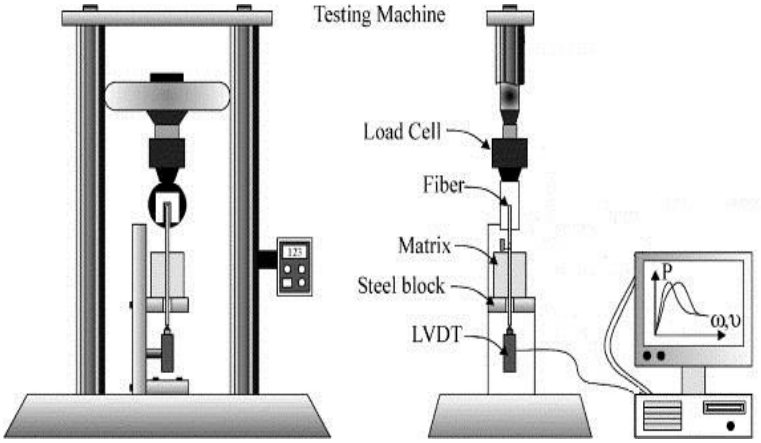

Figure 3.25: The schematic of Pull-out test set up with hydraulic universal test machine

3.10.3 Compressive Strength Test

Compressive strength of concrete cube test provides an idea about all the characteristics of concrete. The compressive strength test is carried out either on cube of hardened concrete 150mm ×150mm × 150 mm (Figure 3.26).

Figure 3.26: The concrete cubes before compressive strength test

These specimens are tested by compression testing machine (Figure 3.27).

Figure 3.27: The compression testing machine

Procedure of compressive strength test of concrete cubes is that after hardening and placing under the appropriate heat concrete specimens were placed under a special pressure jack for testing. Then the vertical force is applied by a fixed speed jack to a cube-shaped specimen so that the specimen is disrupted by the pressure load.

The cubes were placed in the machine in such a manner that the load shall be applied to the opposite sides of the cube. The loading speed should be in the range of 0.14 to 0.34 (MPa/sec). In this study loading speed was considered to be 0.25 (MPa/sec). Finally, as a procedure for cube test:

I. Remove the specimen from water after specified curing time and wipe out excess water from the surface.
II. Set the dimension of the specimen to 150mm × 150mm × 150 mm
III. Clean the bearing surface of the testing machine
IV. Place the specimen in the machine in such a manner that the load shall be applied to the opposite sides of the cube cast.
V. Align the specimen centrally on the base plate of the machine.
VI. Rotate the movable portion gently by hand so that it touches the top surface of the specimen.
VII. Apply the load gradually without shock and continuously at the rate of 0.25 (MPa/Sec) till the specimen fails
VIII. Record the maximum load and note any unusual features in the type of failure.

In this part, four specimens were tested from each selected age and heat group. Strength of the specimens that were varied by more than 15 per cent of average strength, were rejected. Average of four specimens were required to get the crushing strength of concrete. The force required to disassemble the specimen by the device is shown and recorded. The resultant cubic compressive stress is obtained by dividing this force over the cross-sectional area (Equation (3.3)).

$$f'_C = \frac{P}{A} \tag{3.3}$$

Where: f'_C is compressive strength (MPa), P is the maximum compressive force (N)

A is the cross-sectional area of the concrete (mm^2).

Chapter 4

TEST RESULTS AND DISCUSSIONS FOR OBJECTIVE 1

4.1 Introduction

As noted in the previous chapter, the experimental study was divided into two parts due to its size. In this chapter, the results of the first part of the study are presented. The results related to the effect of heat as well as retrofitting with CFRP layers on the compressive strength of concrete are presented. First, the failure patterns and laboratory observations are evaluated. In the following, according to the stress-strain diagrams of the samples, parameters such as final compressive strength, final axial strain, elasticity modulus and stiffness are investigated.

4.2 Test Observation and Failure Mode

All of the concrete specimens were subjected to uniaxial compression load until failure. Images of square specimens after uniaxial compression test can be seen in Figure 4.1. The U-S-O specimens and the square specimens without strengthening and heating had concrete crushing type of specimen failure. Failure of P-S-O specimens were similar to those of U-S-O specimens, except that more cracks or collapse was observed in the P-S-O specimens. On the other hand, for U-S-WR and P-S-WR specimens, failure was owed to concrete crushing which was followed by fracture of CFRP composite jackets at the corners. Brittle fracture is due to stress

concentration near the section corners and the lack of confinement at the flat sides, which eliminated membrane action.

Figure 4.1: Failure of square specimens

Images of circular and modified specimens after uniaxial compression test can be seen in Figure 4.2. Failure of U-C-O specimens was due to the combination of column and shear failure whereas the P-C-O specimens had wedge failure.

The failures of U-C-WR and P-C-WR specimens were sudden and explosive with loud noise. It was caused by rupture in the CFRP composites. The strengthened circular specimens' failure was observed at the middle of its height. The rupture mode in the CFRP layers of these specimens represents the accumulation of a large amount of strain energy created as a result of confinement. When failure of shape-modified specimens without CFRP wrapping (P-M-O) is considered, the layer of expansive concrete separated from the main concrete due to low bond. Hence, after the failure, the main concrete was without fracture. For shape-modified specimens with CFRP wrapping like C-WR specimens, the failure has been sudden and explosive with loud booming noise and was due to rupture at the mid-height of the specimen. However,

separation between the central core and the expansive concrete has also been observed in these specimens.

Figure 4.2: Failure of circular and modified specimens

4.3 The Stress-strain Behavior of Specimens Subjected to Compression

Axial strain has been measured by using two LVDTs. The axial stress was calculated by using the axial compressive load divided by the specimen's cross-sectional area. Figure 4.3 indicates the axial stress versus axial strain response of all specimens with square cross-section including the reference specimens of (U-S-O), reference specimens with wrapping (U-S-WR), and the specimens with square cross-section exposed to heating, P-S-O and U-S-WR. By comparing the stress-strain diagrams related to the un-heated specimens, it is observed that the CFRP wrapping has no significant influence on the initial slope. However, it has a prominent effect on the

strength and ultimate strain of the specimens which can be due to the confinement of the CFRP composite sheets to prevent failures of specimens and to withstand a high strain. On the other hand, the specimens exposed to heating have a significant loss of stiffness and strength while, the maximum strain of these specimens has been increased. The reduction in stiffness could be due to small cracks and the pores created in concrete owing to the water evaporation during heating. As can be seen from Figure 4.3, once the specimens that are strengthened with CFRP composite sheets were subjected to heating, the stiffness and strength of the specimens were increased. However, this growth is not enough for the specimens to reach the stiffness of the baseline specimens. In addition, the increase in strength was almost 56% more than the reference specimens and 20% less than U-S-WR specimens. This reduction is due to the presence of cracks that lead to the loss of strength in the core of heated concrete.

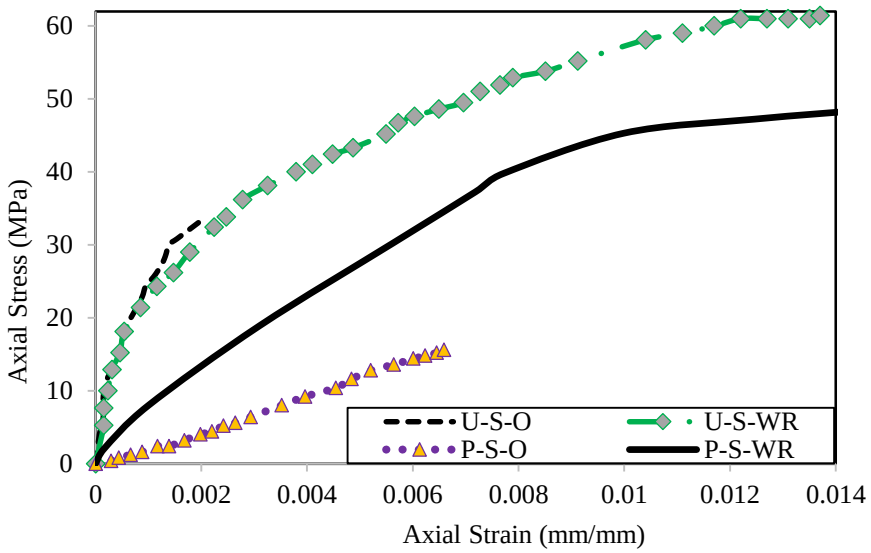

Figure 4.3: Axial stress- strain behaviour of specimens with square cross-section

Figure 4.4 presents axial stress versus axial strain of the specimens with circular cross-section including U-C-O, P-C-O, U-C-WR and P-C-WR specimens for comparison with reference specimens (U-S-O). By studying the diagrams related to specimens

exposed to heating, it can be concluded that, as expected, the stiffness and the strength were significantly dropped according to expectation. But, after strengthening with CFRP composite wrapping the stiffness was enhanced. However, it should be noted that the increased stiffness is not as high as the initial stiffness. The strength of the specimens was considerably improved after strengthening with CFRP which is due to the confinement effect that prevented the destruction of the central core.

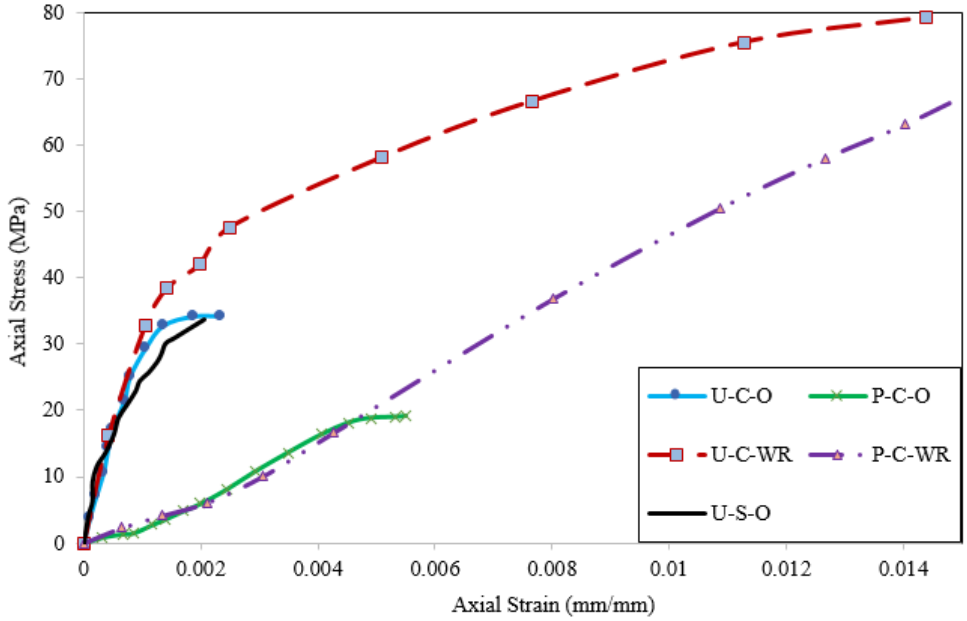

Figure 4.4: Axial stress- strain behaviour of specimens with circular cross-section

Figure 4.5 shows the axial stress-strain curve of P-M-O, P-M-WR, U-S-O, U-C-O, P-S-O and P-C-O specimens. The curves of U-S-O, U-C-O, P-S-O and P-C-O were included for comparison purposes. It is obvious from the Figures 4.3 to 4.5 that stiffness of specimens was increase with the application of shape modification. Moreover, the strength of shape-modified and wrapped specimens has considerably improved whilst the strength of unwrapped specimens was close to the strength of original specimens.

It is noteworthy that shape modification for the damaged specimens could largely compensate the stiffness reduction and the use of CFRP wrapping could considerably improve the compressive strength. However, this was not enough to compensate the stiffness and the strength to return to their initial values.

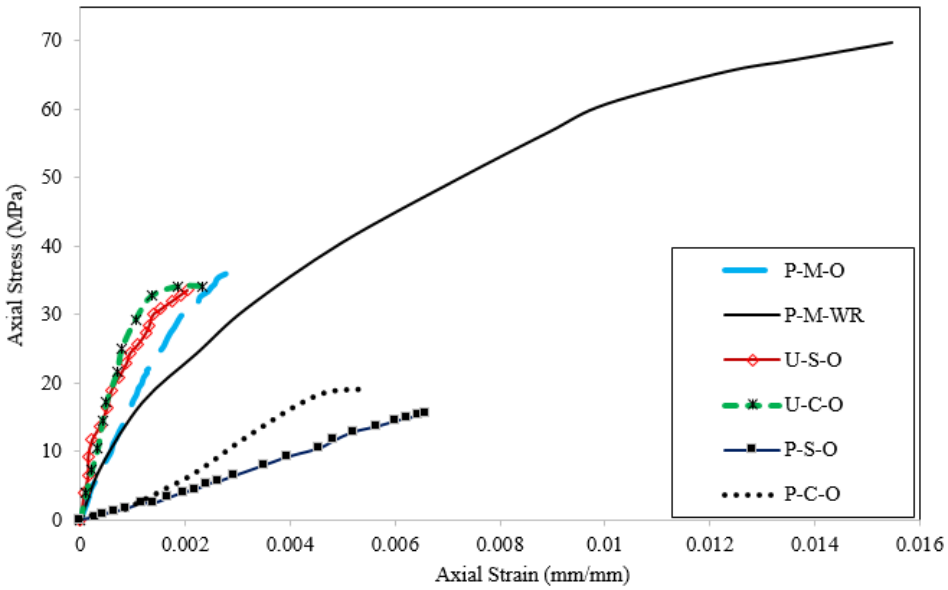

Figure 4.5: Comparison of axial stress- strain behavior between modified and unmodified specimens

4.4 Compressive Strength

The results of compressive strength for the studied specimens are given in Figure 4.6. Compressive strength of the reference specimens was 33.4MPa. When the specimens were heated, the square and the circular specimens had 56% and 42% drop in their compressive strength, respectively. This reduction in strength is attributed to the dehydration of CSH gel as well as to the volumetric expansion resulting from the transformation of the chemical compounds $Ca(oh)_2$to CaO.

Strengthening by CFRP wrapping of the un-heated specimens caused 98.7% and 122% increase in the compressive strength of the square and the circular specimens,

respectively. However, the increase in compressive strength was more remarkable for circular specimens. In addition, strengthening by CFRP composite for specimens subjected to heating led to a prominent increase in their compressive strength which was more than three times higher than those of the P-O specimens. By studying the compressive strength of the square specimens and circular specimens, it is observed that the drop in strength resulted from heating is less for C specimens and also the growth of strength in these series of specimens caused by strengthening with CFRP is more than square specimens. According to the compressive strength of shape-modified specimens, it can be concluded that shape modification and repairing of fire-damaged specimens led to an increase in the compressive strength. This growth was to the extent that for the specimens without wrapping, the compressive strength of shape-modified specimens was reached to the compressive strength of unheated specimens. Once the shape-modified specimens were wrapped by CFRP sheets, their compressive strength showed an increase more than which was two times P-M-O specimens and four times more than P-S-O specimens. This amount is more than U-S-WR and P-S-WR specimens, while it is less than the compressive strength of U-C-WR specimens. This increase in strength is due to both the strength created by expansive concrete and the shape modification of cross sections to circle section. Therefore, exerting uniform stress to CFRP sheets and enhancing the confinement effect.

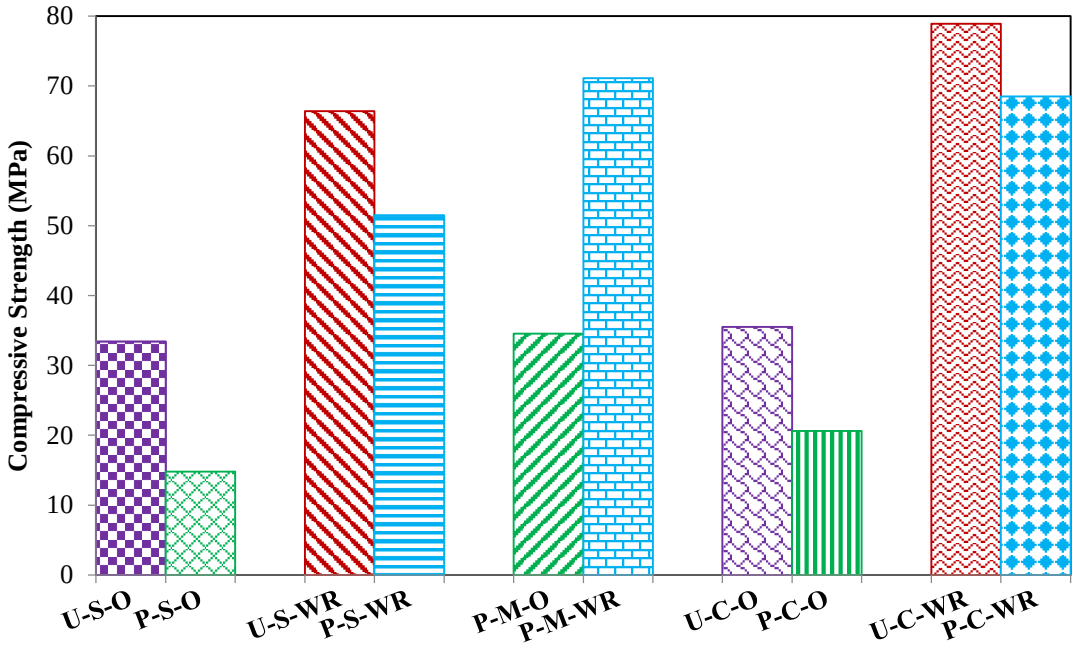

Figure 4.6: Compressive strength of the studied specimens

4.5 Secant Modulus

Figure 4.7 is presented to provide further examination on the effect of cross-section shape modification and also the effect of strengthening with CFRP on the elastic range of loading of the concrete.

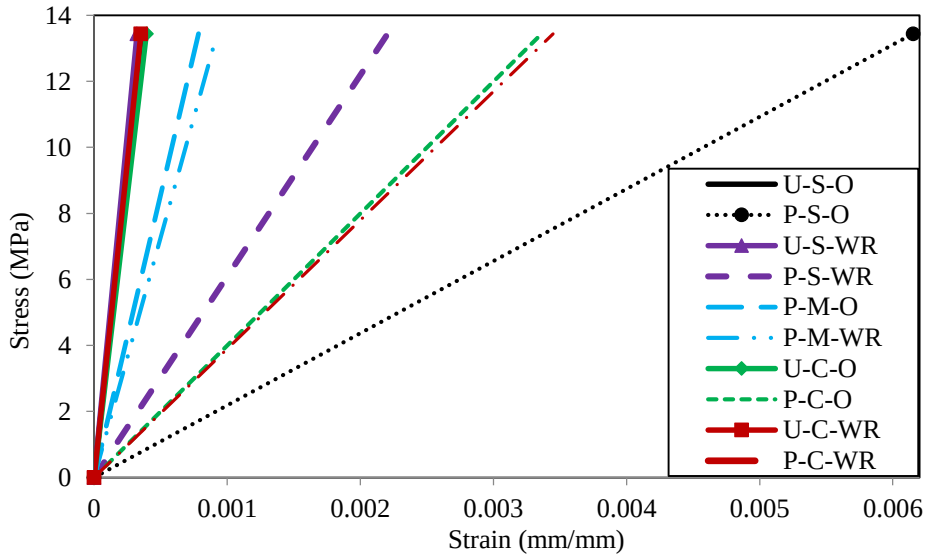

Figure 4.7: Comparison of stress- strain behavior among specimens in elastic range

The primary parts of stress-strain curves are linear (Figure 4.7). The origin point has been linearly connected to a point of stress-strain curve which is corresponding to 40% of maximum stress in reference specimen (U-S-O). It can clearly be concluded (Figure 4.7) that the influence of shape modification and strengthening with CFRP is obvious on the primary slope and stiffness of stress-strain curve for the studied specimens. The slope of curves for U-S-O, U-S-WR, U-C-O, and U-C-WR specimens is almost identical so that the mentioned curves have been overlapped (Figure 4.7).

The compliance of the four mentioned lines shows that the confinement with CFRP has little impact on the stiffness and primary slope (elastic range) of stress-strain curve. In other words, the effect of strengthening with CFRP in elastic state of loading is negligible. It is observed that the slope of curves has significantly dropped after exposure to heating. This issue is clearly visible in P-S-O and P-C-O specimens but the drop in P-S-O specimen is more that P-C-O specimen.

The slope and primary stiffness of specimens has greatly increased owing to the shape modification of cross-sections. However, this growth has not been enough to reach to the initial slope before heating. It is observed that the shape modification can considerably enhance the slope and primary stiffness of stress-strain curve or the stiffness of concrete in elastic state.

Figure 4.8 indicates the effects of heating, shape modification and strengthening with CFRP wrapping on secant modulus of concrete specimens. In this study, in order to examine the effect of fire on the secant modulus of concrete in elastic range and also to investigate the proposed strengthening method on restoring the reduction in stiffness, secant modulus has been used.

Secant modulus is defined as linear slope corresponding to 40% of maximum stress in original specimens (U-S-O) and for P-S-O and P-C-O specimens, it is calculated linear slope according to 40% of maximum stress of these specimens.

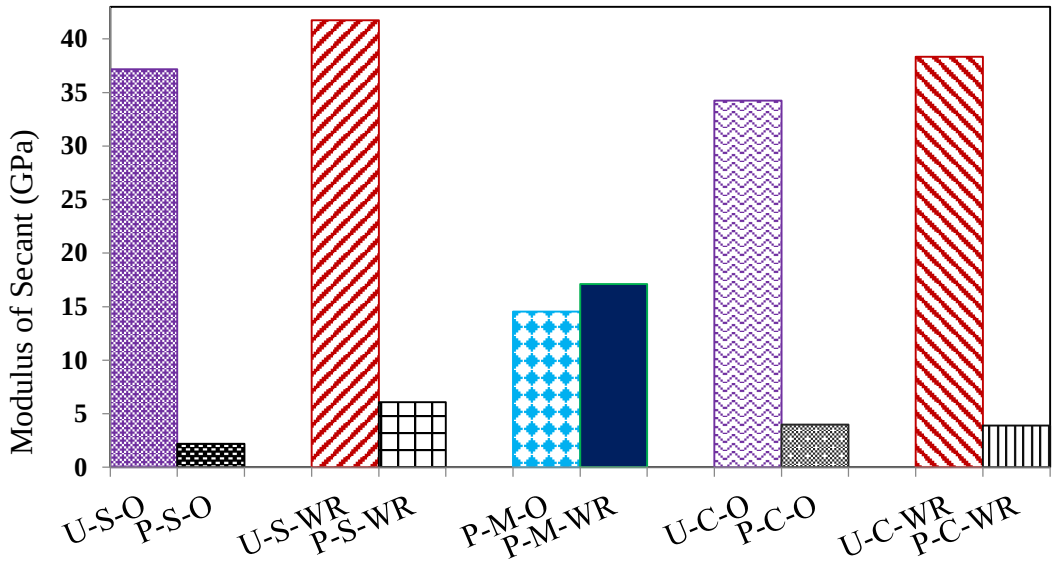

Figure 4.8: Average modulus of secant for the studied specimens

The average amount of secant modulus related to the three studied specimens has been presented in Figure 4.8. This Figure shows that the modulus of secant has sharply fallen due to heating effect. This reduction is due to the creation of micro-cracks and softening of the concrete after heating and reduction in bonds. Moreover, more porosity because of evaporation of concrete water is another factor for the reduction. The modulus of secant can be improved by strengthening with two layers of CFRP.

The modulus of secant for U-S-O specimen is 37.1 GPa that has dropped to 2.1 GPa in P-S-O specimen due to heating. Thanks to shape modification, the modulus of secant for P-S-O specimens has increased by more than eight times and reached to 17.1 GPa showing the effect of shape modification on secant modulus or the stiffness

of elastic range for heated concrete. However, the effect of confinement on modulus secant of concrete is not perceptible.

It is obvious from the Figure 4.8, the numerical value of secant modulus for unheated specimens U-S-O, U-S-WR, U-C-O, and U-C-WR is ranges from 34 to 41 GPa. Once the specimens were exposed to 500 °C temperature, secant modulus sharply drops and reaches to 2 to 4 GPa range. Confinement with CFRP had a little effect on modulus of secant, although the confinement significantly increases the compressive strength of concrete.

Figure 4.8 shows that, shape modification from square to circle in heated specimens causes a significantly growth in secant modulus or in other words the stiffness of elastic range. It is worth being noted that the effect of CFRP wrapping on the overall stiffness has been negligible for heated specimens this may be due to the result of insignificant effect of confinement in the elastic range of loading. The confinement of CFRP layers is activated after reaching the concrete to nonlinear state and by applying continuous pressure on the concrete core, it will continue until reaching the failure of CFRP jacket. Therefore, the behavior of elastic state of the wrapped heated specimens with CFRP is similar to the heated specimens without wrapping.

The increase in modulus of secant can be due to the fact that the central core of shape-modified specimens was made of fire-damaged concrete but the external core of the specimens was consisted of expansive concrete which has high stiffness. It should be noted that the growth of the modulus secant in shape-modified specimens is due to the expansive concrete. Therefore, it is possible to compensate the drop in secant modulus or stiffness in elastic range damaged by heating considerably.

Chapter 5

TEST RESULTS AND DISCUSSIONS FOR OBJECTIVE 2

5.1 Introduction

As outlined in Chapter 3, the experimental plan was divided into two parts due to the size and breadth of study.

In this chapter, the results of the second part of experimental work results are related to the effect of heat, as well as strengthening with CFRP layers and other parameters studied on the bond strength of steel reinforced in concrete are presented. Firstly, the compressive strength of concrete samples studied and the effect of heat on this property was investigated, and then the behavior of the bond strength between steel rebar and concrete was investigated by using the pull-out specimens. The parameters studied on bonding strength include: compressive strength of concrete, concrete covering on the rebar, temperature levels, strengthening by CFRP. The results of the study are reported and presented in the following sections. At first, the experimental observations and the failure modes were discussed. Then, the compressive strength of concrete samples under high temperature were reported. Subsequently, the bonding behavior between the reinforcing rebar and the concrete under varied temperatures was evaluated by the pull-out test and the load-to-displacement ratios of the pull-out samples were presented. Also, the effect of compressive strength of concrete, heat, concrete coating and reinforcement by CFRP on cohesion strength was discussed.

5.2 Test Observations and Failure Modes

Figure 5.1 shows the overall appearance of samples after being exposed to heat and the laboratory observations of these concrete samples are described below.

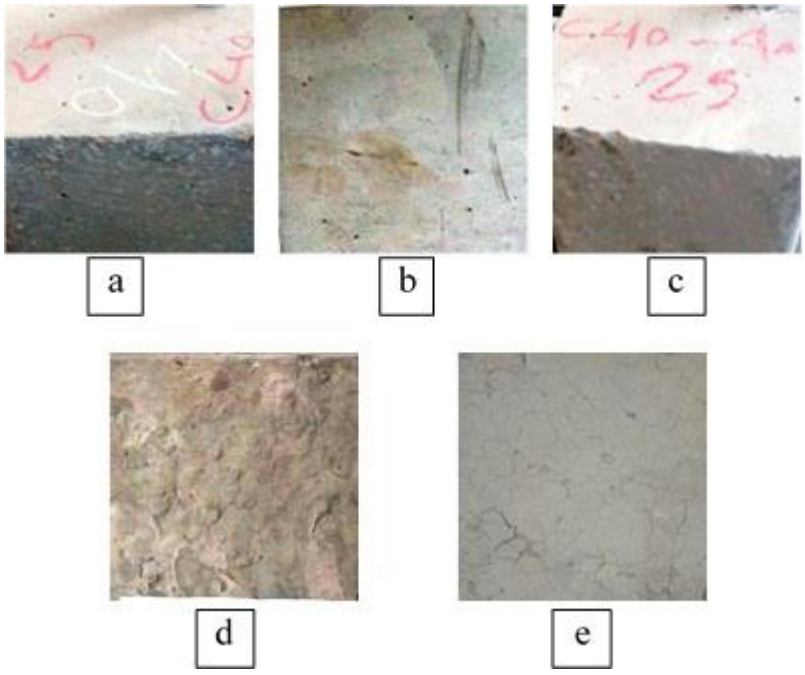

Figure 5.1: The surface appearance of the samples after the heat (a=20°C, b=200°C, c=400°C, d=600°C, e=800°C)

20°C: The surfaces of non-heated samples were dark grey. No surface cracks in concrete due to shrinkage or other factors were considered.

200°C: No spalling has been observed in the specimens and the color of the heated samples was mud grey.

400°C: After heating the surface color of the samples was gray brown. Surface cracks were seen in the specimens but no crushing has been observed.

600°C: The surface of the samples was grey white and the cracks formed by the heat were evident.

800°C: The specimens were lit in grey and red in color. Thermal cracks were evident in concrete levels.

The specimens were subjected to pull-out test after being exposed to heat and CFRP wrapping. As expected, the failure of the samples has occurred in bond behavior testing in two modes: Bar bond splitting and bar pull out.

The failure mode is affected cover to the reinforcing bar and compressive strength of concrete and CFRP sheets wrapping. The failure mode of unconfined specimens was splitting bond failure, regardless of compressive strength and concrete cover, while the failure mode in all wrapped specimens was bar pull out. Generally, failure mode involves the extension of radial cracks and the fragile crushed of concrete specimens in the corner of the sample where the reinforcing bar is present.

On the other hand, failure mode in un-wrapped and unheated specimens was more fragile and exploded with high noise. While for heated specimens exposed to higher temperature, the failure mode occurred but the failure rate was lower than the unheated specimens. In Figure 5.2, the failure mode of some specimens are presented after the pull-out test.

Figure 5.2: The appearance of some specimens after the pull-out test

In the Figure 5.2, the lateral surface of the wrapped specimens are perfectly healthy, without any crack and any damage after pull-out tests. Whereas in the unwrapped specimens, the damages are very severe and cracks are occurred in these specimens and also complete crash observed in some specimens that were exposed to low temperatures and unheated specimens, after pull-out tests.

By wrapping the specimens, the bond failure mode has changed to the pull out of the reinforcing bar. Despite the observation of splitting crack in some of the samples, the CFRP wrap limit the cracks and lead to higher strength. Cracking in specimens that ruptured splitting starts from the middle part of the side of the specimen and then expands to the end of the specimen but confinement by CFRP layer prevents cracking. The CEB-FIB [121] indicated that such failure was partial pull-out bond failure when the specimen had moderate confinement and/or a limited concrete cover. Failure mode in similar specimens with different compressive strength was the same. But in

unwrapped and unheated specimens with a 40 (MPa) compressive strength (C40-U-20 group of specimens) crash was brittle with a lot of noise. Concrete coverings (35mm and 25mm) also have little effect on the type of failure mode and similar specimens with different concrete cover had same behaviour.

5.3 Residual Compressive Strength

The compressive strength of the cube specimens is shown in Figure 5.3. This figure shows the changes in the compressive strength due to varied temperature for two types of concrete (C40-C30). Also, the results presented are the average results of six cubic specimens. However, in the last chapter of thesis, it has been discussed in detail about the effect of heat and a CFRP wrapping on compressive strength. In this chapter, in order to present the compressive strength of the samples and the effect of different temperatures on the compressive strength, an overview of the effect of heat on compressive strength is included. The compressive strength of the non-heated reference samples for the grade C30 and C40 concrete was 30.1MPa and 39.41MPa, respectively.

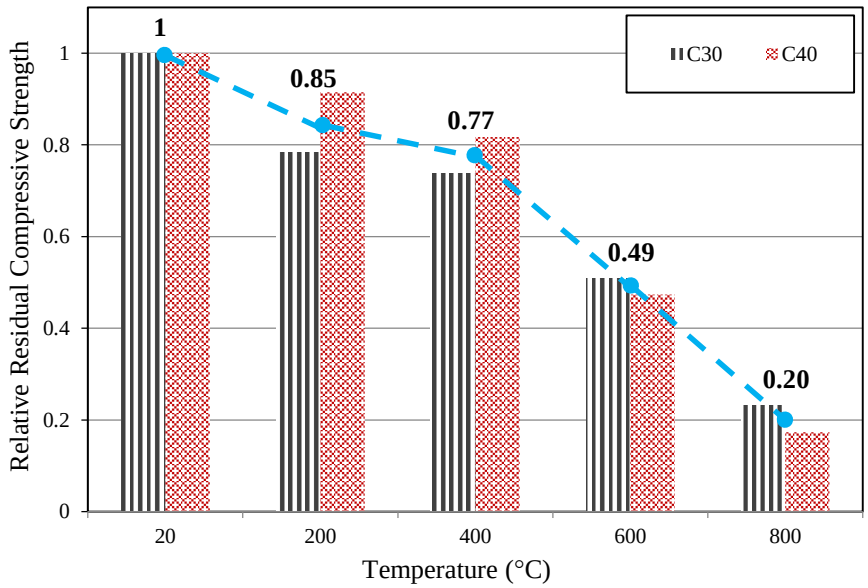

Figure 5.3: Variation of relative residual concrete compressive strength with temperature

In Figure 5.3, the results are presented in relative proportions for better comparison and conclusion. The compressive strength results in each design are divided into the compressive strength results of the corresponding reference samples, and the results are presented in this figure. The results show that compressive strength decreases with increasing heat. The test results show that when the concrete reaches up to 200°C the compressive strength decreases by an average of 15%. At a temperature of 400°C the compressive strength decreases by about 23% and at a temperature of 600°C the compressive strength decreases by about 51%. This reduction in strength is attributed to the dehydration of CSH gel as well as to the volumetric expansion resulting from the transformation of the chemical compounds $ca(oh)_2$ to cao. A sharp drop in compressive strength is observed when samples are heated to 800°C. At this temperature, the compressive strength was reduced by about 80%. This severity of strength deterioration is attributed to the decomposition of CSH gel.

By considering the compressive strength behavior of concrete with two different grades it can be deduced that up to 400°C the drop of compressive strength in grade C30 is greater than grade C40. With increase in temperature it was observed that the drop of compressive strength in the grade C40 specimen has increased and was more than the grade C30 specimen. The loss of compressive strength at 800°C for grade C40 was 6% higher than the grade C30 and finally the compressive strength in the two concrete grades was almost identical. The reason for this behavior could be due to the lower permeability of grade C40 that after a temperature of 400°C there was a large amount of cracking in concrete resulting in a drop of compressive strength.

5.4 Bond Stress-slip Relationship

In this study, in order to estimate the bond stress(τ_b), it was assumed that the bond stress between concrete and the reinforcing bars was distributed uniformly throughout the rebar (l_d). Therefore, the bond stress on the rebar was calculated by the following formula [6, 12]:

$$\tau_b = \frac{f}{\pi d_b l_b} \tag{5.1}$$

Where (τ_b) is the moderate bond stress (MPa), f is the applied force (N), l_b is the embedment length (200 mm) and d_b is the nominal diameter of the rebar (20 mm). In addition, using the force applied in equation 5.2 [6, 12], the axial stress was calculated to determine the current state of the rebar.

$$\sigma = \frac{f}{\pi d_b^2/4} \tag{5.2}$$

In all the test specimens the axial stress (σ) applied to the bars was less than the yield strength of the rebar.

Figure 5.4 and 5.5 show the stress-slip of the end of the rebar for C30-U samples at 20°C and concrete covering of 25 mm and 35 mm, respectively. The peak point of bond strength in the C30-U-20-25 specimen for first and second sample was 5.69 and 5.62 MPa, respectively. However, in the C30-U-20-35 design, the peak point of strength was 8.95 and 8.59 MPa for samples 1 and 2, respectively.

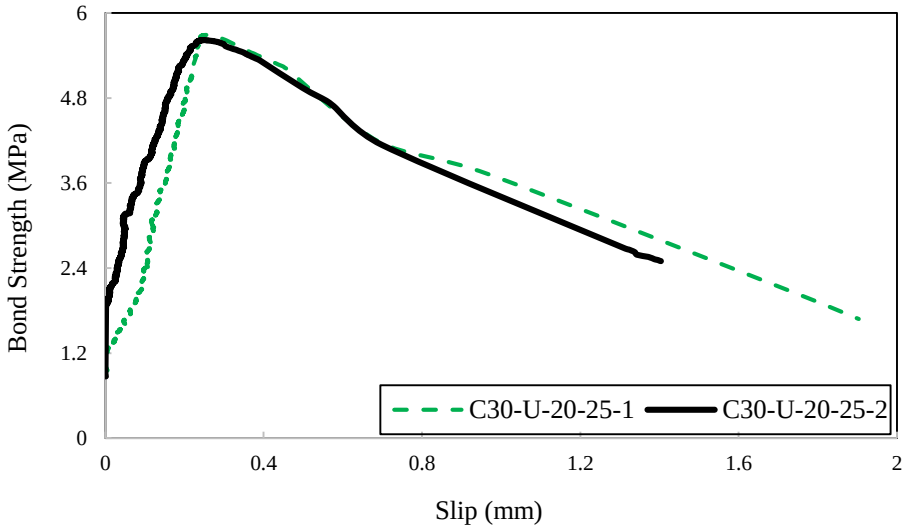

Figure 5.4: Bond stress-slip curves of pull-out specimens (C30-U-20-25)

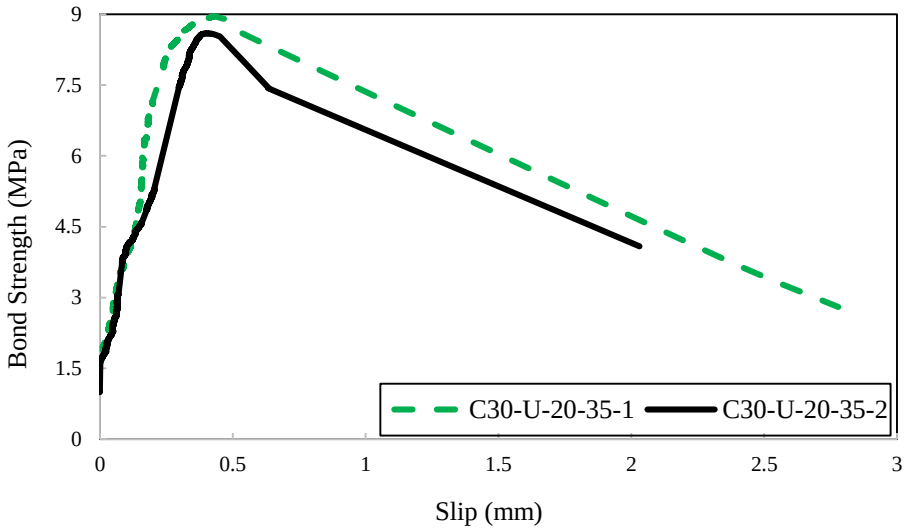

Figure 5.5: Bond stress-slip curves of pull-out specimens (C30-U-20-35)

Figure 5.6 and 5.7 show the stress-slip of the end of the rebar for C30-W specimens at 20°C and concrete covers of 25 mm and 35 mm, respectively. The peak point of bond strength in the C30-W-20-25 specimen was 8.34 MPa and 8.78 MPa for samples 1 and 2, respectively. However, the peak point of strength in the C30-W-20-25 specimen was 8.34 MPa and 8.78 MPa for sample 1 and 2, respectively.

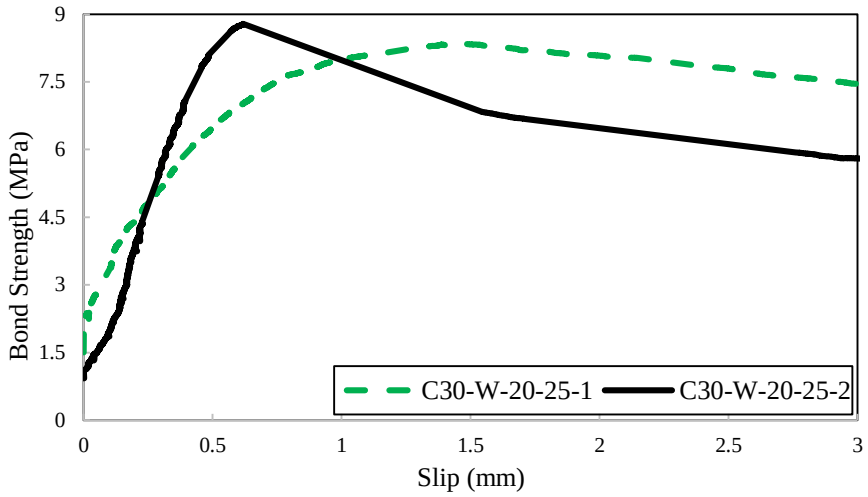

Figure 5.6: Bond stress-slip curves of pull-out specimens (C30-W-20-25)

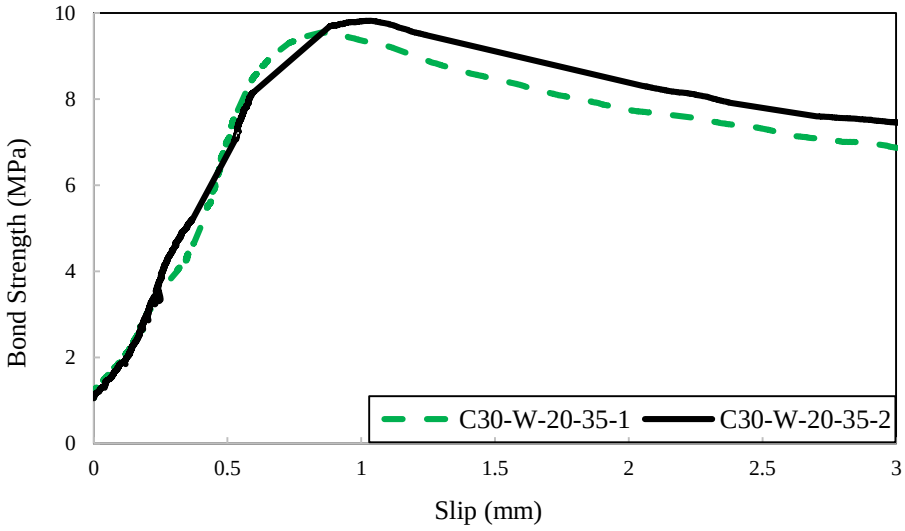

Figure 5.7: Bond stress-slip curves of pull-out specimens (C30-W-20-35)

Figure 5.8 and 5.9 show the stress-slip of the end of the rebar for C40-U samples at 20°C and concrete covers of 25 mm and 35 mm, respectively. The peak point of bond strength in the C40-U-20-25 design was 6.49 MPa and 6.29 MPa for samples 1 and 2, respectively. However, in the C40-U-20-35 design, the peak point of strength was 9.55 MPa and 9.19 MPa for samples 1 and 2, respectively.

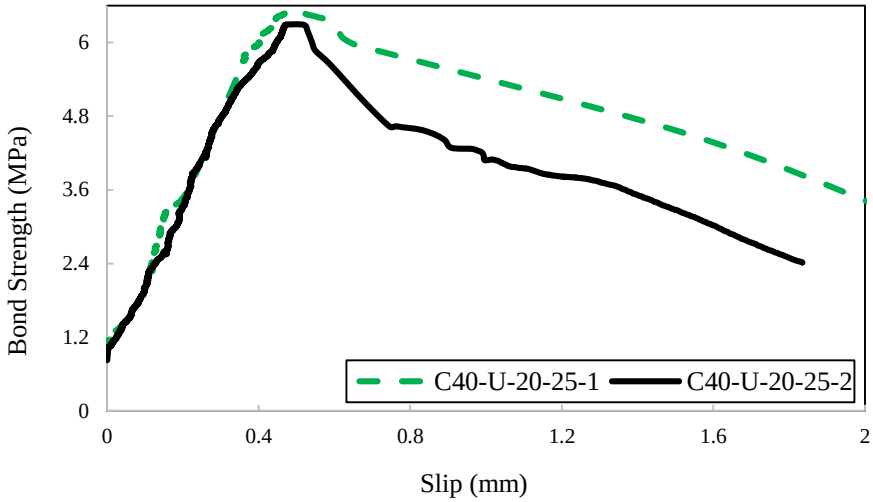

Figure 5.8: Bond stress-slip curves of pull-out specimens (C40-U-20-25)

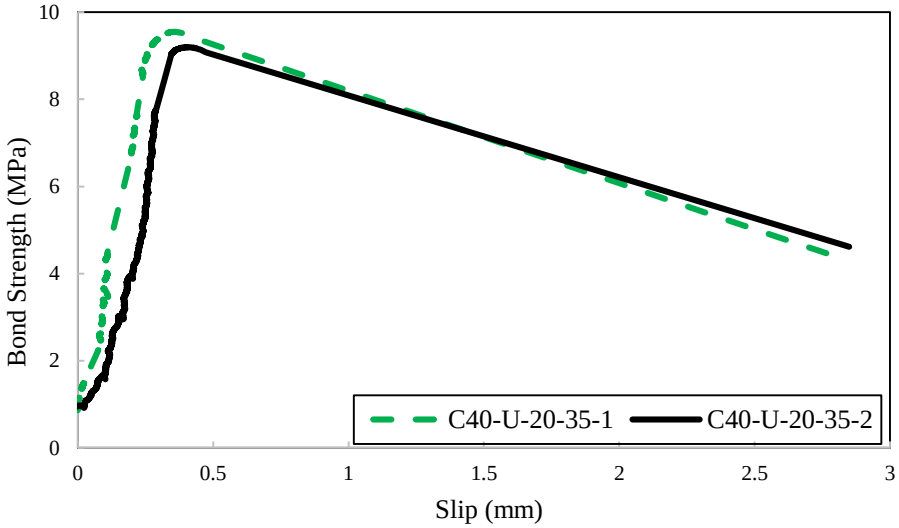

Figure 5.9: Bond stress-slip curves of pull-out specimens (C40-U-20-35)

Figure 5.10 and 5.11 show the stress-slip of the end of the rebar for samples C40-W at 20°C and concrete covers of 25 mm and 35 mm, respectively. The peak point of bond strength in the C40-W-20-25 design was 9.83 MPa and 10.16 MPa for samples 1 and 2, respectively. However, in the C40-W-20-35 design, the peak point of strength was 10.64 MPa and 10.23 MPa for samples 1 and 2, respectively.

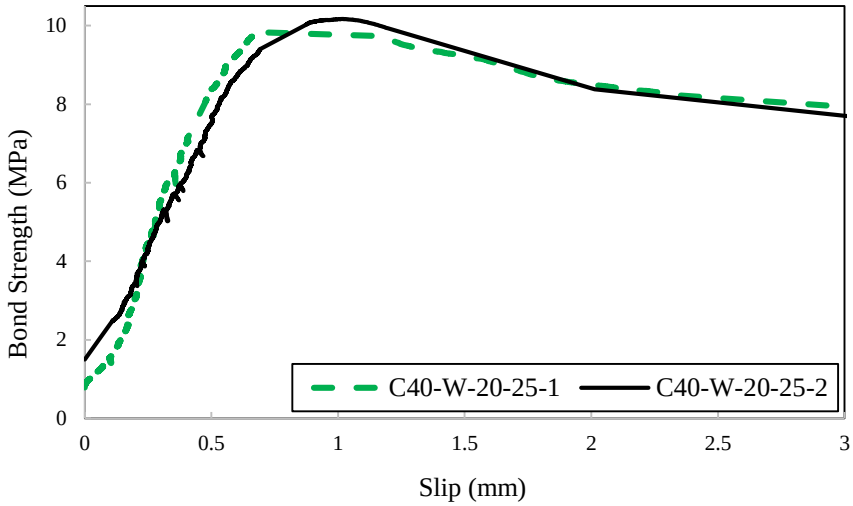

Figure 5.10: Bond stress-slip curves of pull-out specimens (C40-W-20-25)

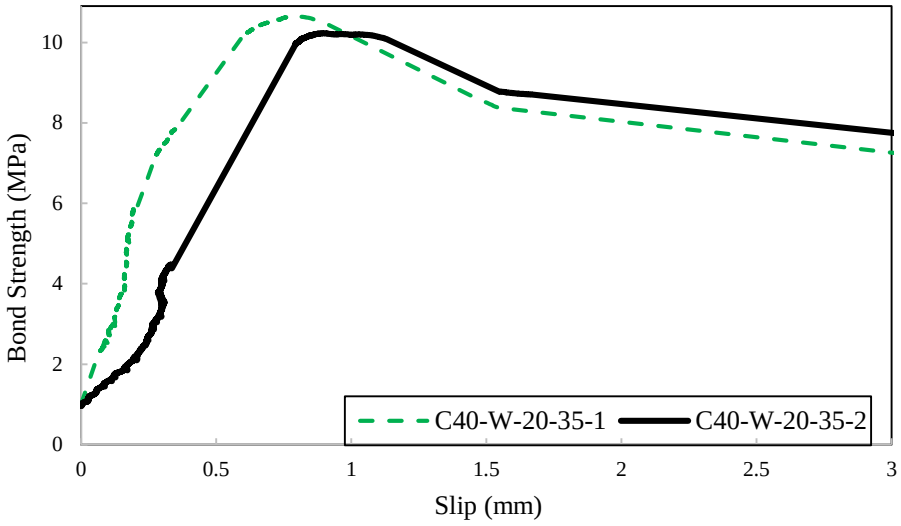

Figure 5.11: Bond stress-slip curves of pull-out specimens (C40-W-20-35)

Figure 5.12 and 5.13 show the stress-slip of the end of the rebar for C30-U samples at 200°C and concrete covers of 25 mm and 35 mm, respectively. The peak point of bond strength in the C30-U-200-25 specimen was 4.07 MPa and 4.21 MPa for sample 1 and 2, respectively. However, in the C30-U-200-35 design, the peak point of strength was 5.78 MPa and 5.57 MPa for sample 1 and 2, respectively.

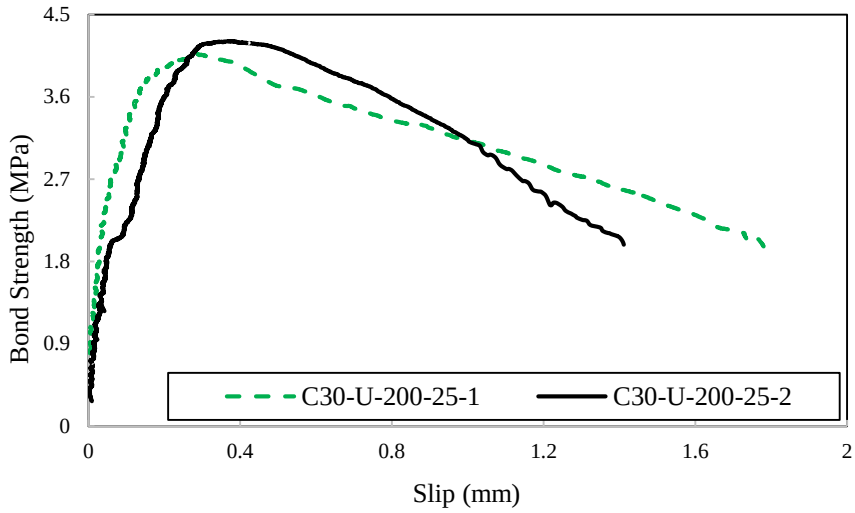

Figure 5.12: Bond stress-slip curves of pull-out specimens (C30-U-200-25)

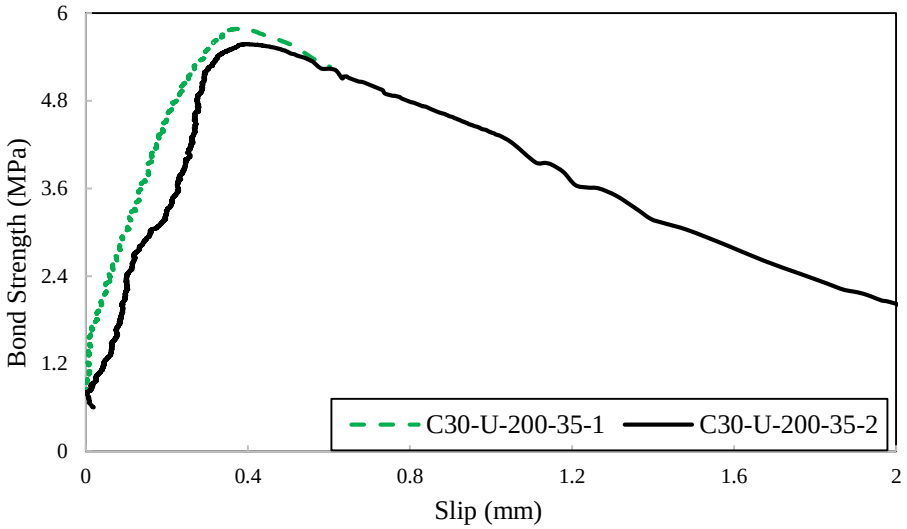

Figure 5.13: Bond stress-slip curves of pull-out specimens (C30-U-200-35)

Figure 5.14 and 5.15 represent the stress-slip of the end of the rebar for C30-W samples at 200°C and concrete covers of 25 mm and 35 mm, respectively. The peak point of bond strength in the C30-U-200-25 specimen was 6.01 MPa and 5.9 MPa for sample 1 and 2, respectively. However, in the C30-W-200-35 design, the peak point of strength was 7.82 MPa and 8.19 MPa for sample 1 and 2, respectively.

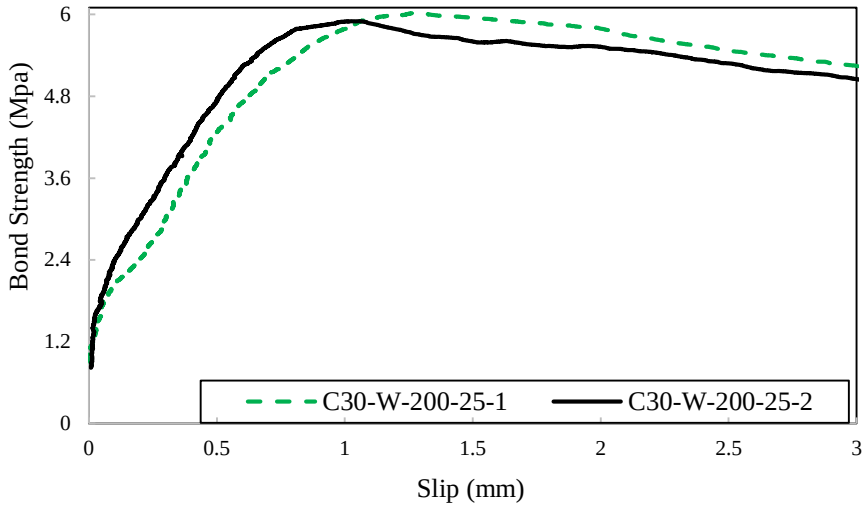

Figure 5.14: Bond stress-slip curves of pull-out specimens (C30-W-200-25)

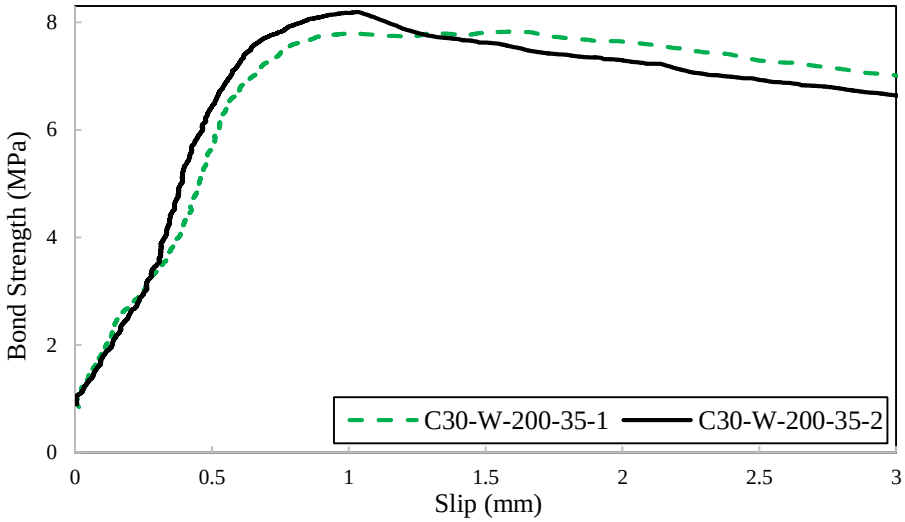

Figure 5.15: Bond stress-slip curves of pull-out specimens (C30-W-200-35)

Figure 5.16 and 5.17 represent the stress-slip of the end of the rebar for C40-U samples at 200°C and concrete covers of 25 mm and 35 mm, respectively. The peak point of bond strength in the C40-U-200-25 specimens was 5.87 MPa and 5.64 MPa for sample 1 and 2, respectively. However, in the C40-U-200-35 design, the peak point of strength was 6.71 MPa and 6.97 MPa for sample 1 and 2, respectively.

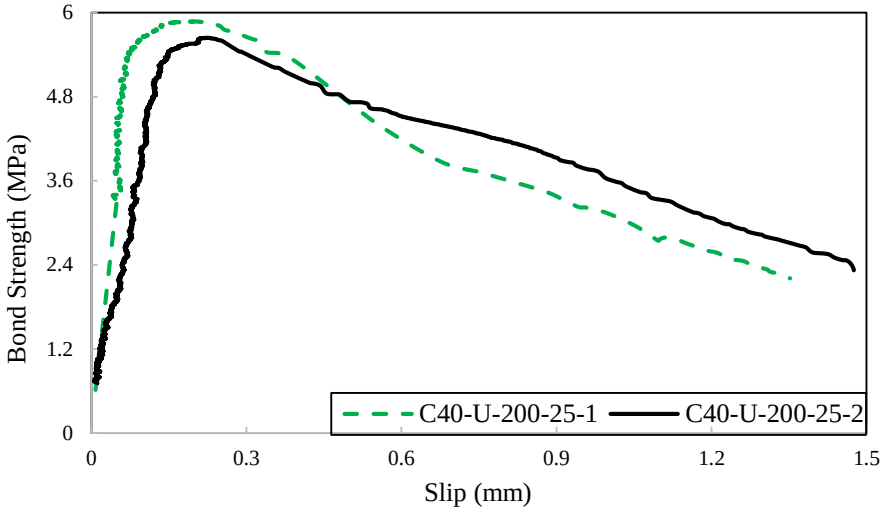

Figure 5.16: Bond stress-slip curves of pull-out specimens (C40-U-200-25)

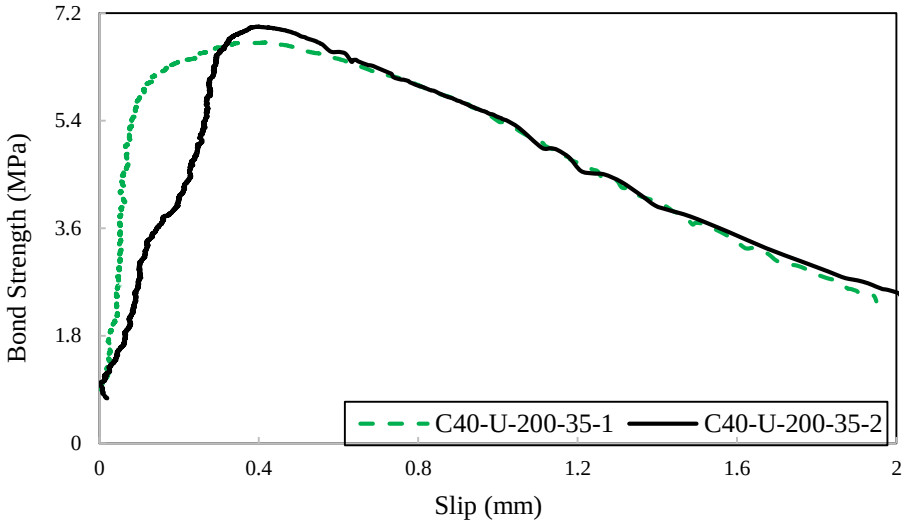

Figure 5.17: Bond stress-slip curves of pull-out specimens (C40-U-200-35)

Figure 5.18 and 5.19 indicate the stress-slip of the end of the rebar for samples C40-W at 200°C and concrete cover of 25 mm and 35 mm, respectively. The peak point of bond strength in the C40-W-200-25 design was 8.45 MPa and 8.44 MPa for sample 1 and 2, respectively. However, in the C40-W-200-35 design, the peak point of strength was 9.87 MPa and 10.14 MPa for sample 1 and 2, respectively.

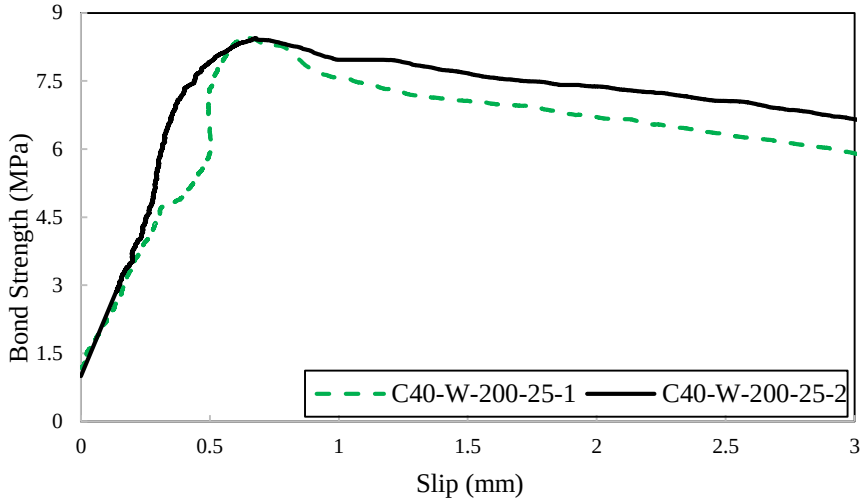

Figure 5.18: Bond stress-slip curves of pull-out specimens (C40-W-200-25)

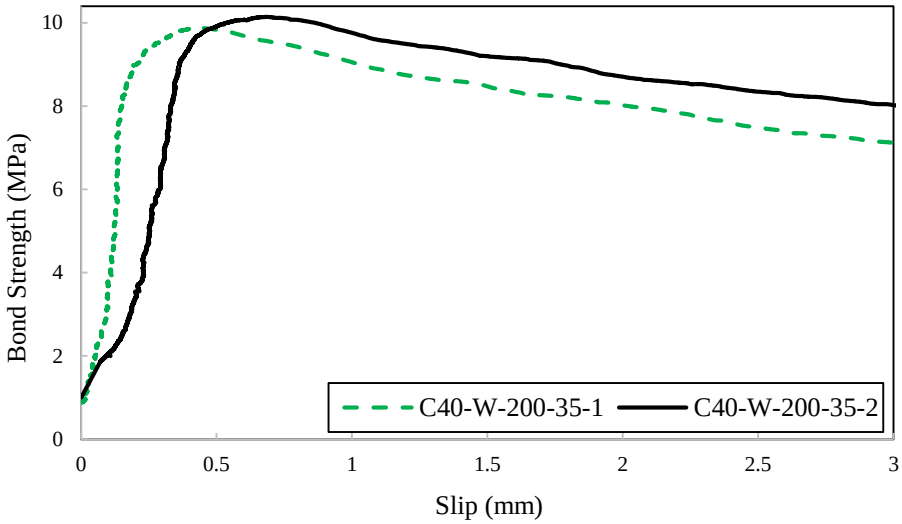

Figure 5.19: Bond stress-slip curves of pull-out specimens (C40-W-200-35)

Figure 5.20 and 5.21 indicate the stress-slip of the end of the rebar for C30-U samples at 400°C and concrete cover of 25 mm and 35 mm, respectively. The peak point of bond strength in the C30-U-400-25 design was 2.92 MPa and 2.8 MPa for sample 1 and 2, respectively. However, in the C30-U-400-35 design, the peak point of strength was 4.47 MPa and 4.72 MPa for sample 1 and 2, respectively.

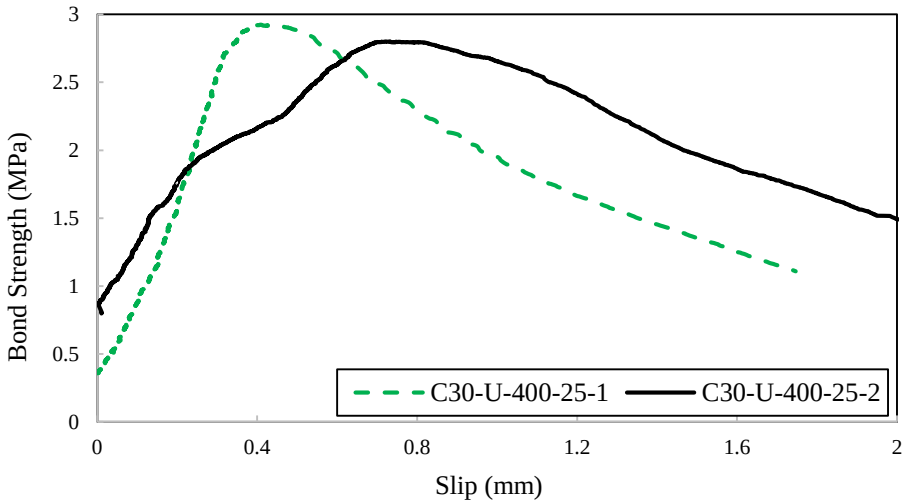

Figure 5.20: Bond stress-slip curves of pull-out specimens (C30-U-400-25)

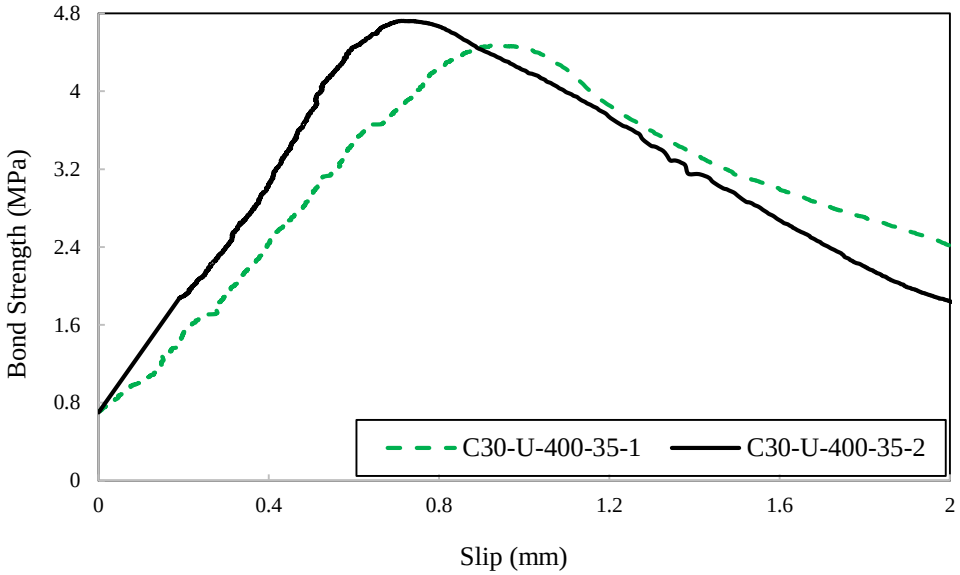

Figure 5.21: Bond stress-slip curves of pull-out specimens (C30-U-400-35)

Figures 5.22 and 5.23 represent the stress-slip of the end of the rebar for C30-W samples at 400°C and concrete cover of 25 mm and 35 mm, respectively. The peak point of bond strength in the C30-W-400-25 design was 6.1 MPa and 6.25 MPa for sample 1 and 2, respectively. However, in the C30-W-400-35 design, the peak point of strength was 7.07 MPa and 7.53 MPa for sample 1 and 2, respectively.

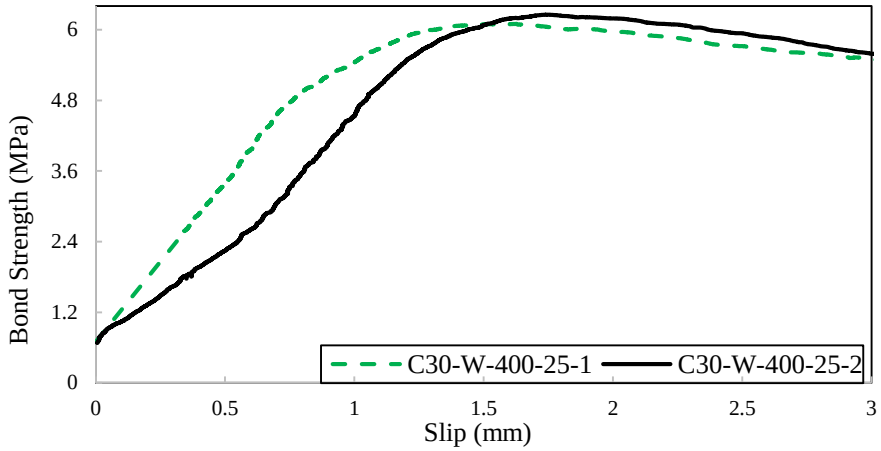

Figure 5.22: Bond stress-slip curves of pull-out specimens (C30-W-400-25)

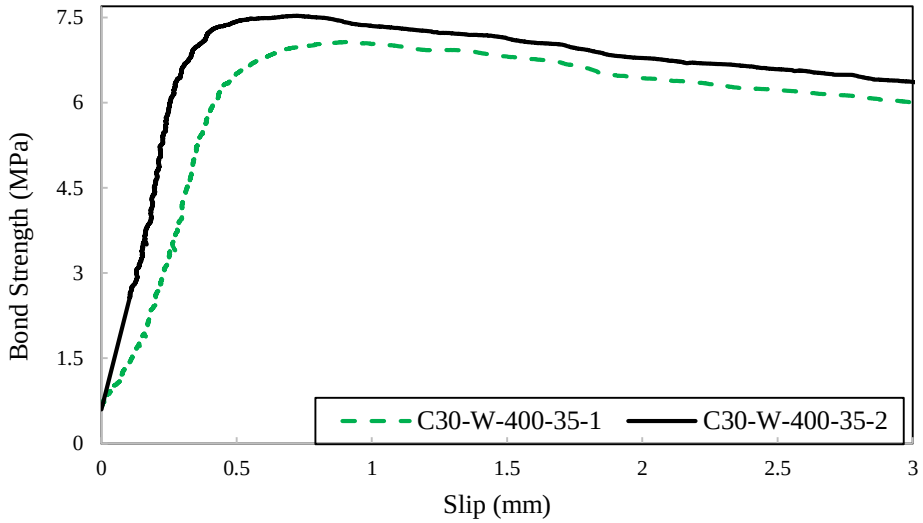

Figure 5.23: Bond stress-slip curves of pull-out specimens (C30-W-400-35)

Figures 5.24 and 5.25 indicate the stress-slip of the end of the rebar for C40-U samples at 400°C and concrete cover of 25 mm and 35 mm, respectively. The peak point of bond strength in the C40-U-400-25 design was 4.43 MPa and 4.29 MPa for sample 1 and 2, respectively. However, in the C40-U-400-35 design, the peak point of strength was 6.29 MPa and 6.02 MPa for sample 1 and 2, respectively.

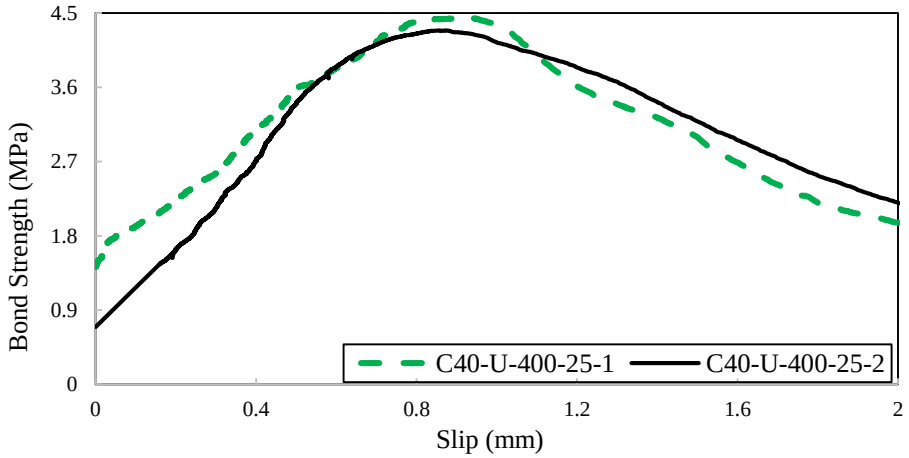

Figure 5.24: Bond stress-slip curves of pull-out specimens (C40-U-400-25)

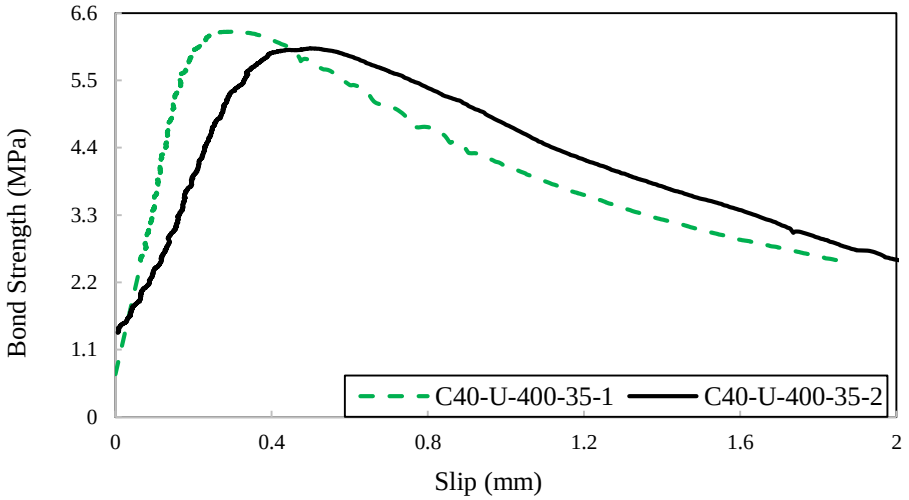

Figure 5.25: Bond stress-slip curves of pull-out specimens (C40-U-400-35)

Figures 5.26 and 5.27 represent the stress-slip of the end of the rebar for samples C40-W at 400°C and concrete cover of 25 mm and 35 mm, respectively. The peak point of bond strength in the C40-W-400-25 design was 6.99 MPa and 7.03 MPa for sample 1 and 2, respectively. However, in the C40-W-400-35 design, the peak point of strength was 7.46 MPa and 7.38 MPa for sample 1 and 2, respectively.

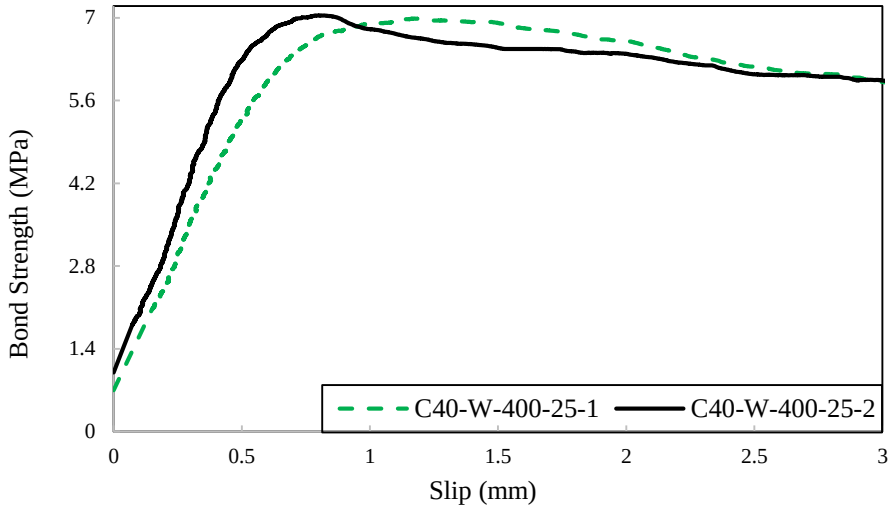

Figure 5.26: Bond stress-slip curves of pull-out specimens (C40-W-400-25)

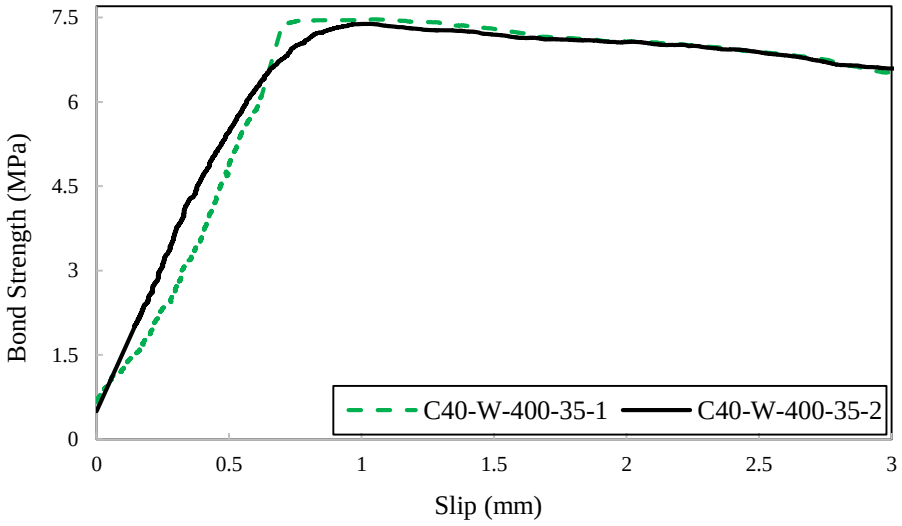

Figure 5.27: Bond stress-slip curves of pull-out specimens (C40-W-400-35)

Figures 5.28 and 5.29 represent the stress-slip of the end of the rebar for C30-U samples at 600°C and concrete cover of 25 mm and 35 mm, respectively. The peak point of bond strength in the C30-U-600-25 design was 1.51 MPa and 1.47 MPa for sample 1 and 2, respectively. However, in the C30-U-600-35 design, the peak point of strength was 2.17 MPa and 2.09 MPa for sample 1 and 2, respectively.

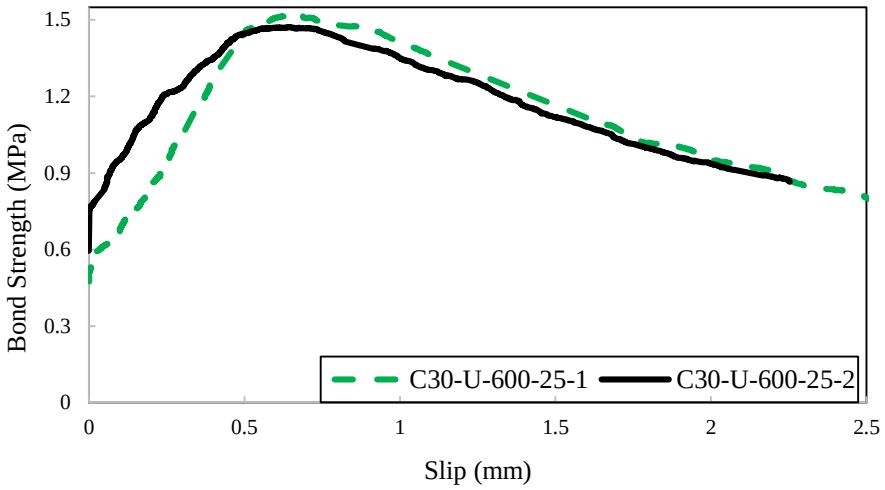

Figure 5.28: Bond stress-slip curves of pull-out specimens (C30-U-600-25)

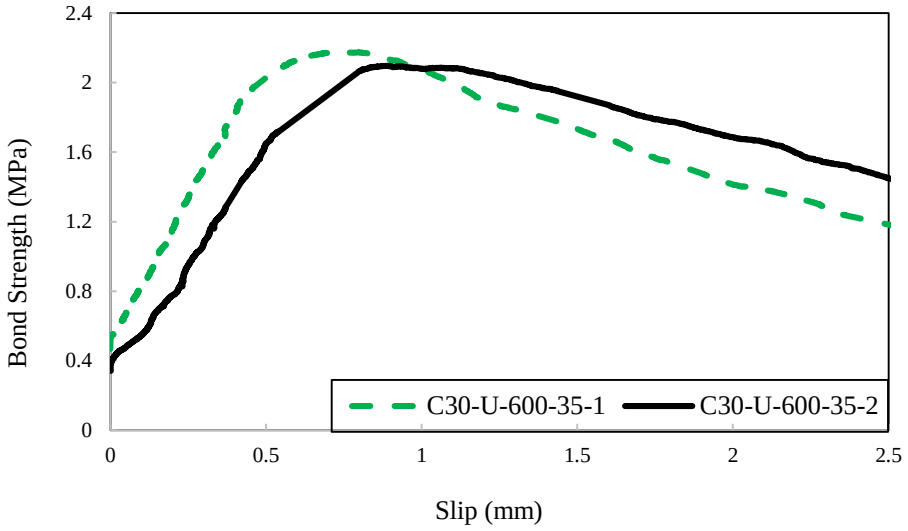

Figure 5.29: Bond stress-slip curves of pull-out specimens (C30-U-600-35)

Figures 5.30 and 5.31 represent the stress-slip of the end of the rebar for C30-W samples at 600°C and concrete cover of 25 mm and 35 mm, respectively. The peak point of bond strength in the C30-W-600-25 design was 3.65 MPa and 3.54 MPa for sample 1 and 2, respectively. However, in the C30-W-600-35 design, the peak point of strength was 5.02 MPa and 4.87 MPa for sample 1 and 2, respectively.

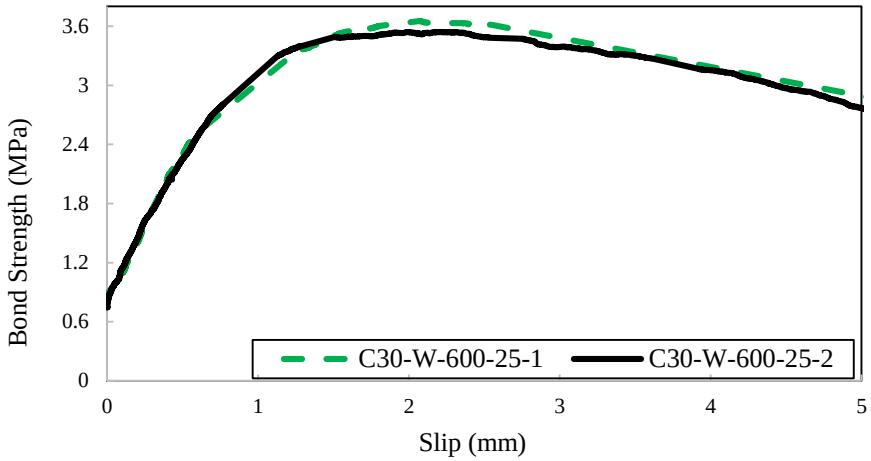

Figure 5.30: Bond stress-slip curves of pull-out specimens (C30-W-600-25)

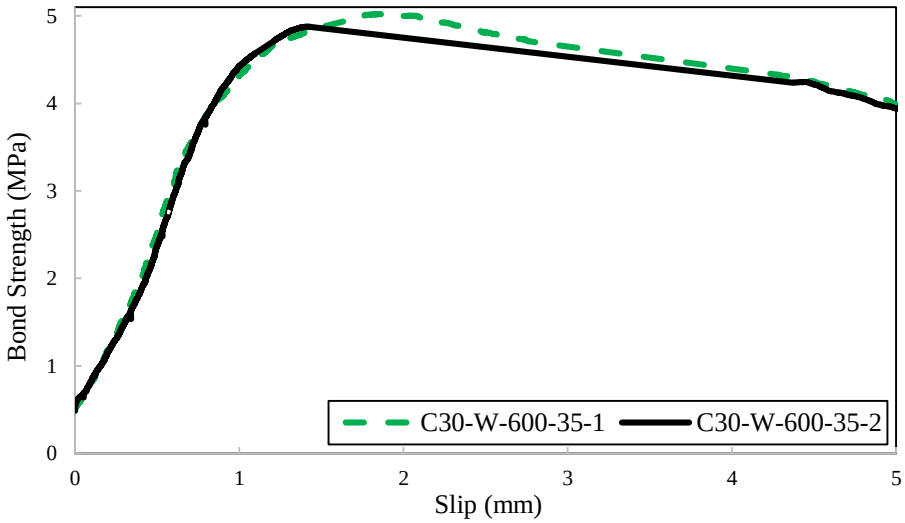

Figure 5.31: Bond stress-slip curves of pull-out specimens (C30-W-600-35)

Figures 5.32 and 5.33 represent the stress-slip of the end of the rebar for C40-U samples at 600°C and concrete cover of 25 mm and 35 mm, respectively. The peak point of bond strength in the C40-U-600-25 design was 1.82 MPa and 1.78 MPa for sample 1 and 2, respectively. However, in the C40-U-600-35 design, the peak point of strength was 2.65 MPa and 2.58 MPa for sample 1 and 2, respectively.

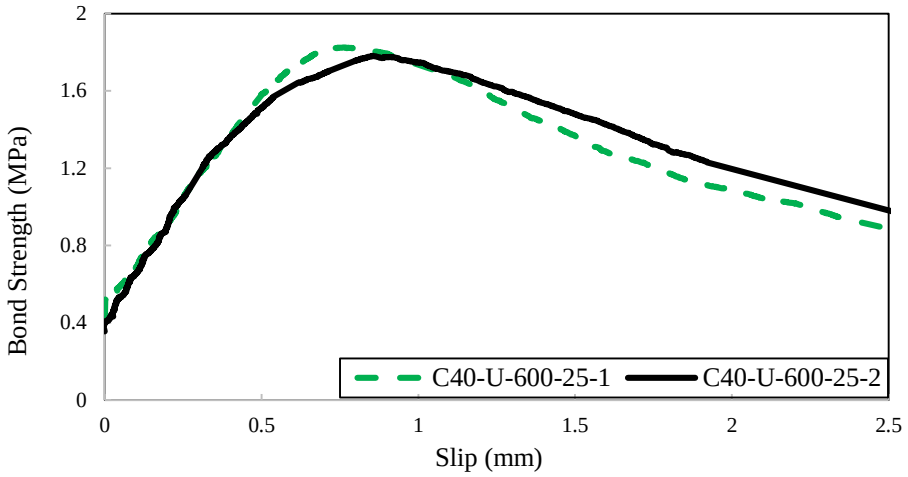

Figure 5.32: Bond stress-slip curves of pull-out specimens (C40-U-600-25)

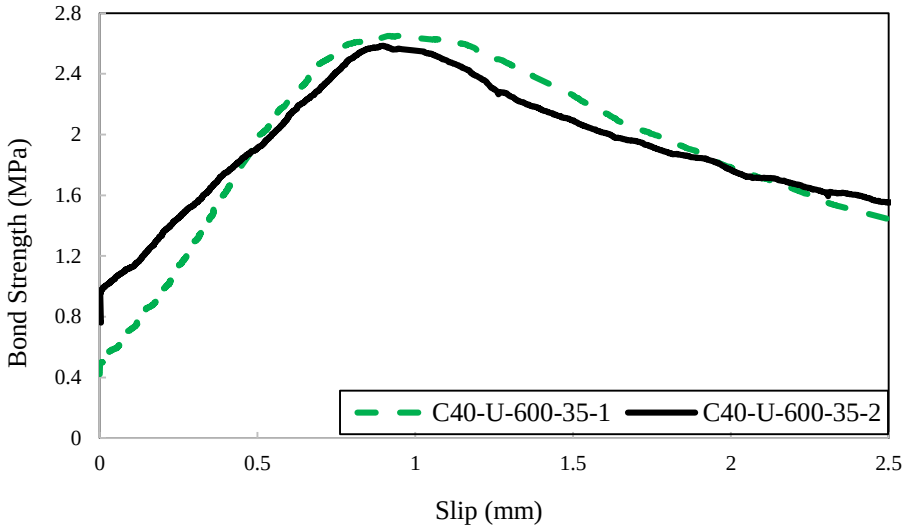

Figure 5.33: Bond stress-slip curves of pull-out specimens (C40-U-600-35)

Figures 5.34 and 5.35 show the stress-slip of the end of the rebar for C40-W samples at 600°C and concrete cover of 25 mm and 35 mm, respectively. The peak point of bond strength in the C40-W-600-25 design was 4.28 MPa and 4.37 MPa for sample 1 and 2, respectively. However, in the C40-W-600-35 design, the peak point of strength was 3.89 MPa and 4 MPa for sample 1 and 2, respectively.

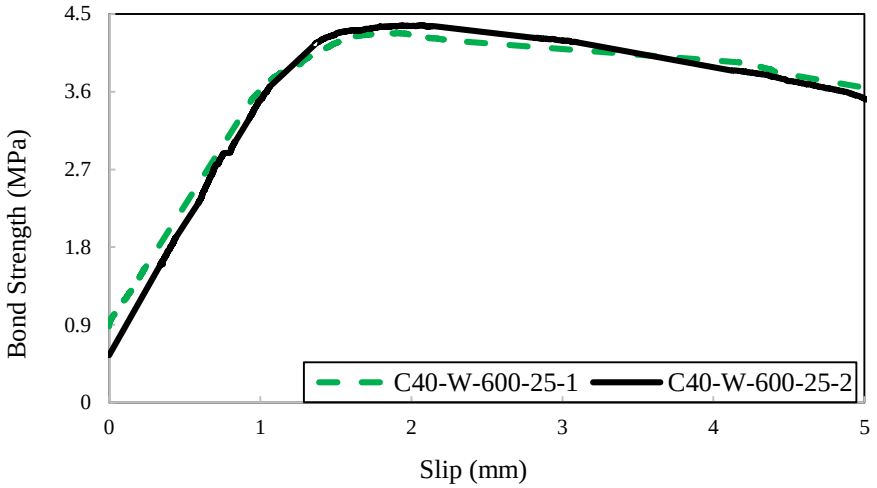

Figure 5.34: Bond stress-slip curves of pull-out specimens (C40-W-600-25)

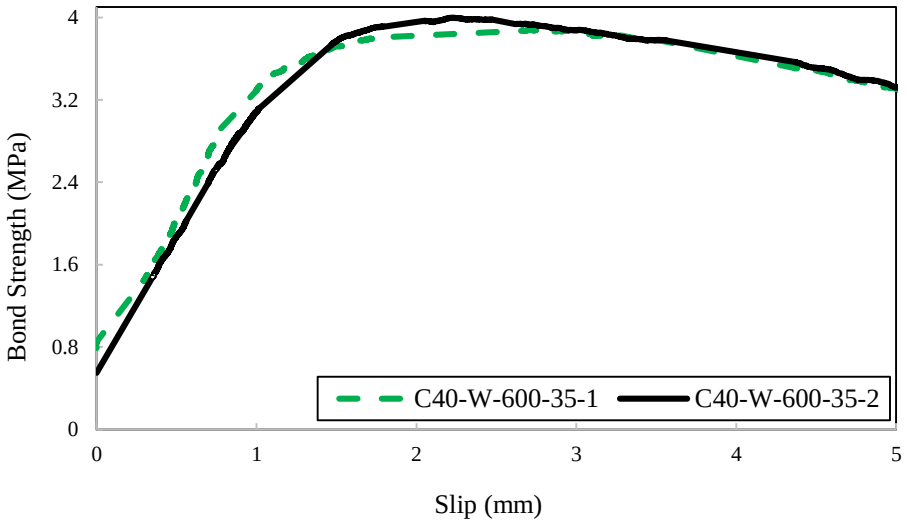

Figure 5.35: Bond stress-slip curves of pull-out specimens (C40-W-600-35)

Figure 5.36 and 5.37 represent the stress-slip of the end of the rebar for C30-U samples at 800°C and concrete cover of 25 mm and 35 mm, respectively. The peak point of bond strength in the C30-U-800-25 design was 0.79 MPa and 0.77 MPa for sample 1 and 2, respectively. However, in the C30-U-800-35 design, the peak point of strength was 1.1 MPa and 1.08 MPa for sample 1 and 2, respectively.

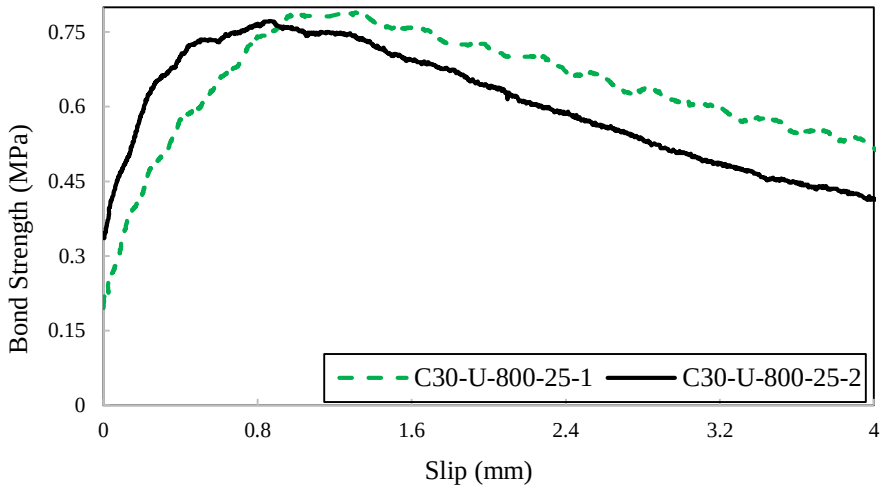

Figure 5.36: Bond stress-slip curves of pull-out specimens (C30-U-800-25)

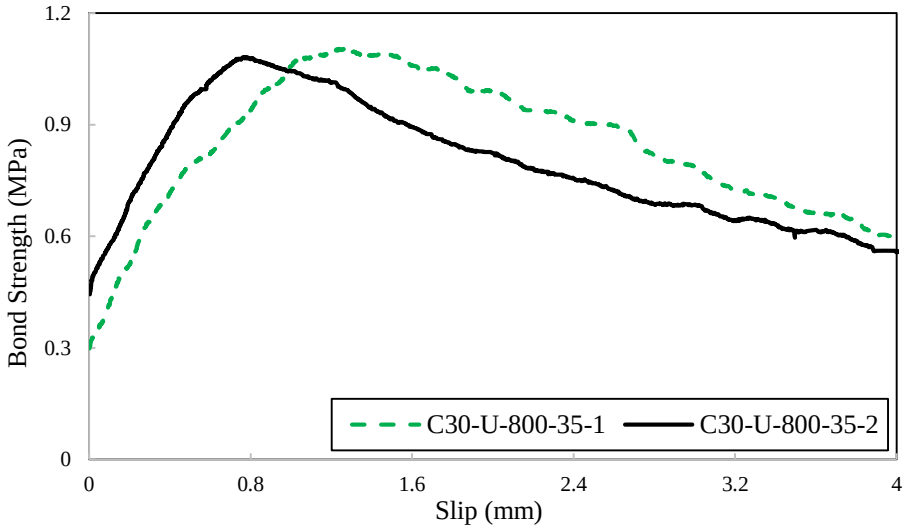

Figure 5.37: Bond stress-slip curves of pull-out specimens (C30-U-800-35)

Figure 5.38 and 5.39 represent the stress-slip of the end of the rebar for C30-W samples at 800°C and concrete cover of 25 mm and 35 mm, respectively. The peak point of bond strength in the C30-W-800-25 design was 1.97 MPa and 2.09 MPa for sample 1 and 2, respectively. However, the C30-W-800-35 has the point of strength of 2.41 MPa and 2.36 MPa for sample 1 and 2, respectively.

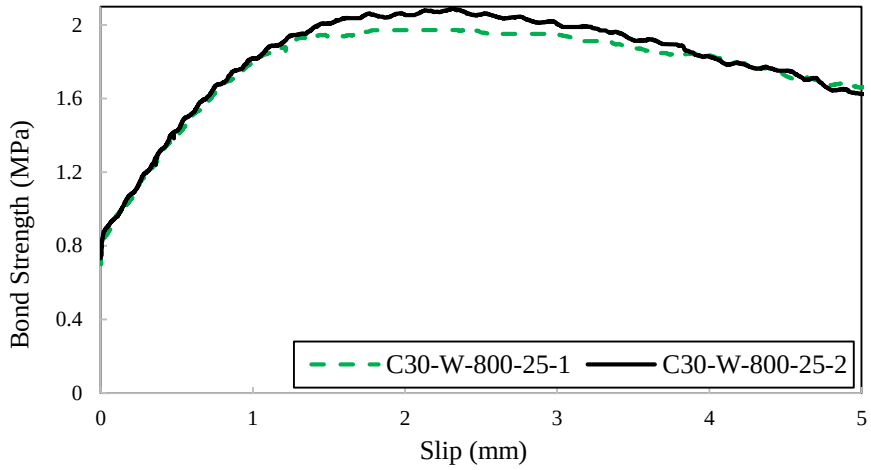

Figure 5.38: Bond stress-slip curves of pull-out specimens (C30-W-800-25)

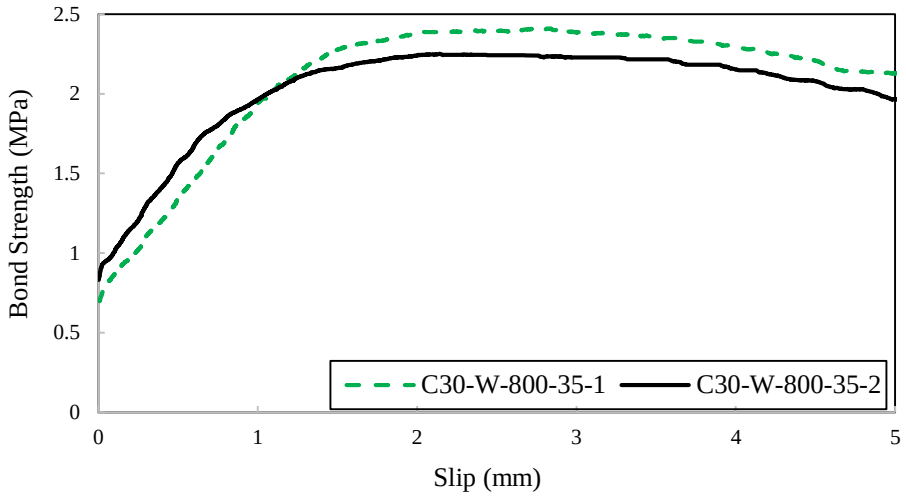

Figure 5.39: Bond stress-slip curves of pull-out specimens (C30-W-800-35)

Figures 5.40 and 5.41 indicate the stress-slip of the end of the rebar for C40-U samples at 800°C and concrete covers of 25 mm and 35 mm, respectively. The peak point of bond strength in the C40-U-800-25 design was 0.85 MPa and 0.88 MPa for sample 1 and 2, respectively. However, in the C40-U-800-35 design, the peak point of strength was 0.96 MPa and 0.99 MPa for sample 1 and 2, respectively.

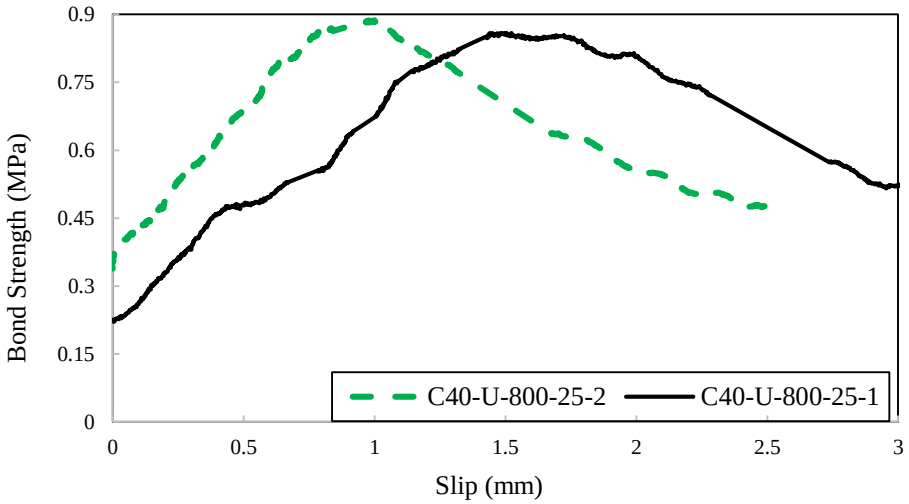

Figure 5.40: Bond stress-slip curves of pull-out specimens (C40-U-800-25)

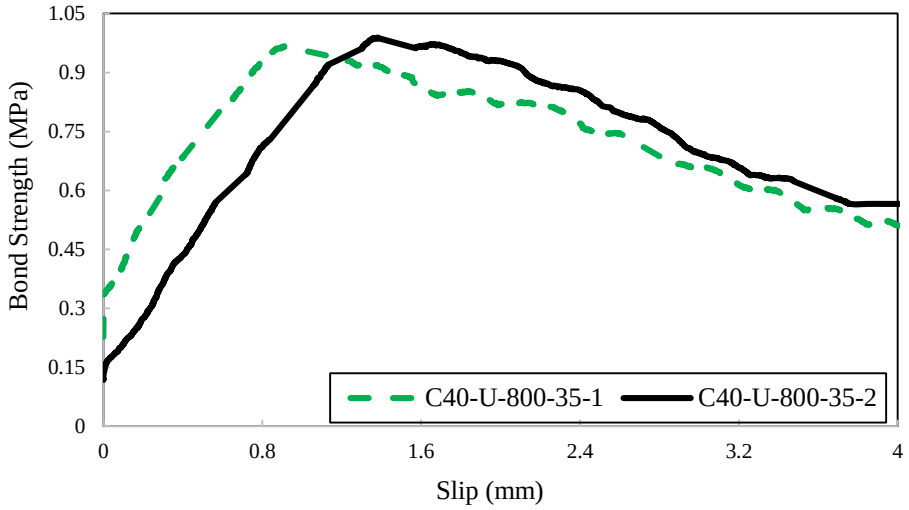

Figure 5.41: Bond stress-slip curves of pull-out specimens (C40-U-800-35)

Figure 5.42 and 5.43 show the stress-slip of the end of the rebar for C40-W samples at 800°C and concrete covers of 25 mm and 35 mm, respectively. The peak point of bond strength in the C40-W-800-25 design was 2.45 MPa and 2.36 MPa for sample 1 and 2, respectively. However, in the C40-W-800-35 design, the peak point of strength was 2.24 and 2.35 MPa for samples 1 and 2, respectively.

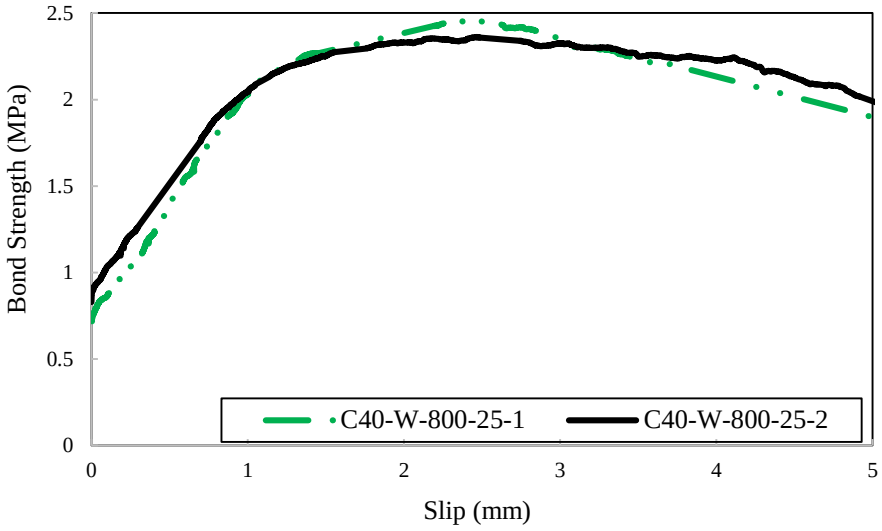

Figure 5.42: Bond stress-slip curves of pull-out specimens (C40-W-800-25)

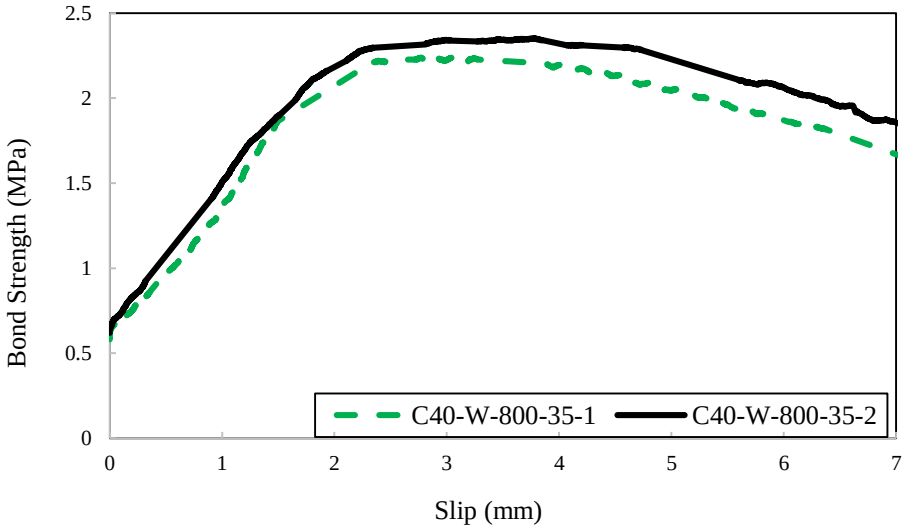

Figure 5.43: Bond stress-slip curves of pull-out specimens (C40-W-800-35)

General information of the specimens after the compressive strength test and pull-out test include compressive strength, bond strength, slip at the end of the bar and failure mode are given in Table 5.1.

Table 5.1: The results of experimental program

Type of specimen	Number of sample	Compressive strength(MPa)	Ultimate bond strength(MPa)	Slip ultimate load (mm)	Failure mode
C30-U-20-25	1	30.1	5.69	0.258	Splitting
	2	30.1	5.62	0.251	Splitting
C30-U-20-35	1	30.1	8.95	0.428	Splitting
	2	30.1	8.59	0.409	Splitting
C30-W-20-25	1	30.1	8.34	1.459	Pull-Out
	2	30.1	8.78	0.618	Pull-Out
C30-W-20-35	1	30.1	9.55	0.851	Pull-Out
	2	30.1	9.82	1.019	Pull-Out
C40-U-20-25	1	39.9	6.50	0.491	Splitting
	2	39.9	6.29	0.473	Splitting
C40-U-20-35	1	39.9	9.55	0.357	Splitting
	2	39.9	9.20	0.407	Splitting
C40-W-20-25	1	39.9	9.83	0.676	Pull-Out
	2	39.9	10.17	1.221	Pull-Out
C40-W-20-35	1	39.9	10.64	1.154	Pull-Out
	2	39.9	10.22	0.900	Pull-Out
C30-U-200-25	1	23.6	4.07	0.272	Splitting
	2	23.6	4.21	0.370	Splitting
C30-U-200-35	1	23.6	5.79	0.382	Splitting
	2	23.6	5.57	0.401	Splitting
C30-W-200-25	1	23.6	6.02	1.260	Pull-Out
	2	23.6	5.90	1.020	Pull-Out
C30-W-200-35	1	23.6	7.83	1.600	Pull-Out
	2	23.6	8.19	1.030	Pull-Out
C40-U-200-25	1	36.5	5.87	0.198	Splitting
	2	36.5	5.64	0.226	Splitting
C40-U-200-35	1	36.5	6.71	0.425	Splitting
	2	36.5	8.45	0.392	Splitting
C40-W-200-25	1	36.5	8.45	2.260	Pull-Out
	2	36.5	8.44	0.905	Pull-Out
C40-W-200-35	1	36.5	9.87	1.710	Pull-Out
	2	36.5	10.14	0.987	Pull-Out

Type of specimen	Number of sample	Compressive strength(MPa)	Ultimate bond strength(MPa)	Slip ultimate load (mm)	Failure mode
C30-U-400-25	1	22.2	2.92	1.078	Splitting
	2	22.2	2.80	0.747	Splitting
C30-U-400-35	1	22.2	4.47	0.907	Splitting
	2	22.2	4.72	1.300	Splitting
C30-W-400-25	1	22.2	6.10	1.870	Pull-Out
	2	22.2	6.25	1.740	Pull-Out
C30-W-400-35	1	22.2	7.07	1.865	Pull-Out
	2	22.2	7.53	0.846	Pull-Out
C40-U-400-25	1	32.6	4.43	0.882	Splitting
	2	32.6	4.29	0.982	Splitting
C40-U-400-35	1	32.6	6.30	0.335	Splitting
	2	32.6	6.02	0.436	Splitting
C40-W-400-25	1	32.6	6.99	1.555	Pull-Out
	2	32.6	7.04	1.220	Pull-Out
C40-W-400-35	1	32.6	7.47	1.041	Pull-Out
	2	32.6	7.39	1.214	Pull-Out
C30-U-600-25	1	15.3	1.52	0.663	Splitting
	2	15.3	1.47	0.640	Splitting
C30-U-600-35	1	15.3	2.18	0.727	Splitting
	2	15.3	2.09	0.889	Splitting
C30-W-600-25	1	15.3	3.65	2.069	Pull-Out
	2	15.3	3.54	2.210	Pull-Out
C30-W-600-35	1	15.3	5.02	1.849	Pull-Out
	2	15.3	4.87	1.400	Pull-Out
C40-U-600-25	1	18.9	1.82	0.760	Splitting
	2	18.9	1.78	0.853	Splitting
C40-U-600-35	1	18.9	2.65	0.913	Splitting
	2	18.9	2.58	0.898	Splitting
C40-W-600-25	1	18.9	4.28	1.855	Pull-Out
	2	18.9	4.37	2.303	Pull-Out
C40-W-600-35	1	18.9	3.89	2.710	Pull-Out
	2	18.9	4.00	2.381	Pull-Out
C30-U-800-25	1	7	0.79	1.307	Splitting

Type of specimen	Number of sample	Compressive strength(MPa)	Ultimate bond strength(MPa)	Slip ultimate load (mm)	Failure mode
	2	7	0.77	0.862	Splitting
C30-U-800-35	1	7	1.10	1.236	Splitting
	2	7	1.08	1.006	Splitting
C30-W-800-25	1	7	1.98	2.445	Pull-Out
	2	7	2.09	2.318	Pull-Out
C30-W-800-35	1	7	2.41	2.820	Pull-Out
	2	7	2.36	2.141	Pull-Out
C40-U-800-25	1	6.9	0.85	2.129	Splitting
	2	6.9	0.89	0.978	Splitting
C40-U-800-35	1	6.9	0.96	0.911	Splitting
	2	6.9	0.99	1.378	Splitting
C40-W-800-25	1	6.9	2.46	2.331	Pull-Out
	2	6.9	2.36	2.465	Pull-Out
C40-W-800-35	1	6.9	2.24	3.057	Pull-Out
	2	6.9	2.35	3.782	Pull-Out

Figure 5.44 is presented for better understanding and easier comparison of all specimens to help arriving conclusions. Figure 5.44 shows the relationship between bond strength and free end slip of rebar for all studied designs. In this figure, to make it easier to deduce charts, just one specimen's data is given in the figure of each model designs. The charts represent a specific temperature at each row and a specific concrete covering is given in each column. In addition, the curves for wrapped and unwrapped designs in a particular mix design are presented in each graph.

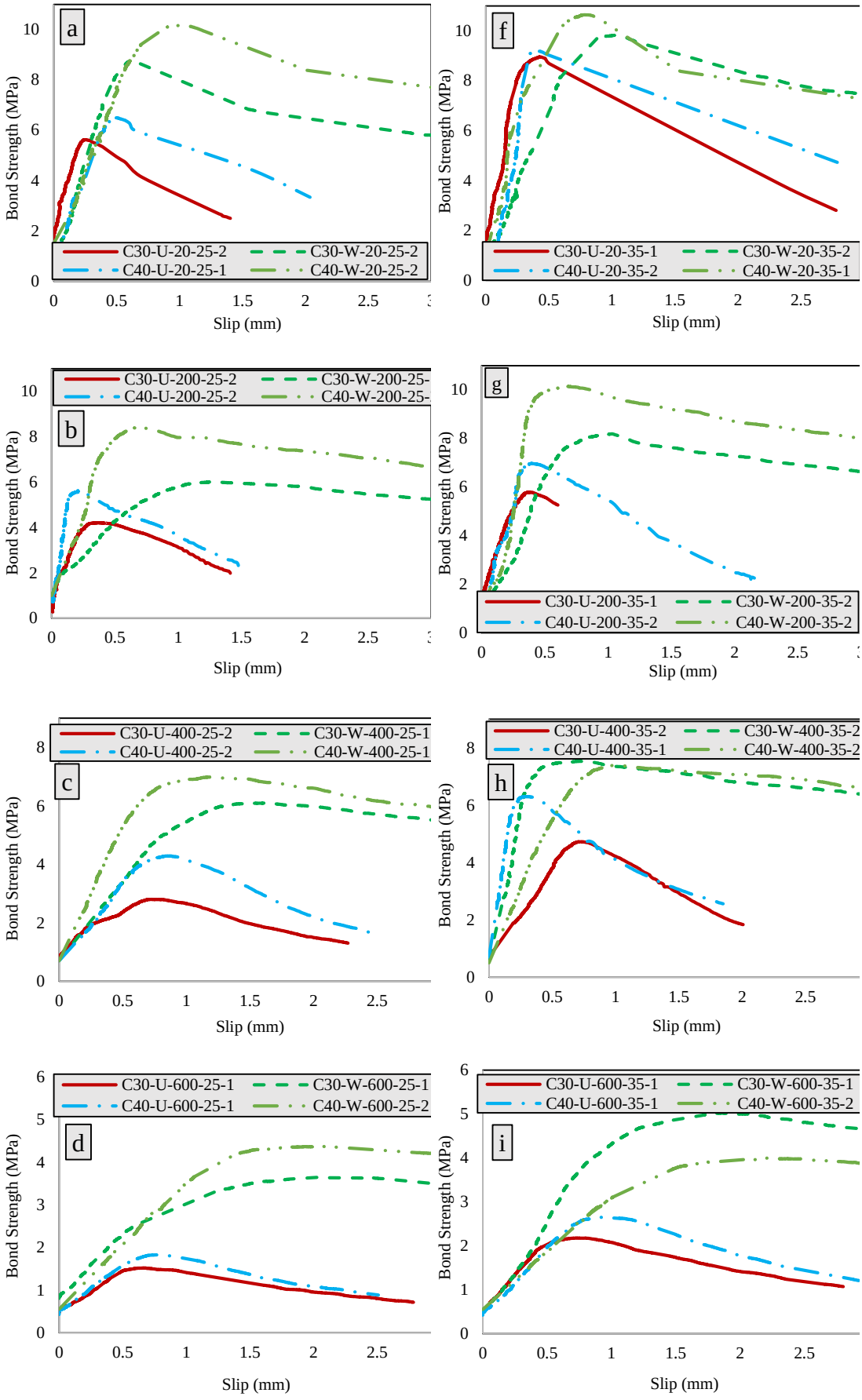
a
Bond Strength (MPa)
Slip (mm)
C30-U-20-25-2
C30-W-20-25-2
C40-U-20-25-1
C40-W-20-25-2
f
C30-U-20-35-1
C30-W-20-35-2
C40-U-20-35-2
C40-W-20-35-1
b
C30-U-200-25-2
C30-W-200-25-
C40-U-200-25-2
C40-W-200-25-
g
C30-U-200-35-1
C30-W-200-35-2
C40-U-200-35-2
C40-W-200-35-2
c
C30-U-400-25-2
C30-W-400-25-1
C40-U-400-25-2
C40-W-400-25-1
h
C30-U-400-35-2
C30-W-400-35-2
C40-U-400-35-1
C40-W-400-35-2
d
C30-U-600-25-1
C30-W-600-25-1
C40-U-600-25-1
C40-W-600-25-2
i
C30-U-600-35-1
C30-W-600-35-1
C40-U-600-35-1
C40-W-600-35-2

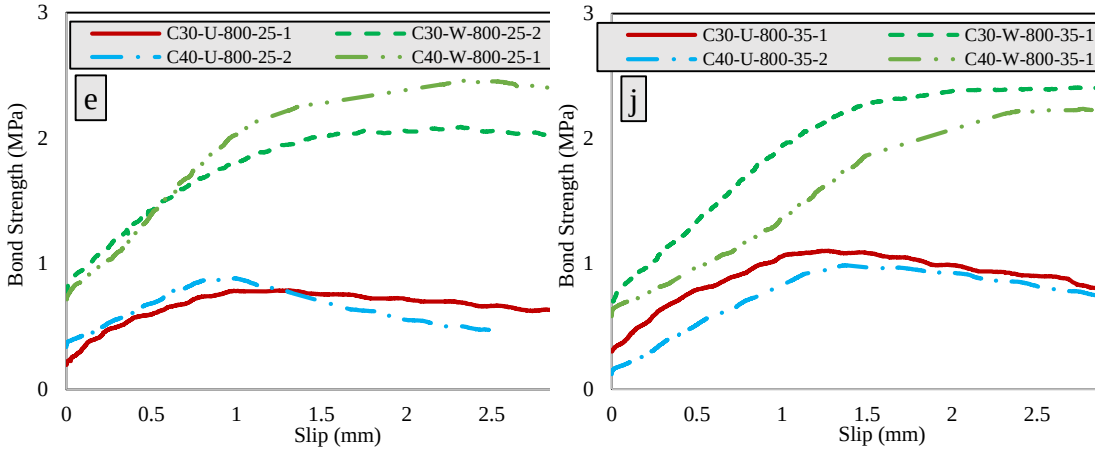

Figure 5.44: Bond stress-slip curves of pull-out specimens

These charts can be obtained when the bond stress increases the slip at a fixed rate to reach the final strength and then the bond strength curve falls. In the initial loading phase, the response consists of a hard linear component in which the bond strength is mainly composed of chemical bonding or friction. As the temperature drops in the sample the bond strength increases. It can be seen from Figure 5.44 that by increasing the temperature the slope of the curves (initial stiffness) also falls sharply. Certainly, this drop is much more obvious in higher temperatures. When the curves are compared, it can be concluded that specimens that are exposed to lower temperatures with increasing compressive strength of the concrete leads to increase in the bond strength of the concrete. This bond strength growth is due to the increased strength of the concrete between the shear keys (treads of the rebar). However, by increasing the temperature concrete gets cracked, compression strength is reduced to the point where the compressive strength is identical in both types of concrete. Therefore, the resistance of the shear keys is greatly reduced and consequently the bond strength of the two types of concrete is uniform at high temperatures and the difference is subtle. By comparing the same curves in the two columns of Figure 5.44 it can be seen that by increasing the concrete cover from 25 mm to 35 mm the slope of the graphs and

also the peak point of the growth were significant. This increase in the strength and stiffness is the result of increased concrete cover and energy stored with this increase.

This can be explained by increasing the enclosure, which leads to more resistance in longitudinal cracks and decreases in the distribution of non-uniform tension in embedded length. By comparing the graphs in different rows it can be concluded that the effect of concrete coverings on different temperatures is evident and the curve representing samples with concrete coverings of 35 mm has been able to exhibit a higher bond stress than those of 25 mm concrete coverings. However, with increase in temperature this difference is reduced but still tangible. Reduction of the bonding strength difference between the two samples with different concrete coverage at high temperatures can be due to the reduction of compressive strength, hence weakness of the concrete, shear keys and the lesser impact of concrete covers.

By observing each graph and comparing the curves of the same specimens wrapped and unwrapped ones it can be concluded that the positive effect of the CFRP sheets wrap on the bond strength is evident. With the presence of CFRP wrapped the bond behavior of pull out specimens has dramatically increased. This growth was more evident in samples that have been exposed to high temperatures. In addition, it is obvious that unwrapped specimens in a brittle and crisp state are suddenly broken with formation of longitudinal cracks, the bond stress was severely reduced, and the graph is cutoff. This can explain the failure mechanism based on the failure energy criterion: Strain energy keeps on accumulating in the materials micro-cracking propagates at about 70-80% of ultimate.

As soon as the primary crack, along the boundary between the steel bar and the concrete, is formed it immediately leads to the release of the crack using stored energy. While in wrapped specimens after the formation of cracks, CFRP sheets prevent the cracks and specimen rupture and the bond behavior is enhanced. This growth continues to the point where the radial stresses are increased and the shearing keys slipped and the steel bar reinforcement removed from the concrete, which is shown as nearly a horizontal line in the graph.

5.5 Bond Strength After Pull-out Test

The results of the pull out test (for example the maximum bond strength and its corresponding slip and compressive strength) are given in Table 5.1 with attention to the corresponding temperature. The results presented in the table have been used to study the basic variables on bond behavior. The variables affecting bond behavior in this study were compressive strength of concrete subjected to heat, concrete covering around steel bars and CFRP wrapped, which are discussed individually for better understanding of the impact of each variable. The maximum of bond strength is presented in Table 5.1 and better understanding of the process of variables' effect, percentages presented in figures 5.45 to 5.49 relative to the non-heated specimen. According to Table 5.1, effect of CFRP wrapping on the bonding strength of the heated samples is very impressive and its effect at temperatures of 20°C, 200°C, 400°C, 600°C and 800°C for C30 group of specimens and 25 mm concrete covering relative to the corresponding heated samples, the increasing of the bond strength is equal to 51%, 44%, 115%, 141% and 160% respectively. Heat and strengthening on other group of samples also had the same behavior.

To obtain these graphs, the numerical value of each plot is divided into the corresponding non-heated reference sample value so that the values can be obtained in relative terms, a better comparison and easier deduction can be made, and on the other hand the effect of the parameters can be easily extracted.

Figure 5.45 is presented for investigate the effect of the temperature, compressive strength of concrete and concrete coverings on bond strength. By observing Figure 5.45, it can be seen that with increasing temperature, bond strength decreases and the severity of strength reduction increases for specimen exposed to higher temperature. The downward trend of bond strength was almost the same for the different compressive strength specimen model (C30 and C40). In the Figure 5.45, by comparing the wrapped and unwrapped specimen diagrams in a row it can be concluded that the process of reducing the bond strength has been slower for wrapped sample. At the temperature of 600°C and 800°C, respectively, the relative residual bond strength is on average 0.26 and 0.11 for unwrapped samples and 0.43 and 0.25 for wrapped samples.

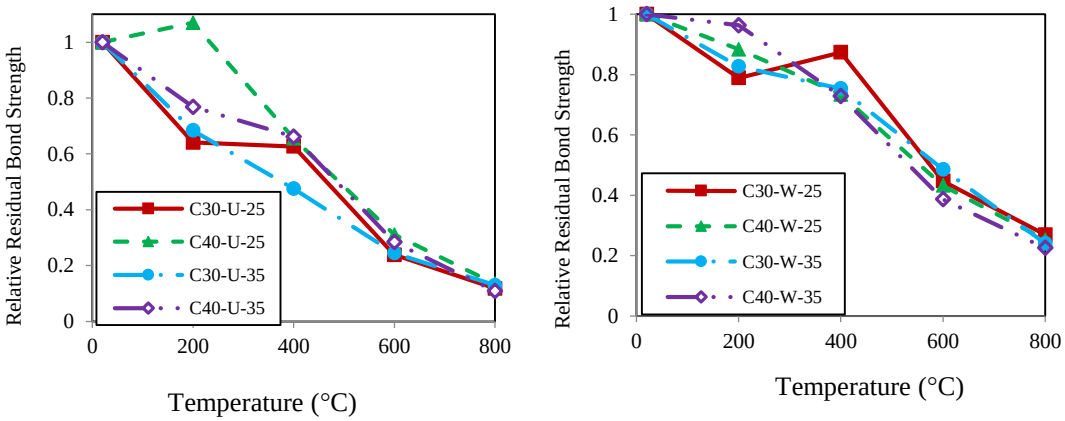

Figure 5.45: Degradation of bond strength of concrete in post-heating specimens (the effect of cover and compressive strength)

Considering both Table 5.1 and Figure 5.45 it can be seen that by increasing compressive strength the bond strength has also increased. When the concrete covering is reduced from 35 mm to 25 mm, the final bond strength decreased and the corresponding slip increased.

Figure 5.46 illustrates the effect of heat, concrete coverage and CFRP wrapped on bond strength. By observing Figure 5.46 it can be seen that in spite of the CFRP wrapped the bond strength has also increased. This increase was higher for 25 mm concrete cover specimen due to the increased enclosure compared to a 35mm concrete cover. Also, the effect of the CFRP wrapped on the exposed high temperature specimen was higher. The effect of CFRP wrapping in the 30C-25 and 30C-35 group of specimens, C40-25 and C40-35 group of specimens was 23%, 14%, 68% and 21% respectively, at ambient temperature while the same growth at the temperature of 800°C was 182%, 113%, 215% and 152% respectively. During the testing process, the CFRP sheets cause a significant pressure on the surrounding concrete resulted in increased elastic confinement, locking and mechanical fastening around the rebar.

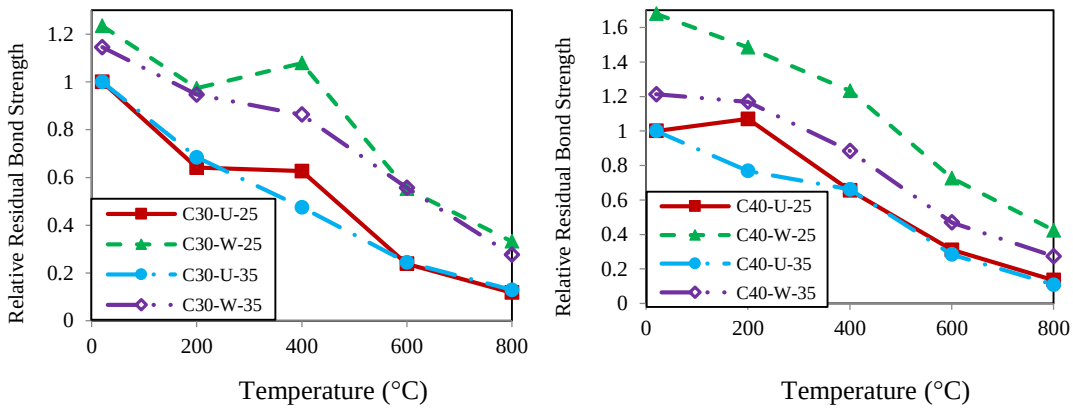

Figure 5.46: Degradation of bond strength of concrete in post-heating specimens (the effect of cover and CFRP wrap)

Figure 5.47 shows the strengthening capability with CFRP to retrieve the bond strength between steel bars and heat-damaged concrete. As can be seen from the figure, strengthening by CFRP can compensate drop in bond strength formed because of heat in pull out specimen to a large extent. It can be deduced from the figure that when a concrete specimen is heated to 400°C, the strengthening with a CFRP layer can compensate almost the entire drop of bond strength. For the C40 group of specimen, the drop of bond strength is completely compensated (up to 400°C). On the other hand, due to the more effective wrapping effect of the concrete samples with less cover, retrieval of bond strength for 25mm concrete cover samples is well compensated for C30 group of specimens. At temperatures of 600°C and 800°C, despite the high efficiency of strengthening due to the serious drop in compressive strength and consequently the bond strength, the strength has not been reached to the initial strength.

The effect of strengthening on bond strength at 20°C, 200°C, 400°C, 600°C, 800°C for C30 designs and 25 mm concrete coverage relative to the reference sample were 23% increase, 2% decrease, 8% increase, 44% decrease, and 66% decrease, respectively.

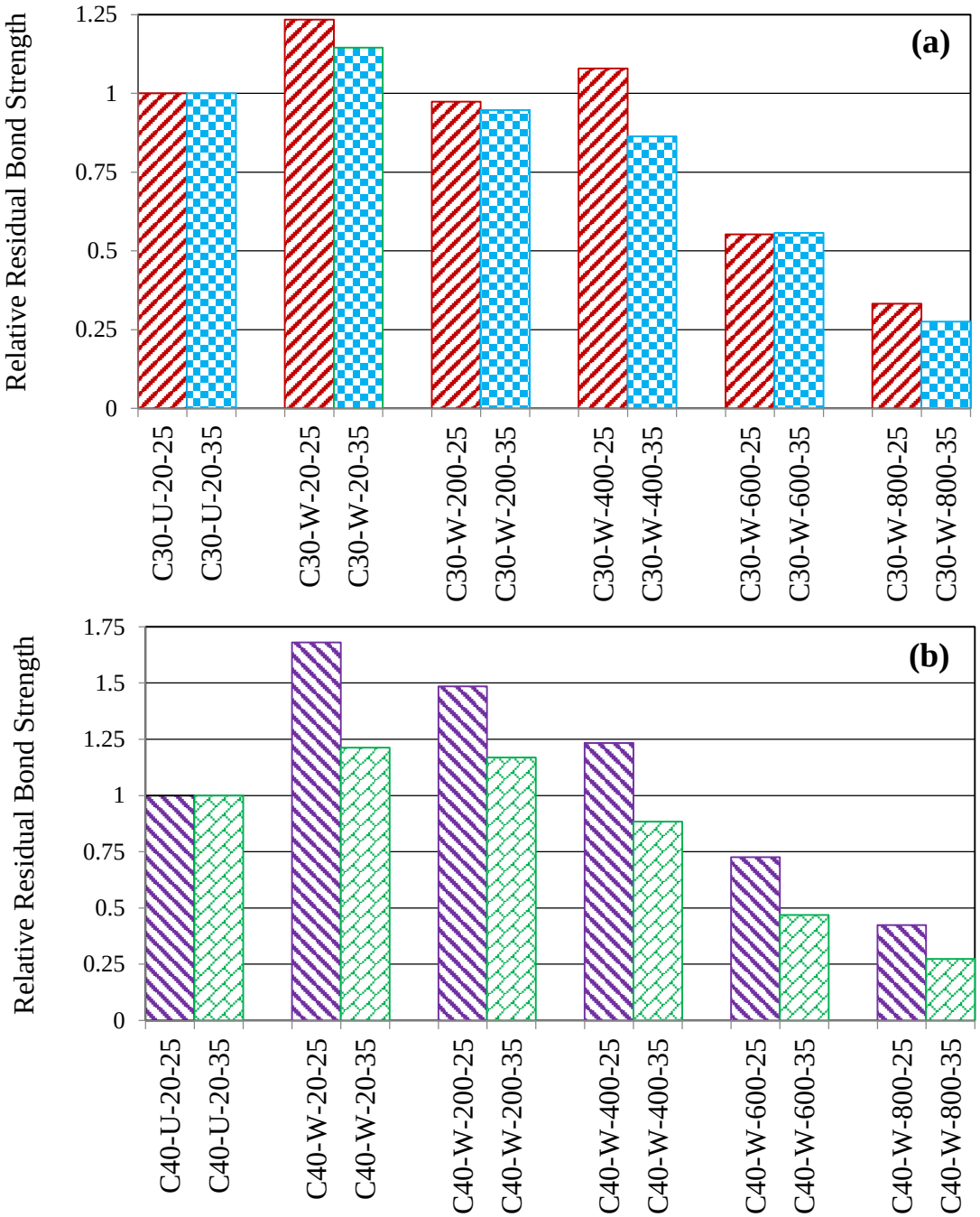

Figure 5.47: Effect of Strengthening in the recovery of bond strength (a: C30, b: C40)

Figure 5.48 shows a comparison between the drop of compressive strength and bond strength of heated and unwrapped group of specimens. Depending on the figure, it can be concluded that the drop of compressive strength is less than the drop of the bond strength. This drop was also noticeable in the C30 group of specimens. So that the relative residual compressive strength of the C30 group of specimens at 200°C, 400°C,

600°C and 800°C was 0.78, 0.73, 0.5, 0.23 respectively and the relative residual compressive strength of the C40 group of specimens at 200°C, 400°C, 600°C and 800°C was 0.91, 0.81, 0.47, 0.17 respectively. While the average relative bond strength (average of different concrete covers) at the above mentioned temperatures for the C30 group of specimens is 0.66, 0.54, 0.24, 0.13 and for the C40 group of specimens it is 0.92, 0.66, 0.30 and 0.12 respectively. This change in behavior is due to the fact that the bond function is a tensional stress and since the tensional strength of the concrete under fire is greater than the compressive strength therefore the further reduction of the bond strength than the compressive strength is reasonable and justified.

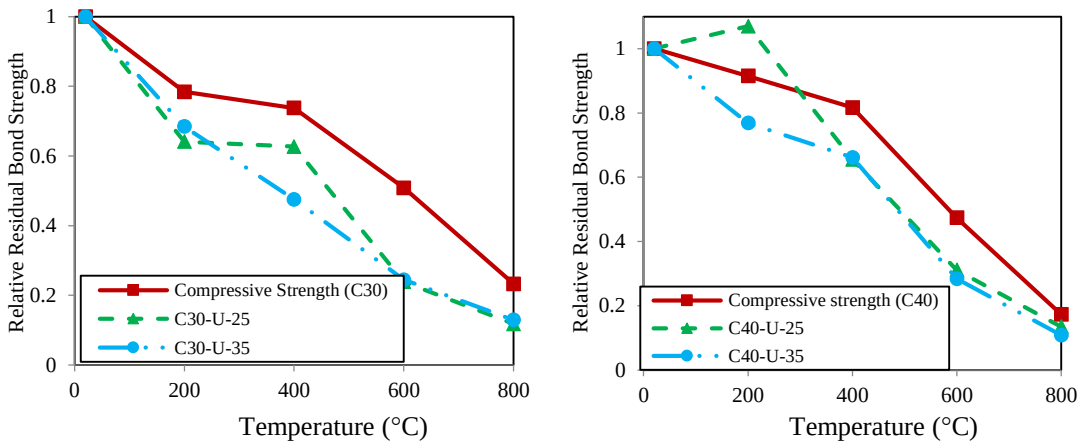

Figure 5.48: Degradation of bond strength and compressive strength of concrete in post-heating unwrapping specimen

Figures 5.49 and 5.50 both show bond strength variations due to increasing in temperature and is prepared for better understanding the effect of the heat on the bond strength. The relative residual bond strength at 200°C, 400°C, 600°C and 800°C temperatures for C30 group of specimens (average for all C30 specimens) was 0.73, 0.68, 0.35 and 0.19 respectively, while this parameter was 0.92, 0.69, 0.35 and 0.18 for C40 group of specimens respectively. By carefully examining these two graphs it can be seen that up to 400°C the drop of bond strength in the C30 specimen was more

and with increasing temperature the C40 drainage curves have been increased and to the extent that at 800°C the bond strength of the two designs is approximately the same. The main cause of the reduction of the concrete strength is the formation of internal cracks due to the evaporation of water from the cavity structure vents at 200°C. At a high temperature of 400°C, the reduction of strength was happened. This reduction is attributed to water losing from CSH and CSH graft decomposition. Therefore, the compressive strength of the concrete with the loss of CSH is almost identical at the high temperatures.

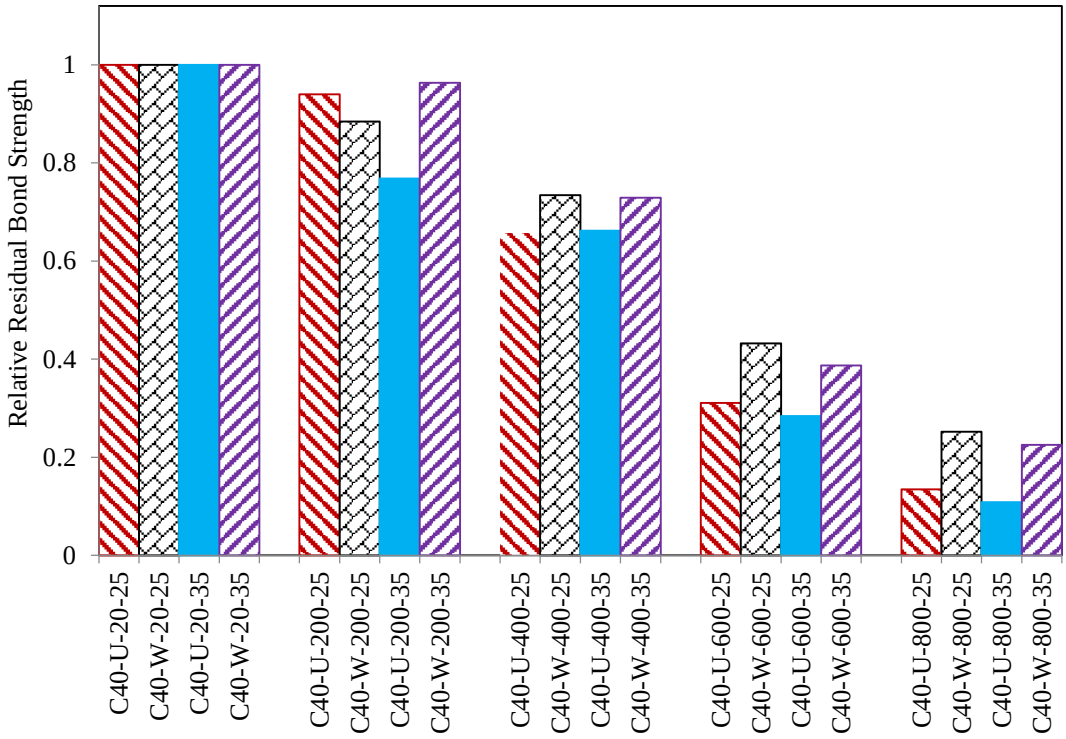

Figure 5.49: Variation of relative residual bond strength with temperature for C30

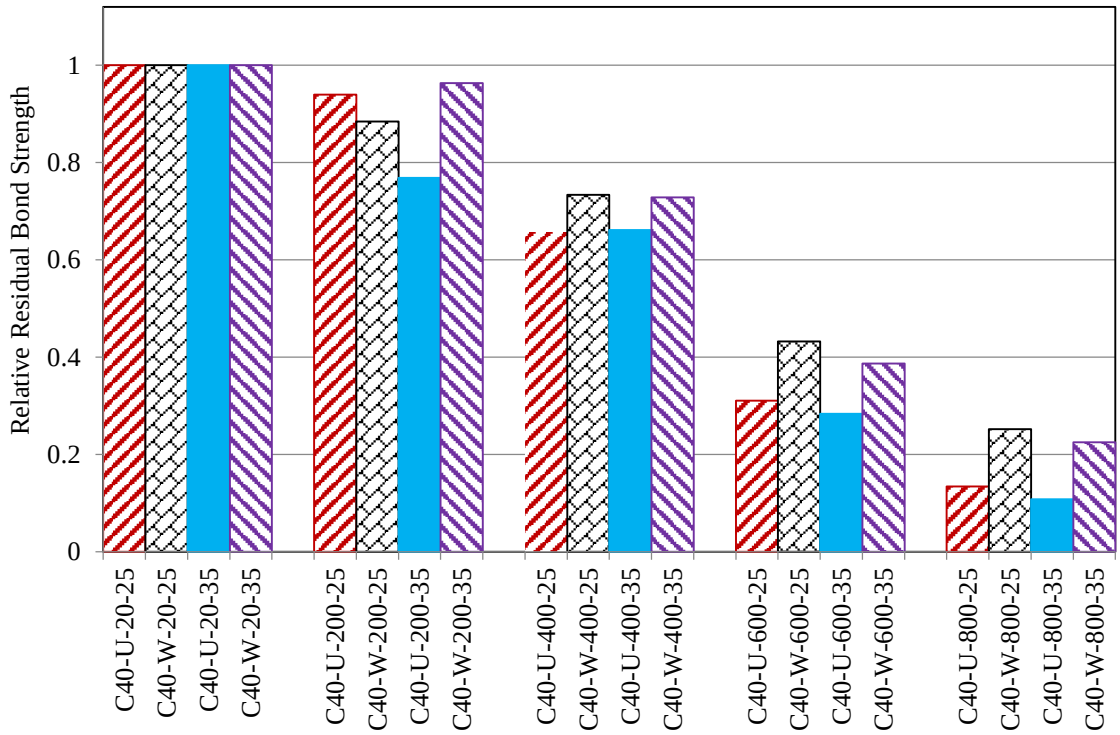

Figure 5.50: Variation of relative residual bond strength with temperature for C40

For the steel rebar, which have lugs on the surfaces, strength against pull out is mainly due to the shear capacity of the concrete around the bars' lugs. Adhesion and friction have a small contribution. When the rebar is pulled out the force works with the two components in the lugs. The horizontal component tries to cut the concrete between the hugs while the vertical component produces radial stresses that cause tensional stresses in surrounding concrete. The horizontal component tries to cut the concrete between the hugs while the vertical component produces radial stresses that cause tensional stresses in surrounding concrete. Compressive strength and tensional strength of concrete are the main parameters affecting the bond strength among the reinforced members with the steel rebar. According to the description given in the above, the concrete specimen exposed to heat, mechanical properties such as compressive strength and tensional strength and thus the bond strength are reduced. By installing the CFRP sheet wrapping and strengthening concrete specimens in the

process of bar pull out testing and applying the tensional force to the bar, the CFRP sheet has a significant pressure on the concrete, which causes the confinement effect and thus improves the bond strength.

Chapter 6

CONCLUSION AND RECOMMENDATIONS FOR FUTURE WORK

6.1 Conclusion

In the first part of the study, repairing and shape modification of fire-damaged specimens using expansive concrete and strengthening affect with CFRP have been studied. The axial compressive strength of shape-modified post-heated specimens and the effect of CFRP wrapping have been investigated and compared with the un-heated specimens as reference specimens.

The second part of the thesis have been studied about simulation of the effects of fire in the building and investigation of the bond behavior of rebar and damaged concrete exposed to fire in different temperatures and the effect of strengthening with carbon fiber reinforced polymer sheets.

Major conclusions from this study can be summarized as:

1. In section 1, failure in specimens without wrapping has been due to concrete crashing. While, in the wrapped specimens, the failure was owing to concrete crashing and followed by rupture of CFRP composite with explosion and a loud booming noise. Failure in shape-modified specimens without wrapping has been in the form of separation of the two concrete layers from each other.

Whereas, failure in shape modified specimens with wrapping was similar to the wrapped circle specimens.

2. The compressive strength of the concrete specimens, which are exposed to heating to 500 °C in section1, has significantly decreased. This reduction for square series specimens and circular series specimens has respectively been 56% and 42% relative to un-heated specimens.
3. The compressive strength of the specimens after strengthening with two layers CFRP wrapping (first section of study) has significantly increased. This increase in the un-heated specimens was more than twice and for fire-damaged specimens was significant and reached to more than three times of the growth for the P-O specimens.
4. Shape modification and repairing of the fire-damaged specimens caused increase in compressive strength and in unwrapped specimens has reached to the strength of square specimens. When they are strengthened, the strength has enhanced more than two times than unwrapped specimens and more than four times than heated square specimens.
5. The initial slope of the curve related to the unheated specimens and also the unheated confined specimens has nearly been identical and consistent with each other. However, by placing the specimens exposed to the heat, the slope in elastic state of specimens has been sharply decreased and confinement also has little effect on the initial stiffness. Therefore, the slope of stress-strain curve in elastic range could be considerably increased and has been largely compensated for fire-damaged specimens using shape modification.

6. The modulus of secant has been sharply decreased due to heating. The reduction in modulus of secant of fire-damaged specimens has been more than the reduction in compressive strength of specimens.
7. The effect of CFRP wrappings on the modulus of secant has been negligible being as a result of weak effect of concrete confinement in elastic state of loading. Although Shape modification of a square section to a circle section has a considerable effect on the modulus of secant of fire-damaged specimens so that with shape modification, the reduction in this parameter was compensated to a large and increased more than eight times with respect to the damaged specimens, while not reaching to the initial value.
8. In the second part of thesis, after the heating process was completed and the samples were removed from the furnace, no crushing was observed in the specimens. Even at a temperature of 200°C, no superficial cracking has been observed. But superficial cracking caused by heat was observed as the temperature rises. Therefore, superficial cracking of the specimens exposed to higher temperature are more visible.
9. In the second part of study, the unwrapped specimens have a break in fragile conditions with high sound and the specimen suddenly becomes disturbed by the development of longitudinal splitting crack. This type of breaking for unwrapped specimens was observed at all temperatures but at lower temperatures it occurred more brittle and louder. However, the strengthening and wrapping specimen by a CFRP layer prevents the cracks from spreading and also changes the failure mode to the pulling out bar as a soft breaking.

10. The remained compressive strength of specimens drops by increasing temperature of heat slowly up to 400°C. But this drop is faster by increasing temperature of heat up to 800°C, insofar as, specimen loses its compressive strength by as much as 80% at 800°C.
11. After the heating of pull-out test specimens, the drop of stiffness and strength was observed in the load-slip diagram at the free end of the rebar. However, with increase in heat, the drop of the above parameters was also more evident. However, the aforementioned drop in specimens with higher compressive strength (C40 specimens) and more concrete covering (35mm concrete cover specimens) was lower than other specimens.
12. The stiffness and bond strength behavior between steel bars and heat damaged concrete in similar specimens of the C40 plan were more than the C30 design. Therefore, increasing compressive strength of concrete causes the growth of bond strength under heat.
13. The bond strength of the specimens has grown dramatically with strengthening by a CFRP layer and also the drop of bond strength with increasing the temperature and un-wrapped specimen was lower significantly.
14. The bond strength of between steel bar and concrete was dropped after exposed to the high temperature. Intensity of this drop goes up by increasing the temperature over 400°C. The CFRP confinement of specimens caused to dramatic increase in bond strength. The growth has been more dramatic in specimens exposed to higher temperatures. The maximum growth in the bond strength of the non-heated specimens is 68% while the growth is above 115% for specimens that have been heated up to 800°C and even insofar as, it reaches to 215% in the C40-25 scheme.

15. When the concrete cover was reduced from 35mm to 25mm, the final bond strength between the steel rebar and the concrete have been reduction while the corresponding slip have been increase. After the CFRP wrapping on the specimens, the bond strength increased, which the increase bond strength of specimen with 25mm concrete cover was more dramatic from the specimen with 35mm cover.
16. Strengthening by a CFRP layer has been very effective in restoring the bond strength of the heated damaged specimens. To the extent that, the strengthening has completely compensated the drop of bond strength of heated samples that were exposed to temperatures of up to 400°C. However, the effect of retrofit in concrete samples with 25 mm cover was more impressive than concrete samples with 35 mm cover and the loss of bond strength (up to 400°C) is was completely compensated.

6.2 Recommendations for Future Work

Since the problem of repairing and retrofitting structures under heat in structural engineering is a completely new subject, there are a lot of opportunities for future work and research. Hence, there are a series of recommendations for future researchers who want to work in conjunction with this subject that the mentioned in below:

a) Investigation of the bonding behavior between steel bars and low-strength concrete with different cross-sectional thickness and diameter.
b) Evaluation of the bonding behavior of steel bars in low strength concrete under cyclic loading.
c) Use of high-strength repair concrete such as RPC concrete.

d) Investigating the effect of heat on square columns with longitudinal and transverse bars.

e) Providing some methods of enhance the elastic modulus

REFERENCES

[1] Medina, C., Zhu, W., Howind, T., Sánchez de Rojas, M. I., & Frías, M. (2014). Influence of mixed recycled aggregate on the physical – mechanical properties of recycled concrete. *Journal of Cleaner Production*, 68, pp.216–225.

[2] Boris Kolle. (2006). Behaviour of Steel Fibre Reinforced High Performance Concrete under Biaxial Loading Conditions", PhD Thesis, University of Glasgow.

[3] I.A. Fletcher, S. Welch, J.L. Torero, R.O. Carvel, A. (2007). Usmani, Behaviour of concrete structure in fire, Therm. Sci. 11(2), pp.37–52.

[4] Ismail M A F. (1970). "Bond deterioration in reinforced concrete under cyclic loading". Houston, Texas, USA: College of Engineering, Rice University.

[5] Panda A K. (1984). Bond of deformed bars in steel fiber reinforced concrete under cyclic loading [D]. Vancouver, Canada: College of Civil Engineering, University of British Columbia.

[6] R, Popov E P, Bertero.(1983). Local bond stress-slip relationships of deformed bars under generalized excitations [R]. Berkeley: University of California.

[7] Lee, J. Y., Kim, T., Kim, T. J., Yi, C. K., Park, J. S., You, Y. C., & Park, Y. H. (2008). Interfacial bond strength of glass fiber reinforced polymer bars in high-strength concrete. Composites Part B: Engineering, 39(2), pp.258–270.

[8] Cosenza, E., Manfredi, G., & Realfonzo, R. (1997). Behavior and modeling of bond of FRP rebars to concrete. *Journal of Composites for Construction*, 2(1994), pp.40–51.

[9] Okelo, R., & Yuan, R. L. (2005). Bond strength of fiber reinforced polymer rebars in normal strength concrete. *Journal of Composites for Construction*,9(3), pp.203–213.

[10] Achillides, Z., & Pilakoutas, K. (2004). Bond behavior of fiber reinforced polymer bars under direct pullout conditions. *Journal of Composites for Construction*, 8(April), pp.173–181.

[11] Aiello, M. A., Leone, M., & Pecce, M. (2007). Bond Performances of FRP Rebars-Reinforced Concrete. *Journal of Materials in Civil Engineering*, 19(March), pp.205–213.

[12] Rossetti, V. A., Giammatteo D. G. M. M. (1995). Local bond stress-slip relationships of glass fibre reinforced plastic bars embedded in concrete. *Materials and Structures*, 28, pp.340–344.

[13] Arias, J. P. M., Vazquez, a., & Escobar, M. M. (2012). Use of sand coating to improve bonding between GFRP bars and concrete. *Journal of Composite Materials*, 46(18), 2271–2278.

[14] Benmokrane, B., Zhang, B., Laoubi, K., Tighiouart, B., & Lord, I. (2002). Mechanical and bond properties of new generation of carbon fibre reinforced polymer reinforcing bars for concrete structures. Can. J. Civ. Eng, 29, 338–343.

[15] Hao, Q., Wang, Y., He, Z., & Ou, J. (2009). Bond strength of glass fiber reinforced polymer ribbed rebars in normal strength concrete. Construction and Building Materials, 23(2), 865–871.

[16] P. Morely, R. Royles, (1983). Response of the bond in reinforcing concrete to high temperatures, Mag. Concr. Res,35(123), pp.67–74.

[17] R. Haddad, L. Shannis. (2004). Post-fire behavior of bond between high strength pozzolanic concrete and reinforcing steel, Construction. Build. Mater, 18, pp.425–435.

[18] R.H. Haddad, R.J. Al-Saleh, N.M. Al-Akhras. (2008). Effect of elevated temperature on bond between steel reinforcement and fiber reinforced concrete, *Fire Safety Journal*, 43, pp.334–343.

[19] A.F. Bingol, R. Gul. (2009). Residual bond strength between steel bars and concrete after elevated temperatures, *Fire Safety Journal*, 44 ,854–859.

[20] Yaqub, M. Bailey, C.G. (2011). "Repair of fire damaged circular reinforced concrete columns with CFRP composites", *Construction and Building Materials*, 25, pp.359–370.

[21] Assessment design and repair of fire-damaged concrete structures. Technical Report-68, Concrete Society, Camberley, UK.

[22] Marchant.E.W. (1972). A complete guide to fire and buildings. Medical and Technical Publishing, London.

[23] Assessment of fire-damaged concrete structures and repair by gunite. Concrete Society Technical Report No.15.

[24] Assessment and repair of fire-damaged concrete structures. Concrete Society Technical Report No.33.

[25] Repairability of fire damaged structures CIB W14 Report. (1990). *Fire Safety Journal*, 16(4), pp. 251-336.

[26] Concrete for fire resistant construction. (1979). A Cembureau Report prepared with the assistance of FIP.

[27] Abrams.M.S. (1977).Performance of concrete structures exposed to Fire. PCA, Research and Development Bulletin.

[28] Hertz.K.D. (2005). Concrete strength for fire safety design. Magazine of Concrete Research 2005; 57(8), p.445-453.

[29] Malhotra.H.L. (1956). The effect of temperature on the compressive strength of concrete. *Magazine of concrete research* 1956, 23(8), pp.85-100.

[30] Lee.J,Xi.Y and William.K, Properties of concrete after high-temperature heating and cooling. *ACI, Materials Journal*. 105(4), pp. 334-341.

[31] Fire resistance of concrete structures. Report of a Joint Committee of the Institution of Structural Engineers and the Concrete Society.

[32] Phan.L.T.(1996).Fire performance of high strength concrete. A report of the state of the art. Maryland 20899, NISTIR 5934. Building and Fire Research Laboratory, National Institute of Standards and Technology Gaithersburg.

[33] Perkins.P.H, Repair protection and waterproofing of concrete structures. *Elsevier applied science publishers Ltd*.

[34] Abrams.M.S.(1977). Compressive strength of concrete at temperatures to 1600 F fire. PCA, Research and Development Bulletin.

[35] Neville.A.M, Properties of concrete, 4th edition. Pearson Prentice Hall

[36] Lankard.D.R,Birkimer.D.L,Fondriest.F and Snyder,M.J. (1971). Effects of moisture content on the structural properties of Portland Cement Concrete exposed to temperatures up to 500F. American Concrete Institute, Detroit, 1971, 25(SP25-03), pp.59-102.

[37] Kaplan.M.F and Roux.F.J.P. (1981). Variations in properties of concrete at elevated temperatures. In transactions of the 6th international conference on structural mechanics in reactor technology, Paris, France.

[38] Khoury.G.A, Grainger.B.N and Sullivan.P.J.E. (1985). Strain of concrete during first heating to cooling from 600°C under load. Magazine of Concrete Research1985,37 (133), pp.195-215.

[39] Harada.T, Takeda.J, Yamane.S and Furumura.F. (1972). Strength, elasticity, and thermal properties of concrete subjected to elevated temperatures. *ACI Structural Journal*,34(SP34-21), pp.377-406.

[40] Purkiss.A.J. (2007). Fire safety engineering design of structures,2nd edition.

[41] Bessey.G.E. (1950). The visible changes in concrete mortar exposed to high temperatures. Technical paper.No.4: part-II. National Building Studies, HMSO, London.

[42] Komarovskii.A.N. (1965). Design of Nuclear Plants, 2nd edition.

[43] Li.M, Qian.X and Sun.W. (2004). Mechanical properties of high strength concrete after fire. Cement and Concrete Research .2004,34(6), pp.1001-1005.

[44] Davis.H.S. (1967). Effect of high-temperature exposure on concrete. Materials Research and Standards.1967,7(10), pp.452-459.

[45] Arioz.O. (2009). Retained properties of concrete exposed to high temperatures: Size effect. Fire and Materials; 2009, 33(5), pp.211-222.

[46] Cho.T.L,Chih.C.H,Chun.Y.C and Chun.C.M. (2005). Tracking concrete strength under variable high temperature. *ACI Material Journal*. 2005,102(5), pp.322-329.

[47] Carette.G.G, Painter.K.E and Malhotra.V.M. (1982). Sustained high temperature effect on concrete made with normal Portland Cement, normal Portland Cement and slag, or normal Portland Cement and fly ash concrete international. Design and Construction.1982, 4(7), pp.41-51.

[48] Nasser.K.W and Lothia.R.P.(1971). Mass concrete properties at high temperatures. ACI Structural.1971, 68(3), pp.180-188.

[49] Kassir.M.K,Bandyopadhyay.K.K and Reich.M. (1996).Thermal degradation of concrete in the temperature range from ambient to 315°C, Un ited States Department of Emergency report, Washington D.C.

[50] Mohamedbhai.G.T.G. (1986). Effect of exposure time and rates of heating and cooling on the residual strength of heated concrete. Magazine of Concrete Research.1986;38(136), pp.151-158.

[51] Chang.Y.F, ChinY.H, Sheu.M.S and Yao.G.C. (2006). Residual stress-strain relationship for concrete after exposure to high temperatures. Cement and Concrete Research .2006; 36(10), pp.1999-2005.

[52] Castillo.C and Durrani A.J. (1990). Effect of transient high temperature on high strength concrete. ACI Materials.1990,87(1), p.47-53.

[53] Harada.T. (1959). Transactions of the Architectural Institute of Japan, report 63, October, Architectural Institute of Japan, Tokyo.

[54] Smith.P, Resistance to fire and high temperatures, Research and Development Branch, Ontario Ministry of Transportation, Downs view, Ontario, Canada.

[55] Cruz.C.R. (1966). Elastic properties of concrete at high temperature. Portland Cement Association Research and Development Laboratory,PCA Bulletin 191,January1966.

[56] Marechal.J.C.(1972). Creep of concrete as function of temperature. ACI Structural.1972; 34(SP34-30), pp.547-564.

[57] Potyrala P. B. (2011). Use of Fibre Reinforced Polymer Composites in Bridge Construction. Universitat Politécnica de Catalunya. 93 p.

[58] Sonnenschein, R., Bilcik, J., Gajdosova, K. (2016). Crack Width Control in Concrete Structures with FRP Reinforcement, Engineering Mechanics 2016, Svratka.

[59] Tuakta,C. (2005). Use of Fiber Reinforced Polymer Composite in Bridge Structures, Massachusetts Institute of Technology.

[60] Zobel ,H. (2004). Composites Bridges, 50. Jubileuszowa Konferencja Naukowa KILiW PAN i KN PZITB, Krynica (in Poland).

[61] Gardiner,G. (2016). Disruptive composite infrastructure. Composites World. http://www.compositesworld.com/blog/post/disruptive-compositeinfrastructure

[62] Carolin, A. (2003). Carbon Fibre Reinforced Polymers for Strengthening of Structural Elements. Doctoral thesis. Lulea: Lulea University of Technology, 194 p.

[63] Concrete Society Assessment. (2008). "design and repair of fire-damaged concrete structures", Technical report, no. 68, Camberley, Surrey, UK.

[64] Bastami, M. Chaboki-Khiabani, A. Baghbadrani, M. Kordi, M. (2011). "Performance of high strength concretes at elevated temperatures", *Scientia Iranica*, 18(5), pp.1028–1036.

[65] Mehta, P.K. and Monteiro, P.J.M. (2006). "Concrete: Microstructure, Properties, and Materials", McGraw-Hill, New York, NY, USA.

[66] Chen, G.M. He, Y.H. Yang, H. Chen, J.F. Guo, Y.C. (2014). "Compressive behavior of steel fiber reinforced recycled aggregate concrete after exposure to elevated temperatures", *Construction and Building Materials*, 71, pp.1–15,

[67] Gupta, T. Siddique, S. Sharma, R. K. Chaudhary, S. (2017). "Effect of elevated temperature and cooling regimes on mechanical and durability properties of concrete containing waste rubber fiber", *Construction and Building Materials* ,137, pp.35–45.

[68] Huang, Z. Liew, J.Y.R. Li, W. (2017). “Evaluation of compressive behavior of ultra-lightweight cement composite after elevated temperature exposure”, *Construction and Building Materials*, 148, pp.579–589.

[69] Baradaran-Nasiri, A. and Nematzadeh, M. (2017). “The effect of elevated temperatures on the mechanical properties of concrete with fine recycled refractory brick aggregate and aluminate cement”, *Construction and Building Materials*, 147, pp.865–875.

[70] Xiong, M.X, Liew, J.Y.R. (2016). “Mechanical behaviour of ultra-high strength concrete at elevated temperatures and fire resistance of ultra-high strength concrete filled steel tubes”, Materials and Design, 104, pp.414–427.

[71] Li, L. Jia, P. Dong, J. Shi, L. Zhang, G. Wang, Q. (2017). “Effects of cement dosage and cooling regimes on the compressive strength of concrete after post-fire-curing from 800°C”, *Construction and Building Materials*, 142, pp.208–220.

[72] Xiao, J. Li, Zh. Xie, Q. Shen, L. (2016). “Effect of strain rate on compressive behaviour of high-strength concrete after exposure to elevated temperatures”, *Fire Safety Journal*, 83, pp.25–37.

[73] Choi, E. Kim, Y.W. Chung, Y.S. Yang, K.T. (2010). “Bond strength of concrete confined by SMA wire jackets”, Phys Proc, 10, pp.210–215.

[74] Choi, E. Chung, Y.S. Kim, Y.W. Kim, J.W. (2011). "Monotonic and cyclic bond behavior of confined concrete using NiTiNb SMA Wires", *Smart Mater Structure*, 20(7), pp.1–11.

[75] Calderón, P.A. Adam, J.M. Ivorra, S. Pallarés, S.F. Giménez, E. (2009). "Design strength of axially loaded RC columns strengthened by steel caging", Materials & Design, 30(10), pp. 4069–4080.

[76] Turgay,T. Polat, Z. Koksal, H.O. Doran, B. Karakoç, C. (2010). "Compressive behavior of large-scale square reinforced concrete columns confined with carbon fiber reinforced polymer jackets", Materials & Design, 31(1), pp. 357–364,

[77] Bisby, L.A. Green, M.F. Kodur, V.K.R. (2005). "Fire endurance of fiber-reinforced polymer confined concrete columns", *ACI Structure Journal*, 102(6), pp.883–891.

[78] Chowdhury, E.U. Bisby, L.A. Green, M.F. Kodur, V.K.R. (2007). "Investigation of insulated CFRP wrapped reinforced concrete columns in fire", *Fire Safety Journal*, 42(6), pp.452–460.

[79] Maghsoudi, A.A and Akbarzadeh Bengar, H. (2011). "Acceptable lower bound of the ductility index and serviceability state of RC continuous beams strengthened with CFRP sheets", Scientia Iranica, 18(1), pp. 36-44.

[80] Ghasemi, S. Maghsoudi, A.A. Akbarzadeh Bengar, H. Ronagh, H.R. (2016). "Sagging and Hogging Strengthening of Continuous Unbonded Posttensioned HSC Beams by NSM and EBR", J. Compos. Construction, 20(2).

[81] Balaguru, P. Nanni, A. Giancaspro, J. (2009). "CFRP composites for reinforced and prestressed concrete structures", Taylor and Francis, New York.

[82] Yan, Z. (2005). "Shape modification of rectangular columns confined with CFRP composites", Phd thesis, Salt Lake City (UT), Dept. Civil and Environmental Eng. University of Utah.

[83] Behzard, P. Sharbatdar, M.K. Kheyroddin, A. (2016). "Different NSM CFRP technique for strengthening of RC two-way slabs with low clear cover thickness", Scientia Iranica, 23(2), pp.520-534.

[84] Shin, J. Scott, D.W. Stewart, L.K. Yang, Ch. Wright, T.R. Roches, R.D. (2016). "Dynamic response of a full-scale reinforced concrete building frame retrofitted with CFRP column jackets", Engineering Structures,125, pp.244–253.

[85] Hadi, M.N.S. (2009). "Behaviour of eccentric loading of CFRP confined fibre steel reinforced concrete columns", Construction Build Mater,23(2), pp.1102–1108.

[86] Parvin, A. Altay, S. Yalcin, C. Kaya, O. (2010). "CFRP rehabilitation of concrete frame joints with inadequate shear and anchorage details", J Compos Construction,14(1).

[87] Teng, J.G. Chen, J.F. Smith, S.T. Lam, L. (2002). “CFRP strengthened RC structures”, Wiley Chichester.

[88] Debaiky, S.A. Green, M.F. Hope, B.B. (2002). “Carbon fibre-reinforced polymer wraps for corrosion control and rehabilitation of reinforced concrete columns.”, ACI Mater J, 99(2), pp.129–137.

[89] Ilia, E. Mostofinejad, D. Moghaddas, A. (2015). “Performance of corner strips in CFRP confinement of rectilinear RC columns”, Scientia Iranica,22(6), pp. 2024–2032.

[90] Issa, M.A. Rajai, Z.A. (2009). “Experimental and parametric study of circular short columns confined with CFRP composites”, J Compos Construction, 13(2), pp.35–147.

[91] Maaddawy, T. (2008). “Post-repair performance of eccentrically loaded RC columns wrapped with CFRP composites”, Cement Concr Compos, 30(9),pp. 822–830.

[92] Toutanji, H. Han, M. (2009). Gilbert, J. Matthys, S. “Behaviour of large scale rectangular columns confined with CFRP composites”, J Compos Constr (ASCE), 29.

[93] Chowdhury, E.U. Bisby, L.A. (2008). Green, M.F. Kodur, V.K.R. “Residual behaviour of fire exposed reinforced concrete beams prestrengthened in flexure with fibre reinforced polymer sheets.”, J Compos Constr, 12(1), pp. 44–52.

[94] Haddad, R.H. Shannag, M.J. Hamad, R.J. (2007). “Repair of heat damaged reinforced concrete T-beams using FRC jackets”, J Mag Concr Res, 59(3), pp. 223–231.

[95] Yan, Z. Zhisheng, X.U. (2005). “Experimental study on safety test for reinforced concrete columns strengthened with carbon fibre reinforced polymers after fire.”, Disaster Prevention Science and Safety Technology Institute, Central South University, Changsha, China.

[96] Zhong, T. Lin-Hai, H. (2007). “Behaviour of fire-exposed concrete-filled steel tubular beam columns repaired with CFRP wraps”, J Thin-walled Struct, 45(1), pp.63–76.

[97] Zhong,T. Lin-Hai, H. Ling-Ling, W. (2007). “Compressive and flexural behavior of CFRP-repaired concrete-filled steel tubes after exposure to fire.”, J Constr Steel Res, 63(8), pp.1116–1126.

[98] Karbhari, V.M, Gao, Y. (1997). “Composite jacketed concrete under uniaxial compression verification of simple design equations.” J Mater Civil Eng ASCE, 9(4), pp.185–193.

[99] Rochette, P. Labossière, P. (2000). “Axial testing of rectangular column models confined with composites”, J Compos Constr ASCE, 4(3), pp.129–136.

[100] Maaddawy, T.E. Sayed, M.E Abdel-Magid, B. (2010). “The effects of cross-sectional shape and loading condition on performance of reinforced concrete

members confined with Carbon Fiber-Reinforced Polymers", Materials & Design, 31, pp.2330–2341.

[101] Yan, Z. Pantelides, C.P. (2011). "Concrete column shape modification with FRP shells and expansive cement concrete", Construction and Building Materials, 25, pp.396–405.

[102] Ma, Ch. Apandi, N. Yung, S. Hau, Ng. Haur, L. Awang, A. Omar, W. (2017). "Repair andrehabilitation of concrete structures using confinement: A review", Construction and Building Materials, 133, pp. 502–515.

[103] Shin, J. Scott, D.W. Stewart, L.K. Yang, C.S. DesRoches, R. (2016). "Dynamic response of a full-scale reinforced concrete building frame retrofitted with FRP column jackets", Engineering Structures, 125, pp. 244–253.

[104] I.A. Fletcher, S. Welch, J.L. Torero, R.O. Carvel, A. (2007). Usmani, Behaviour of concrete structure in fire, Therm. Sci.11(2), pp.37–52.

[105] U. Diederichs, U. Schneider. (1981). Bond strength at high temperatures, Mag. Concr. Res. 33 (115), pp75–84.

[106] C.A. Menzel. (1943). Tests of the fire resistance and thermal properties of solid concrete slabs and their significance, in: Proceedings, American Society for Testing and Materials (ASTM) 43, pp.1099–1153.

[107] C.R. Binner, C.B. Wilkie, P. Miller. (1949). Heat Testing of High Density Concrete, Supplement, Declassified Report HKF-1, U.S. Atomic Energy Commission.

[108] H.L. Malhotra. (1956). The effect of temperature on the compressive strength of concrete, Mag. Concr. Res. (Lond.),8(22), pp.85–94.

[109] J. Xiao, G. König. (2004). Study on concrete at high temperature in China—an overview, *Fire safety Journal.* 39, pp.89–103.

[110] N. Yuzer, F. Akoz, L. Dokuzer ozturk. (2004). Compressive strength–color change relation in mortars at high temperature, Cem. Concr. Res. 34, pp.1803–1807.

[111] Hwang, Y. Lee, Y. Kwak, H. Kim, W. Hwang. (2016). Fire-resistant capacity of RC structures considering time-dependent creep strain at elevated temperature‖, Magazine of Concrete Research, 68(15), pp.782–797.

[112] Ö. Arıöz. (2007). Effects of elevated temperatures on properties of concrete, *Fire Safety Journal*. 42, pp.516–522.

[113] M.A. Youssef, M. Moftah. (2007). General stress-strain relationship for concrete at elevated temperatures, Eng. Struct. 29, pp.2618–2634.

[114] M. Husem. (2006). The effects of high temperature on compressive and flexural strengths of ordinary and high-performance concrete, *Fire Safety Journal*. 41, pp.155–163.

[115] L. Biolzi, S. Cattaneo, G. Rosati. (2008). Evaluating residual properties of thermally damaged concrete, Cem. Concr. Compos. 30, pp.907–916.

[116] Roy, A. Bhargava, P. Sharma, U. (2016). Confinement strengthening of heat damaged reinforced concrete columns, Magazine of Concrete Research, 68(6), pp. 291– 304.

[117] R. Zheng, Y. Zhang, Z. (2015). Behavior of steel reinforced concrete beams considering overall fire stages, Magazine of Concrete Research, 67(6), pp.294–307.

[118] B. Georgali, P.E. Tsakiridis. (2005). Microstructure of fire-damaged concrete. A case study, Cem. Concr. Compos. 27, pp.255–259.

[119] Y.-H. Chen, Y.-F. Chang, G.C. Yao, M.-S. Sheu. (2009). Experimental research on postfire behaviour of reinforced concrete columns, *Fire Safety Journal*. 44, pp741–748.

[120] Eligehausen, R., Popov, E. P., and Bertero, V. V. (1983). “Local bond stress-slip relationships of deformed bars under generalized excitations.” Rep. No. UCB/EERC-83/23, Univ. of Calif., Berkeley, Calif.

[121] CEB-FIB. (2000). Bond of reinforcement in concrete, International Federation for Structural Concrete.

[122] Yalciner H, Eren O, Sensoy S. (2012). An experimental study on the bond strength between reinforcement bars and concrete as a function of concrete cover, strength and corrosion level. Cem Concr Res; 42, pp.643–55.

[123] Malvar LJ. (1992). Bond of reinforcement under controlled confinement. *ACI Mater Journal*; 89(6), pp.593–601.

[124] M. H. Harajli1. (2009). Bond Stress–Slip Model for Steel Bars in Unconfined or Steel, FRC, or FRP Confined Concrete under Cyclic Loading, (ASCE)0733.

[125] Panedpojaman, P. and pothisiri, Th. (2014). bond characteristics of reinforced normal strength concrete beams at elevated temperatures‖, *ACI structural Journal*, 111(6), 1351-1362.

[126] Kodur, V.K.R. and Agrawal, A. (2017). Effect of temperature induced bond degradation on fire response of reinforced concrete beams‖, engineering structures, 142, 98- 109.

[127] Abdallah, S. fan, M. cashell, K.A. (2017). Bond-slip behavior of steel fiber in concrete after exposure to elevated temperatures, construction and building materials, 140, 542-551.

[128] A.F. Bingol, R. Gul. (2009). Residual bond strength between steel bars and concrete after elevated temperatures, *Fire Safety Journal*. 44, pp.854–859.

[129] Aslani F, Nejadi S. (2012). Bond behavior of reinforcement in conventional and self-compacting concrete. Adv Struct Eng; 15(12), pp.2033–51.

[130] Al-Hammoud R, Soudki K. (2013). Topper TH. Confinement effect on the bond behavior of beams under static and repeated loading. Construction Build Mater; 40, pp.934–43.

[131] Choi E, Kim YW, Chung YS, Yang KT. (2010). Bond strength of concrete confined by SMA wire jackets. Phys Proc; 10:210–5.

[132] Choi E, Chung YS, Kim YW, Kim JW. (2011). Monotonic and cyclic bond behavior of confined concrete using NiTiNb SMA Wires. Smart Mater Struct; 20(7), pp.1–11. 075016.

[133] Lee H, Choi E, Cho SC, Park T. (2012). Bond and splitting behavior of reinforced concrete confined by steel jackets without grouting. Mag Concr Res; 64(3), pp.225–37.

[134] Bournas DA, Triantafillou TC. (2011). Bond strength of lap-spliced bars in concrete confined with composite jackets. J Compos Constr, 15(2), pp.156–67.

[135] Dagher, F., and Harajli, M. H. (2007). “Seismic strengthening of bondcritical regions in rectangular RC columns using external FRP jackets.” Research Rep.

Submitted in Partial Fulfillment of the Requirements of M.S. Degree in CE, American Univ. of Beirut, Beirut, Lebanon.

[136] Ghosh, K. K., and Sheikh, A. S. (2007). “Seismic upgrade with carbon fiber-reinforced polymer of columns containing lap-spliced reinforcing bars.” *ACI Structure Journal,* 104(2), pp. 227–236.

[137] Harajli, M. H. (2008). “Seismic behavior of RC columns with bond critical regions: Criteria for seismic strengthening using external FRP jackets.” J. Compos. Constr., 12(1), pp.69–79.

[138] Harajli, M. H., and Rteil, A. (2004). “Effect of confinement using FRP or FRC on seismic performance of gravity load-designed columns.” *ACI Structure journal,*101(1), pp. 47–56.

[139] Harries, K. A., Ricles, J. R., Pessiki, S., and Sause, R. (2006). “Seismic retrofit of lap splices in nonductile square columns using carbon fiber reinforced jackets.” *ACI Structure Journal,* 103(6), pp.874–884.

[140] ASTM Standard C33, (2006), "Specification for Concrete Aggregates," ASTM International, West Conshohocken, PA, 2006, DOI: 10.1520/C0033- 03R06, www.astm.org .

[141] G.T.G. Mohamedbhai. (1986). Effect of exposure time and rates of heating and cooling on residual strength of heated concrete, Mag. Concr. Res. 38 (136), pp.151–158.

[142] Jianzhuang Xiao, Yizhao Hou, Zhanfei Huang. (2014). “Beam test on bond behavior between high-grade rebar and high-strength concrete after elevated temperatures” *Fire Safety Journal*, 69, pp.23–35.